

D. Brigante

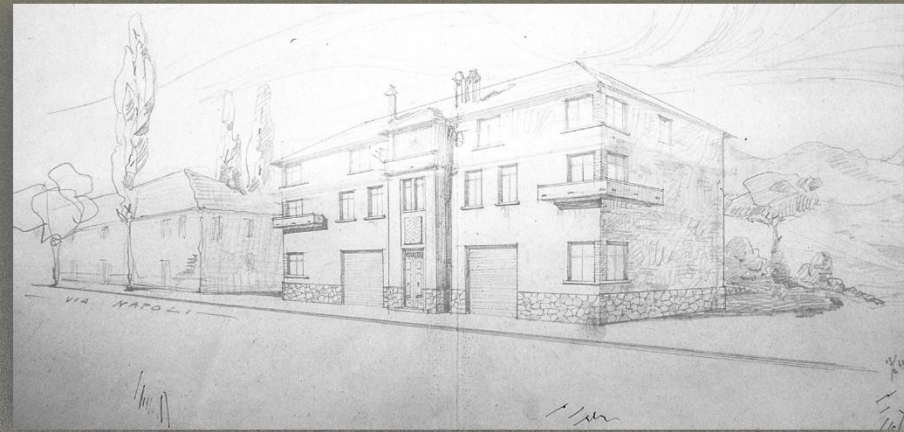
Vibration based methods for the structural assessment of historical structures



Università degli studi  
del Molise

# VIBRATION BASED METHODS FOR THE STRUCTURAL ASSESSMENT OF HISTORICAL STRUCTURES

ICAR/09



Daniele Brigante

**UNIVERSITY OF MOLISE**  
**DEPARTMENT OF BIOSCIENCE AND TERRITORY**

*PHD COURSE - CURRICULUM TERRITORIALE*

**XXXI CICLO**



***VIBRATION BASED METHODS FOR THE  
STRUCTURAL ASSESSMENT OF HISTORICAL  
STRUCTURES***

*ICAR/09*

DANIELE BRIGANTE

TUTORS:  
PROF. FILIPPO SANTUCCI DE  
MAGISTRIS

COORDINATOR:  
PROF.SSA  
GABRIELLA STEFANIA SCIPPA

PROF. GIOVANNI FABBROCINO

Academic year: 2019

*To my family*

# Acknowledgements

*Completion of this doctoral dissertation was possible with the support of several people. I would like to express my sincere gratitude to all of them. First of all, I am extremely grateful to my research guide, Professor Giovanni Fabbrocino, for his valuable guidance, scholarly inputs and consistent encouragement I received throughout the research work. The joy and enthusiasm he has for his research was contagious and motivational for me, even during tough times in the Ph.D. pursuit. I would also like to thank my other supervisor, Professor Filippo Santucci De Magistris for his interest, care and continuous encouragement. I am deeply grateful to Professor Carlo Rainieri for helping me with his very kind amicable and positive disposition. I am grateful to Professor Salvatore Gerbino, for his suggestions for the numerical models analysis.*

*I thank Professor Stefania Scippa, Coordinator of the Phd Course - Curriculum Territoriale, for the academic support and the facilities provided to carry out the research work at the University.*

*Some faculty members of the University have been very kind enough to extend their help at various phases of this research, and I do hereby acknowledge all of them.*

*I would like to express my deep gratitude to my guidance, in the foreign research period, Professor Paulo Lourenço from the University of Minho, for welcoming me in to Institute for Sustainability and Innovation in Structural Engineering (ISISE). I thank him for the academic support and the facilities provided to carry out the research work at the Institute.*

*I would like to thank heartily my co-guidance, in the visiting period, Dr. Maria Giovanna Masciotta from the University of Minho. She has been very kind and patient and always willing to lend her service whenever I approached her and I acknowledge and appreciate her for all her efforts. I would also like to thank all the technicians of the Structural Laboratory LEST, of Civil Engineering Department, of University of Minho, for their support during the experimental phases I am particularly grateful to Antonio Matos who helped me during the all activities.*

*I could not omit the excellent and continuous collaboration, help and guidance that were offered to me by my friend and colleague Dr. Danilo Gargaro for which I am really grateful.*

*During the course of this work, I had an opportunity to interact with many fellow students. I thank them for their friendship and for their support during this work. I would like to thank in particular Massimina and Dipendra.*

*I cannot forget to thank my flatmates Beatrice, Nicoletta and Antonio who supported me a lot during the period in Guimarães, and which also long distance, they continued to encourage me in this last months.*

*I take this time to express my gratitude to my new friends and colleagues that I met in Portugal. I gained a lot from them, through their personal and scholarly interactions and their suggestions for the life.*

*I owe a lot to my parents, who encouraged and helped me at every stage of my personal and academic life, and longed to see this achievement come true.*

*I would also like to thank all of my friends who supported me in writing, and incited me to strive towards my goal.*

*I want to dedicate this work to my friend Fra Peppe. Thank you for supporting me for everything, and especially I can't thank you enough for encouraging me throughout this experience.*

*“No one can pass through life, any more than he can pass through a bit of country, without leaving tracks behind, and those tracks may often be helpful to those coming after him in finding their way.”*

*With this thought of the founder of the modern Scouting movement Baden Powel, at last but not least, I would like to thank God Almighty for giving me the strength, knowledge, ability and opportunity to undertake this research study and to persevere and complete it satisfactorily. Without his blessings, this achievement would not have been possible. “*



---

# TABLE OF CONTENTS

TABLE OF CONTENTS .....	I
LIST OF FIGURES.....	V
INDEX OF TABLES.....	XV
<b>CHAPTER 1 INTRODUCTION .....</b>	<b>1</b>
<b>1.1 BACKGROUND OF THE SEISMIC VULNERABILITY FOR THE     ARCHITECTURAL HERITAGE .....</b>	<b>3</b>
<b>1.2 MOTIVATION FOR THE RELIABLE PROCEDURES FOR PERFORMANCE     ASSESSMENT OF HISTORICAL STRUCTURES IN SEISMIC AREAS .....</b>	<b>7</b>
<b>1.3 OUTLINE OF THE THESIS.....</b>	<b>14</b>
<b>CHAPTER 2 VIBRATION BASED OF DYNAMIC IDENTIFICATION: BACKGROUND AND OPEN ISSUES .....</b>	<b>17</b>
<b>2.1 INTRODUCTION.....</b>	<b>17</b>
<b>2.2 BASICS OF DYNAMIC.....</b>	<b>18</b>
2.2.1 Theory and classical formulation .....	19

## Index

---

<b>2.3 METHODS FOR OPERATIONAL MODAL ANALYSIS (OMA)</b> .....	<b>24</b>
2.3.1 Frequency Domain Decomposition method.....	26
2.3.2 Stochastic Subspace Identification Method .....	29
<b>2.4 SOME REMARKS ON THE DYNAMICS OF HERITAGE STRUCTURES</b> .....	<b>31</b>
<b>2.5 AN OVERVIEW OF EXPERIMENTAL SUBSTRUCTURING TECHNIQUES</b> .....	<b>46</b>
2.5.1 The substructuring approach to dynamic analysis.....	47
2.5.2 The Modal Assurance Criterion (MAC) in the dynamic substructuring.....	52
2.5.3 Modal Assurance Criterion (MAC).....	53
2.5.4 Substructure Modal Assurance Criterion (SUMAC).....	54
<b>CHAPTER 3 MODEL UPDATING VS. DAMAGE ASSESSMENT</b>	<b>59</b>
<b>3.1 INTRODUCTION</b> .....	<b>59</b>
<b>3.2 CLASSIFICATION OF VIBRATION-BASED DAMAGE IDENTIFICATION     METHODS</b> .....	<b>60</b>
<b>3.3 SPECTRUM DRIVEN DAMAGE IDENTIFICATION METHOD</b> .....	<b>61</b>
3.3.1 Basic theory .....	62
<b>CHAPTER 4 A MAC BASED APPROACH: DYNAMIC IDENTIFICATION OF THE STRUCTURAL BEHAVIOUR</b> .....	<b>65</b>
<b>4.1 THE ROLE OF THE DYNAMIC IDENTIFICATION</b> .....	<b>65</b>
4.1.1 Introduction .....	65
4.1.2 Masonry buildings in aggregates.....	67



---

4.1.3 An approach to discriminate global or local mode.....	71
<b>4.2 A NOVEL USE OF THE MAC: ASSESSMENT OF THE METHOD.....</b>	<b>74</b>
4.2.1 Explanatory numerical cases: Regular masonry structure .....	76
4.2.2 Single Cell.....	79
4.2.3 Double Cell.....	100
4.2.4 L-Shaped aggregate.....	107
4.2.5 Monitoring strategies.....	115
<b>4.3 FINAL REMARKS .....</b>	<b>116</b>
<b>CHAPTER 5 FIELD VALIDATION ON AN ITALIAN MASONRY BUILDING .....</b>	<b>119</b>
<b>5.1 INTRODUCTION.....</b>	<b>119</b>
<b>5.2 KNOWLEDGE PATH OF THE STRUCTURE .....</b>	<b>120</b>
5.2.1 Knowledge path .....	120
5.2.2 Historical evolution.....	121
5.2.3 Structural assessment .....	124
5.2.4 Description of the structural systems .....	127
<b>5.3 DESCRIPTION OF THE NUMERICAL MODEL .....</b>	<b>135</b>
5.3.1 Introduction .....	135
5.3.2 Equivalent Frame Model.....	136
<b>5.4 DYNAMIC IDENTIFICATION SYSTEM.....</b>	<b>144</b>
5.4.1 System identification test .....	144
5.4.2 Dynamic identification campaign.....	147
5.4.3 Identification of modal parameters.....	150

## Index

---

5.4.4 Assessment of the modal shapes by means the MAC based procedure .....	155
<b>5.5 CLOSING FINAL REMARKS .....</b>	<b>158</b>
<b>CHAPTER 6 DAMAGE ASSESSMENT: AN OLD ARCH REPLICA</b>	<b>161</b>
<b>6.1 INTRODUCTION.....</b>	<b>161</b>
<b>6.2 ARCH MODEL DESCRIPTION.....</b>	<b>163</b>
6.2.1 Arch construction description .....	163
6.2.2 Numerical Model description.....	165
6.2.3 Modal Dynamic Analysis.....	170
6.2.4 Numerical prediction of damage locations.....	173
<b>6.3 ARCH DAMAGE TEST IN DISPLACEMENT CONTROL.....</b>	<b>176</b>
6.3.1 System identification tests.....	178
6.3.2 Test setup.....	182
6.3.3 Types of Input data acquisition.....	190
6.3.4 Modal identification: Result for the damage evolution .....	191
6.3.5 Application of the spectral damage analysis.....	200
6.3.6 Results.....	203
<b>CHAPTER 7 CONCLUSIONS AND FUTURE DEVELOPMENTS</b>	<b>207</b>
<b>REFERENCES.....</b>	<b>210</b>

---

## LIST OF FIGURES

Figure 1.1. Collapse mechanisms.....	8
Figure 2.1. System scheme for the Experimental Modal Analysis approach (Benjamin Greiner, 2009).....	19
Figure 2.2. Free vibration of an undamped system (Chopra, 2001): (a) system; (b) and (c) different representations of the first natural vibration mode .....	19
Figure 2.3. Total response as superposition of modal components (Clough & Penzien, 1993) .....	24
Figure 2.4. Stochastic Subspace Identification method: (a) model calibration; (b) model parameter estimation dilemma; and (c) data driven with the poles selection through the several test setups (Ramos 2007).....	30
Figure 2.5. a) Distribution of the main modal shapes of some churches in the field of frequency and active modal mass participating; Mode contribution in terms of mass participating : b) S.Maria in Donnaromita, c) S. Agostino	

## Index

---

alla Zecca, d) S. Giovanni Maggiore. Adapted to Boscato et al 2016.....	35
Figure 2.6. a) Distribution of the main modal shapes of some palaces in the field of frequency and active modal mass participating; Mode contribution in terms of participating mass: b) Palazzo Bosco Lucarelli; c) Beylerbeyl Palace. (Adapted from Boscato et al 2016.....	36
Figure 2.7. Different structural configuration of Bell Tower.....	38
Figure 2.8. a) Bell Tower view of the San Bartolomeo church; b) layout of the sensor at each floor; c-d) 3D model of the church aggregate.....	39
Figure 2.9. a) Graph of PMR in $y$ [%]; b) experimental mode and frequency values of the Bell Tower .....	41
Figure 2.10. Layout of the accelerometers at each floor of the Tower .	43
Figure 2.11. a) Damage survey of the Osservatorio Vesuviano Tower; b) damage detail on vaulted .....	44
Figure 2.12. Assembly using interface displacements (adapted from van der Valk. 2010).....	50
Figure 2.13. Assembly using interface forces (adapted from van der Valk. 2010) .....	51
Figure 2.14. Mixed interface method (adapted from van der Valk. 2010) .....	51
Figure 2.15. Yaw system of a 2.3. MW Siemens wind turbine adapted from P.L.C van der Valk (2010) .....	56

---

Figure 2.16. SUMAC of the models from the total assembly and he modes of the component assembly adapted from van der Valk (2010).....	57
Figure 3.1. Classification of Vibration-based Damage Identification Methods by (M.G. Masciotta, 2015) .....	61
Figure 4.1. Classification of the type of behaviour of the existing masonry building .....	68
Figure 4.2. Sample MAC matrix .....	73
Figure 4.3. 3D Model of the aggregate .....	77
Figure 4.4. Location of virtual sensors .....	78
Figure 4.5. a) 3D Model of the isolated building; b)Finite mesh view .	80
Figure 4.6. Model 1: schematic plan view of the aggregate reference basic cell with restrained floor (A), and unrestrained floor (B).....	81
Figure 4.7. Single cell: set of virtual sensor: a) view in plan of the verticals (16 alignments), the number of the sensors increase (b), (c), (d) .....	83
Figure 4.8. M.1.A: modal analysis results for rigid and restrained floor .....	85
Figure 4.9. M.1.B: modal analysis results for rigid and restrained floor .....	86
Figure 4.10. Results M.1.A.16: the MAC matrix associated with the global modes a-b) and local mode d); c) schematic plan view of the virtual alignments.....	87

## Index

---

Figure 4.11. Results M.1.B.16: the MAC matrix associated with the global modes a-b) and local mode d); c) schematic plan view of the virtual alignments.....	88
Figure 4.12. Plan view of the reference numerical model .....	90
Figure 4.13. 3D View of the reference numerical model .....	91
Figure 4.14. Results multi-storey table mode 1: a) deformed shape view in plan; b) 3D view of mode shape; c) the MAC matrix associated with the first mode and vector norm values. ....	92
Figure 4.15. Results multi-storey table mode 2: a) deformed shape view in plan; b) 3D view of mode shape; c) the MAC matrix associated with the first mode and vector norm values. ....	93
Figure 4.16. Results multi-storey table mode 3: a) deformed shape view in plan; b) 3D view of mode shape; c) the MAC matrix associated with the first mode and vector norm values. ....	94
Figure 4.17. Results multi-storey table mode 4: a) deformed shape view in plan; b) 3D view of mode shape; c) the MAC matrix associated with the first mode and vector norm values .....	95
Figure 4.18. Results multi-storey table mode 5: a) deformed shape view in plan; b) 3D view of mode shape; c) the MAC matrix associated with the first mode and vector norm values .....	96

Figure 4.19. Results multi-storey table mode 6: a) deformed shape view in plan; b) 3D view of mode shape; c) the MAC matrix associated with the first mode and vector norm values .....	97
Figure 4.20. Results multi-storey table mode 7: a) deformed shape view in plan; b) 3D view of mode shape; c) the MAC matrix associated with the first mode and vector norm values .....	98
Figure 4.21. Double cell: geometry modelling with restrained floor (A); and unrestrained floor with 0.02 m gap (B) configuration.....	101
Figure 4.22. Double cell: set of virtual sensor: the number of the sensors and the vertical increase. ....	102
Figure 4.23. M.2.A: modal analysis results for rigid and restrained floor (a) and rigid and unrestrained floor (b) .....	104
Figure 4.24. M.2.B: model analysis results for rigid and restrained floor (a) and rigid and unrestrained floor (b) .....	104
Figure 4.25. Results M.2.A.30: the MAC matrix associated with the global modes a-b) and local mode d); c) schematic plan view of the virtual alignments.....	105
Figure 4.26. Figure 4.27. Results M.2.B.30: the MAC matrix associated with the global modes a-b) and local mode d); c) schematic plan view of the virtual alignments.....	106
Figure 4.28.a) L-Shape aggregate: schematic plan view of the aggregate with restrained floor (A). ....	107

## Index

---

Figure 4.29.b) L-Shape aggregate: schematic plan view of the aggregate with unrestrained floor - application of a 0.02 m gap - (B).....	108
Figure 4.30. L-Shape aggregate: set of virtual sensor alignments .....	109
Figure 4.31. Results for building aggregate: M.3.A- Modal analysis with rigid and restrained floor; .....	111
Figure 4.32. Results for building aggregate: M.3.B- Modal analysis with rigid and unrestrained floor;.....	111
Figure 4.33. Results: M.3.A.40: the MAC matrix associated with global mode a- b) and local modes d).....	113
Figure 4.34. Results: M.3.B.40: the MAC matrix associated with global mode a- b) and local modes c) .....	114
Figure 4.35. a) Schemes in plan of the sensors distribution b) results in terms of MAC index.....	116
Figure 5.1. The artefact printing.....	122
Figure 5.2. Plans and section of the building 1951 .....	123
Figure 5.3. Plan of the building in which the relevant investigations are marked.....	126
Figure 5.4. Geometry relief: a) view of the plan; b) drawing of main prospectus.....	128
Figure 5.5. Result of thermographic testing of walls: a) ground floor; b) first floor .....	129
Figure 5.6. a) infrared thermos camera type FLIR E60bx; b) endoscopy .....	130



---

Figure 5.7. Direct investigation: a) front of Masonry Class A3 - Group Ib ; b) cross sections .....	131
Figure 5.8. Direct investigation: a) front of Brickwork; b) cross section .....	132
Figure 5.9. a) IR image of weaving floor; b) detail of concrete curb ..	133
Figure 5.10. a) detail between S.A.P and concrete curb; b) cross section of S.A.P. ( <a href="http://www.leca.it">www.leca.it</a> ) .....	134
Figure 5.11. View of the wooden trusses .....	134
Figure 5.12. Identification of the main structural system .....	136
Figure 5.13. Analysed building: drawing of the equivalent frame ....	137
Figure 5.14. SAP modelling: equivalent frame .....	138
Figure 5.15. Equivalent Frame Model of the building .....	139
Figure 5.16. Modelling building: plastic hinges' location in the equivalent frame model of the wall façade.....	142
Figure 5.17. Principal mode shapes .....	143
Figure 5.18. PCB models: capacitive accelerometer .....	145
Figure 5.19. Coaxial cable for the piezoelectric accelerometers with MIL-C-5015 BNC connection ( <a href="http://www.pcb.com">www.pcb.com</a> ) .....	146
Figure 5.20. The cables system .....	146
Figure 5.21. Modular chassis and modules for the acquisition system. ....	147
Figure 5.22. a) View of the installed sensors; b) detail of the sensor with the plate .....	148
Figure 5.23. Experimental monitoring: a) plan view of the localization of the sensors; b) global view of the verticals .....	149

## Index

---

Figure 5.24. The Assign DOF Information Task displaying all sensors of the three test setups. The purple arrows are the reference sensors.....	151
Figure 5.25. Stabilization diagram for SSI techniques from ARTeMIS .....	152
Figure 5.26. Mode shapes of experimental data .....	152
Figure 5.27. The complexity plots for the corresponding mode shapes .....	153
Figure 5.28. Results: a) The shape mode; b) MAC matrix associated with torsional mode; c) Location of the verticals .....	156
Figure 5.29. Results: a) The shape mode; b) MAC matrix associated with torsional mode; c) Location of the verticals .....	157
Figure 6.1. a) Mortar Cylinder compression test for Elastic modulus; b) flexural strength test of prism specimen; c) compressive test of prism specimen .....	163
Figure 6.2. Arch geometry .....	164
Figure 6.3. Arch model phases in the construction of masonry arches .....	165
Figure 6.4. Arch 3D model : Tensile (a) and compressive behaviour (b) .....	167
Figure 6.5. The CHX60 solid element.....	169
Figure 6.6. Arch 3D: view of the mesh type and the boundary conditions .....	169
Figure 6.7. a) Numerical modal results - mode shape and frequency values .....	171

---

Figure 6.8. b) Numerical modal results - mode shape and frequency values .....	172
Figure 6.9. Edit boundary conditions.....	173
Figure 6.10. Numerical crack sequence prediction.....	175
Figure 6.11. Prediction model analysis: (a)View of the control points; (b) displacement control of the arch .....	176
Figure 6.12. a) View of the actuator pre-test; b) rolls system design .	177
Figure 6.13. Actuator test: a) View of LVDT controller; b) result of displacement test .....	178
Figure 6.14. Arch test: a) view of the test apparatus; b) vertical LVDT .....	179
Figure 6.15. a) View of the LVDTs location during the static tests; b) results for the arch displacement control .....	180
Figure 6.16. Arch damage: a) view of crack location; (b) crack C1; c) crack C2; d) crack C3.....	181
Figure 6.17. BeanDevice® AX-3D XRange wireless vibrations sensor .....	184
Figure 6.18. Sensors location: a) top view of the strain gauge systems; b) view from below of the strain gauge systems; c) strain gauges surface base across 3 bricks; d) disposition of the accelerometers.....	184
Figure 6.19. Location of the measuring points for the dynamic tests: (a) front view; (b) top view. Ai indicates accelerometers and Si indicates strain gauges. ....	185
Figure 6.20. Dynamic test sequence, with the different setups .....	189

## Index

---

Figure 6.21. Data collection: a) ambient excitation; b) random impact excitation.....	190
Figure 6.22. a) Reference scenario: diagram of estimated state space model with ambient excitation input ( FDD method) ....	192
Figure 6.23. b) Reference scenario: diagram of estimated state space model with ambient excitation input (SSI-PC method) .	193
Figure 6.24. a) Reference scenario: diagram of estimated state space model with random excitation input (FDD method) .....	194
Figure 6.25. b) Reference scenario: diagram of estimated state space model with random excitation input (SSI-PC method)..	195
Figure 6.26. Mode shapes configuration for the reference scenario...	200
Figure 6.27. Spectral value decomposition for the random impact excitation.....	201
Figure 6.28. Relative frequency values for the identified modes obtained from the dynamic test.....	202
Figure 6.29. Damage analysis results (RS -DS <sub>I</sub> ) for acceleration responses by BB index (light grey bars) and NB index (dark grey bars).....	204
Figure 6.30. Damage analysis results (RS -DS <sub>VII</sub> ) for acceleration responses by BB index (light grey bars) and NB index (dark grey bars).....	205

---

## INDEX OF TABLES

Table 2.1. Experimental values .....	43
Table 4.1. Matrix of the numerical simulation .....	79
Table 4.2. Single cell: numerical simulation of virtual sensors .....	82
Table 4.3. Modal analysis results: modal shape definition codes: T- X=Translational along X axis; T-Z=Translational along Z; R- Y=Rotational in Y axis.....	84
Table 4.4. Double cell: numerical simulation of virtual sensors .....	100
Table 4.5. Summary of the results : Modal shape definition codes: T- X=Translational along X axis; T-Z=Translational along Z; R- Y=Rotational in Y axis.....	103
Table 4.6 L-Shape aggregate: numerical simulation of virtual sensors .....	109
Table 4.7. Results : Modal shape definition codes: T-X=Translational along X axis; T-Z=Translational along Z; R-Y=Rotational in Y axis.....	110
Table 5.1. Reference value for the masonry mechanical parameters.	140

## Index

---

Table 5.2. Reference value for the concrete and steel mechanical parameters .....	141
Table 5.3. Results OMA: natural frequencies ( $f$ ), damping ( $\xi$ ) and MAC .....	153
Table 5.4. Comparison between numerical and experimental values of the natural frequency of the fundamental modes of the building .....	155
Table 6.1. Mechanical properties of the masonry arch model .....	166
Table 6.2. Test setups for accelerometers, n indicate normal direction and t tangential direction.....	187
Table 6.3. Global scenario: FDD results from the ambient excitation test.....	196
Table 6.4. Global scenario: FDD results from the ambient excitation test.....	196
Table 6.5. Global scenario: dumping results for the ambient excitation test.....	197
Table 6.6. MAC values results.....	197
Table 6.7. Global scenario: FDD results from the random impact test .....	198
Table 6.8. Global scenario: SSI-PC results from the random impact test .....	198
Table 6.9. Global scenario: dumping results for the random excitation test.....	199
Table 6.10. MAC values results.....	199

# Chapter 1

## INTRODUCTION

Protection of cultural and architectural heritage represents an interdisciplinary challenge due to the coexistence of historical, artistic and structural issues (Marra 2015). Aging of materials and components due to either time or environmental effects represents one of the problems to be tackled in preserving cultural heritage. This is quite visible in many European Countries, including Italy, where many modern cities grew around historical centres thus the historical centres are being affected by continuous and irregular evolution over time, so that the present structural condition is very complex due to the effect of extensive interactions.

On the other hand, the destructive effects of recent earthquakes - Emilia, 2012; Gorkha, Nepal, 2015; Central Italy, 2016-17 - confirmed the need of developing effective and reliable procedures for performance assessment of historical structures in seismic areas (EN1998-3 2005). The activity of the Italian Authorities showed a strong effort in this field with the release of a comprehensive program

## Chapter 1 - Introduction

---

aimed at assessing the seismic vulnerability of critical buildings and infrastructures including historical and architectural assets. Such programme is also integrated with a continuous development of national seismic code provisions. With the help of an interdisciplinary effort focused on the application of the seismic performance assessment procedures to cultural and architectural heritage, standard results can be obtained in compliance with the conservation principles (The Charter of Krakow 2000) In addition, the probabilistic approach of seismic safety management of structures is becoming very popular in the scientific and technical community, due to the enhancement of analysis techniques and the increment in the computational capabilities of non-linear analysis software programmes.

However, numerical analyses are often very complex due to significant uncertainties in the characterization of material properties and structural behaviour. Besides this, the reliability of seismic analyses is often jeopardized by the need of definition of an appropriate structural and dynamic model. The unique structural configurations, the old construction techniques and the presence of stratified structural modifications that took place over the centuries make the definition of an appropriate and reliable numerical model very challenging. The possibility of applying the dynamic procedures for the seismic assessment can represent a valid tool in understanding the seismic behaviour of the existing historical constructions.



## **1.1 BACKGROUND OF THE SEISMIC VULNERABILITY FOR THE ARCHITECTURAL HERITAGE**

Masonry buildings are the most common structural typology in the Italian historical centres. They are often the result of continuous urban development in a particular areas yielding large structural aggregates (Formisano et al. 2015). Due to the progressive transformation of the urban centres, distinguishing the structurally independent units and identifying the global response of the building as a whole are often very difficult tasks. In fact, distribution of seismic actions strongly depends on the dynamic properties of the architectural complex and its geometrical and mechanical configurations (Elnashai and Di Sarno 2015). Thus, seismic vulnerability assessment of masonry aggregates in the Italian historical centres represents a challenging problem due to the difficulties in reliably predicting their behaviour under earthquake loadings and defining appropriate seismic protection measures in the presence of structural weakness.

The problem of the characterization of the reference unit/component for the evaluation of seismic performance of masonry buildings is fully within the approach of the regulatory framework, not only in the case of historic constructions but also in the case of the traditional masonry building stocks in many historical sites in the big cities, towns and villages in Italy. It is obvious that historical buildings are integral part of the built environment and thus deserve to be preserved (Lagomarsino and Cattari 2015).

The urban texture of historical city centers, in terms of their construction, reveals considerable differences in terms of geographical, cultural and technical backgrounds. The differences result in buildings with typical local characteristics and authenticity that justify conservation of heritage structures.

Apart from this, the high vulnerability of historic masonry buildings to seismic actions needs to be considered, mainly due to the lack of proper connections between the various structural elements (masonry walls, wooden beams in the floors and wooden beams on the roof). These conditions often lead to overturning collapse of the perimeter walls under seismic excitation. Simplified limit state analysis methods are often used for safety analysis and design of strengthening interventions (Direttiva 2011).

The preservation of the cultural heritage in seismic areas, therefore, requires a strategic plan and a suitable methodology that includes a rational approach of multidisciplinary knowledge.

The issue of seismic vulnerability assessment of existing masonry building takes on particular characteristics due to the difficulties in reliably forecasting their behaviour in the seismic field or provide suitable seismic prevention measures in the presence of structural weakness. To this end, the seismic assessment involves over the historical structures also the traditional masonry buildings present in many historical centers of the big cities or the numerous villages. Also, the architectural and cultural heritage can be viewed as strong social

and economic contributions for the cities and countries by providing an attraction.

Recent Italian guidelines (CNR DT 212. 2012), in agreement with the seismic design code (NTC 2018), suggests the adoption of a probabilistic approach for seismic safety management of structures due to the enhancement of analysis techniques and advancement in computational capabilities of non-linear software programmes. Numerical analysis is a complex task, because of several uncertainties associated with the mechanical properties of materials, structural scheme and structural details. This is a very relevant difference between modern constructions and existing masonry buildings. So, relevant codes at national and international level recommend the assessment of local as well as global mechanisms whenever existing constructions are concerned. The implementation of policies to seismic prevention, whose aim is safeguarding the protected artistic assets, requires knowledge, on a different scale, of the risk which existing artefacts are subjected for the seismic safety assessment and design of the interventions of cultural heritage is therefore necessary to reach an adequate knowledge of the structure, in order to identify the characteristics of the elements that determine the structural behaviour. It can be obtained with different levels of details, according to criteria based on the accuracy of the reliefs and historical investigations, in recognition of the use of rules of art, identification of the level and type of damage, ability to reconstruction of the history of the building in relation to seismic events, results of experimental investigations, of

assess the impact of any evidence including weak earthquakes, in the preservation of the building.

The acquisition of a sufficient level of security and protection with respect to seismic risk is guaranteed, for architectural artefacts of historical and artistic interest, considering three limit states: The Limit State of Protection of Life (LPS), in the case of rare and strong intensity earthquakes, and for the Damage Limit State (DLS) for earthquakes less intense but more frequent. In the case in which the artefact analysed has some characteristics in parts of it or localized in defined areas of the same environment such that a reference earthquake with intensity and frequency can cause damage to parts or elements that entail an irretrievable loss to the cultural heritage, it is necessary to define a new specific limit state called Artistic Limit State (ALS). The analysis to the Artistic Limit State is done exclusively at the local level, in the parts of the building that are characterized by elements whose loss would result in irreparable damage to cultural heritage which is, not recoverable with the procedures and methods of conservation.

A significant attention has been aimed at investigating the seismic behaviour of buildings and historical and monumental complex and about methods of restoration, to establish criteria and methods to operate interventions that are respectful of cultural values and at the same time rational and efficient.

## **1.2 MOTIVATION FOR THE RELIABLE PROCEDURES FOR PERFORMANCE ASSESSMENT OF HISTORICAL STRUCTURES IN SEISMIC AREAS**

Heritage Constructions (HC) are exposed to natural and anthropogenic hazards and need a careful consideration from the technical point of view whenever their preservation and protection are concerned. The task is very complex for all the competences involved in the process and above all for structural engineers who must deal with the safety of structure and users.

The high seismic risk and the large number of historical buildings and distributed over the territory make Italy a unique laboratory for the development and testing of innovative procedures for seismic vulnerability assessment of the cultural heritage. Many studies on protection forma seismic risk of cultural heritage have been produced in recent years.

More attention has been expected at investigating the seismic behaviour of artefacts and architectural complexes and methods of restoration, to establish criteria and methods to operate interventions with respect to cultural values and at the same time rational and efficient.

The damage scenarios related to masonry buildings, show that the earthquake does not affect the entire complex severely in total, but the damage would be concentrated to some structural parts and the weakest technological solutions, activating mechanisms that are easily

identifiable and catalogable in many cases. To overcome this problem, an approach based on the concept of the macroelements has been proposed a few years ago and since then repeatedly used to recognize the collapse mechanisms in the different macroelements.

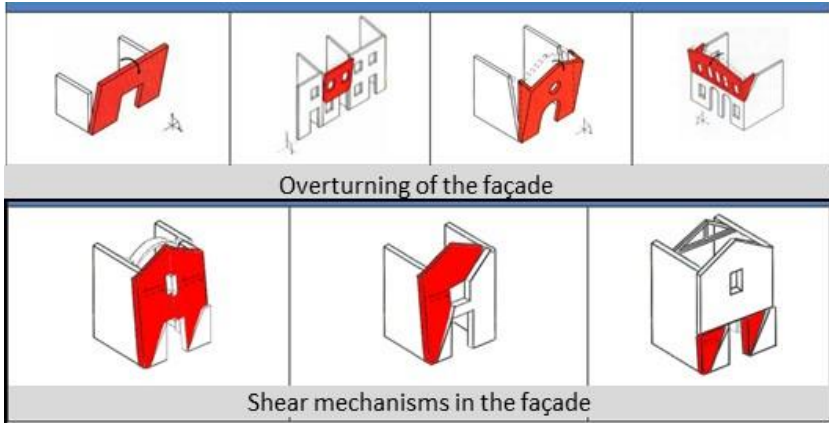


Figure 1.1. Collapse mechanisms

The Architectural heritage are particularly vulnerable to dynamic actions, with a special focus on seismic action. Owing to the age as well as environmental factors, many cultural heritage buildings, as well as structures planned and constructed in the past, are vulnerable to dynamic loads, which may unpredictably induce a collapse of a portion or lead the whole structure to a rapid failure.

The absence of adequate connections between the various parts, irregularities in plan and elevation and presence of flexible floors increase the vulnerability of historical masonry buildings to seismic

actions. The systematic documentation of damage identifies two categories of architectural complexes: The first includes all those structures historically affected by interventions that have led to the presence of significant percentages of stiff floors connected to the masonry. For this class of buildings, the participating mass ratios associated with the fundamental modes are appreciable and thus application of non-linear static analysis methods can be expected easily. The second category consists of structures characterized by very small values of participating mass ratios, suggesting the existence of local vibration modes. In the former case, a global “box-like” behaviour can be observed; whereas in the latter, subdivision of the building into subassemblies of relevant structural elements (macro-elements) that can be extracted and analysed separately from the rest of the complex, and analysis of local mechanisms according to the kinematic approach are recommended. In the literature, there are some approaches employed to analyse the seismic behaviour of masonry building. Accurate simulation of the structure subjected to seismic action should be in principle carried out by means of Non-Linear Dynamic Analysis (NLDA). This means that an exhaustive knowledge of the cyclic response of materials and structural components exists and it can be integrated in the non-linear constitutive laws implemented in dedicated software programs. It is easy to recognize that a similar approach can be unsuitable for general applications, not only due to the high level of complexity of the procedure, but also due

to the need of field investigations aimed at assessing the actual properties of materials and components.

This is the reason why, simplified methodologies of structural analyses have been defined during time. They are based on the application of a distribution of quasi-static forces, which depends on the dynamics of the structure. The structural analysis is carried out in the elastic field (Elastic Static Analysis, ESA). For this reason, it can be reasonably applied to the design of new structures, but it shows some drawbacks and limitations in the analysis of the existing ones.

Another analysis option is the Response Spectrum Analysis (RSA) that, starting from a de-tailed knowledge of the dynamics of the structure, this combines the different contributions of the most relevant modes of vibration to the demand parameters (displacements, forces). The seismic performance assessment is again carried out under the assumptions of elastic response of materials and components and reduced spectral intensities of the seismic action, consider the structural energy dissipation.

In recent years, non-linear static analyses - Push-Over Analyses, POA - have become very popular because of the moderate computational efforts and the possibility to track inelastic phenomena associated to the energy dissipation of the structure. On the analogy with ESA, POA are strictly related to the distribution of inertial forces acting on the structure during the loading process, so that the drawbacks and limitations of the approach are similar to those of the ESA. In particular, both ESA and POA are based on the existence of modes that



dominate the dynamics of the structure, so that the response of the structure under the seismic action basically depends on the same modes.

This is the reason why limitations in terms of participating mass of the fundamental modes are defined for both ESA and POA, and a target cumulative mass participation factor (0.85) is prescribed to modal analysis-based RSA.

The participating mass ratio is a measure of the amount of the total mass participating in the mode of interest: a mode characterized by a large effective mass can be addressed as a significant contributor to the total structural response. It is therefore clear that the dynamics of the structure under consideration for seismic performance assessment, and the nature and characteristics of the local and global constitutive relationships dictate the complexity of the seismic calculations: the more regular the structure from the dynamic standpoint, the simpler the structural analysis would be.

The above concepts are clearly reflected in the seismic codes aimed at providing rules for design and assessment of structures depending on the selected structural system and the associated material for construction. Use of traditional construction materials such as masonry and wood are common in cultural heritage structures, whose structural response also depends on construction techniques.

In addition, fundamental mode shapes do not necessarily characterize the dynamics of the whole structure, so that local mechanisms, for instance out-of-plane overturning of walls, represent the key features

of the structure subjected to seismic actions. The coexistence of local and global mechanisms and their interaction represents one of the most relevant issues in the seismic structural analysis of historical structures.

A general approach to seismic safety assessment should analyse the building within the complex, but this approach requires extensive analyses of the entire architectural complex. As a consequence, an appropriate structural modelling (spatial scale, structural scheme and type of analysis) should start by classifying the investigated building:

1. Structures which tend to an isolated building behaviour;
2. Structures that have a global configuration behaviour;
3. Structures characterized by a complex interaction among the buildings.

In other words, the complex dynamics of historical structures, that depends on many components, in principle can be analysed by dividing the structure in the so-called macro-elements (the basic element of the local analyses) or in structural units, i.e. buildings or assemblage of horizontal and vertical structures that can be extracted and separately analysed from rest of the complex without any loss of significance of the seismic analyses.

The concept is not completely new, since it is a traditional problem in other engineering fields like the mechanical one (De Klerk et al 2008). The most relevant problem in selecting the macro-elements is the lack of operational recommendations in seismic codes, so that sub-assembling is sometimes avoided.

When macro-elements are considered, their identification is usually based on the engineering judgment of the operator without the support of rational tools of analysis

In any case it is easy to recognize the fundamental role of modal analysis, which cannot be disregarded in relation to its complexity. Modern instruments and software packages for the architectural and structural representation are effective options for the analyst, so that detailed modal analyses can be carried out. An effective support to the analysis of historical structures comes from Operational Modal Analysis - OMA - (Rainieri e Fabbrocino 2014) and model updating techniques (Friswell & Mottershead 1995), which have been proved to be valuable tools for indirect non-invasive structural assessment (Rainieri et al 2014, Conte et al 2011). However, an extensive experimental analysis of large architectural complexes is definitely expensive and sometimes infeasible. Nevertheless, some tools traditionally used in the context of experimental modal analysis can be profitably used also to compare the results of purely numerical analyses and check the effectiveness of sub-structuring.

In addition, monuments significantly contribute to the economy of cities and countries by providing key attractions. In this context, structural damage identification at an early stage plays an important role for developing effective and reliable procedures for performance assessment of historical structures in seismic areas (L F Ramos et al., 2010). Damage on masonry structures mainly relates to cracks, foundation settlements, material degradation and displacements.

When cracks occur, they are generally localized, splitting the structures in macroblocks. Dynamic based methods to assess the damage are an attractive tool to this type of structures because they are non-destructive methods and are able to capture the global structural behaviour. Moreover, being motivated by the above reasons, this work aims at exploring damage in masonry structures at an early stage by vibration measurements.

### 1.3 OUTLINE OF THE THESIS

The thesis is organized in seven chapters as follows:

- **Chapter 1** is the introduction to the work, with the motivation, the background, the focus of the thesis, as well as the outline of the thesis;
- **Chapter 2** addresses the state of the art on system identification based on vibration measurements. Secondly presents some remarks on the dynamics of heritage structures. Finally, an overview of experimental substructuring methods is presented;
- **Chapter 3** reviews the main analysis procedures about dynamic based damage identification techniques. The principal algorithm-based methods developed hitherto are described;

- **Chapter 4** presents the numerical study on a well-established vector correlation index frequently used in the field of experimental modal analysis;
- **Chapter 5** performs the validation of the Modal Assurance Criteria (MAC) procedure identification carried out in the context of an isolated masonry building.
- **Chapter 6** describes the experimental campaign carried out on the masonry arch replica. The arch model was built in the laboratory where a controlled damage not recoverable (support movement) was applied. The dynamic response of the system was processed based on the spectral output. Issues addressed are the preliminary numerical model simulations for static and dynamic behaviour of the arch, the description of the static tests series, including the observed damage pattern, the system identification tests on each scenario;
- **Chapter 7** summarizes the main conclusion from each chapter and a proposal for future works.



## Chapter 2

# VIBRATION BASED OF DYNAMIC IDENTIFICATION: BACKGROUND AND OPEN ISSUES

### 2.1 INTRODUCTION

The present chapter is dedicated to description of fundamental theoretical of the system identification based on vibration signatures. Basic notions to approach the topics analysed in the below of the thesis was provides. The chapter deals briefly with the differences between the classical experimental modal analysis approach such as conducted in the MST - and the OMA approach. This chapter introduces the theory of two major methods used in OMA: Frequency Domain Decomposition (FDD) and Stochastic Subspace Identification (SSI). Issues addressed include sensors selection, data acquisition systems and test planning.

## 2.2 BASICS OF DYNAMIC

A preliminary, review about the signals and systems would be definitely useful in the field of experimental dynamics.

The theory notions about signals, systems and structural dynamics and indirectly defines the required cultural background with respect to the Operational Modal Analysis (OMA).

A *signal* is any physical quantity varying with respect to one or more independent variables and associated to information of interest. A *system* converts an input signal into an output signal (Rainieri & Fabbrocino, 2014).

The evaluation of the structural conditions to a given stimulus detects important information about the system. For instance, the analysis under wind load (input signal) and the swinging of a building (output signal) makes possible the identification of dynamic parameters of the structures investigated.

Nevertheless, attention is herein focused on inverse approaches; where the output is known but either the input or the system characteristics are unknown. The attention is focused around the identification of the characteristics of the system when the output signal is known and some assumptions for the input are considered.

The term *noise* refers to any undesired signal superimposed on the signal of interest. Thus, suitable data acquisition strategies must be adopted to reduce the level of noise that necessarily affects measurements.



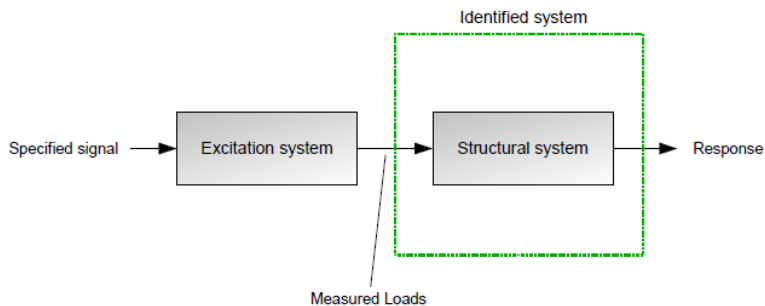


Figure 2.1. System scheme for the Experimental Modal Analysis approach (Benjamin Greiner, 2009)

### 2.2.1 Theory and classical formulation

Structural dynamics theory outlines that an undamped structure with multiple degrees of freedom owns simple harmonic motion without changing the deflected shape, if free vibration is initiated under particular conditions (Chopra, 2001).

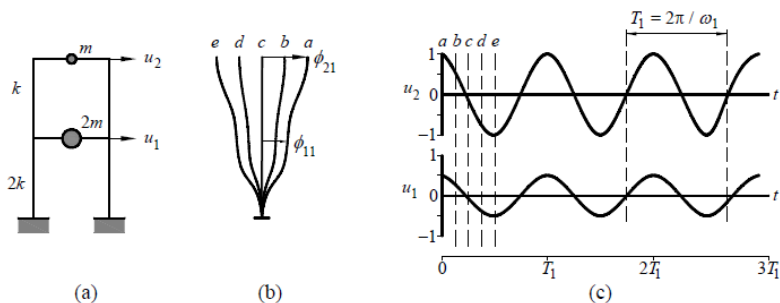


Figure 2.2. Free vibration of an undamped system (Chopra, 2001): (a) system; (b) and (c) different representations of the first natural vibration mode

## Chapter 2 - Vibration based of dynamic identification: background and open issues

---

Whenever the initial static equilibrium position changes- whether by applying external dynamic forces or by imparting some initial displacement -, the structural system starts vibrating with a certain frequency until the mechanisms controlled by the damping and other sources of energy dissipation gradually reduce the amplitude of the motion and cause its decline (Figure 2.2).

Thus, the dynamic response of a structure can be described by three main characteristics of dynamic systems: mode shape, frequency and damping ratio that define the modal properties of the system. However, the main property of a dynamic system from a mechanical and physical point of view are mass and stiffness. Considering the direct interdependence between dynamic and physical properties makes modal-based methods suitable tools for detecting the structural. The important role played by this relationship will be extensively discussed in Chapter 3.

The mathematical methods used to characterize the dynamic behaviour of the systems are: The Classical Formulation, the Steady-State Formulation and Auto-Regressive Models. The attention is focused on the Classical formulation. Main difference between the dynamic and the static analysis is the time dependency of the dynamic approach. In fact, the response of the structure in terms of displacements, velocities, accelerations or internal forces is connected to the accelerations that take place due to inertia forces. The observed free vibration response of a Single-Degree-of-Freedom (SDOF) system

under a set of initial conditions is an example of deterministic data, since it is governed by an explicit mathematical expression depending on the mass and stiffness properties of the system:

$$m\ddot{q}(t) + c\dot{q}(t) + k_e q(t) = p(t) \quad (2.1)$$

where  $m$  is mass of the system,  $c$  is the damping constant,  $k_e$  is the system stiffness and  $p(t)$  is the load vector, which is also time dependant. Here, the time derivates  $\ddot{q}(t)$  and  $\dot{q}(t)$  represent the acceleration and the velocity of the system respectively. When an arbitrary force is acting in the system, the solution of this second order differential equation can be obtained by the Duhamel's integral, valid for linear systems (Chopra, 2001).

Another possibility is to achieve the solution of linear differential equation in the frequency domain, by applying the Fourier transform to the functions on both sides of (2.2). The *Fourier* transform  $X(\omega)$  of a function  $x(t)$  is given by:

$$X(\omega) = \int_{-\infty}^{+\infty} x(t)e^{-\omega t} dt \quad (2.2)$$

where  $j$  is the imaginary number ( $j^2 = -1$ ). As the time derivate of the frequency transform functions are given by the product  $j \omega$  in the frequency domain, Eq.(2.1) can be rewritten as:

$$-m\omega^2 Q(\omega) + cj\omega Q(\omega) + k_e Q(\omega) = P(\omega) \quad (2.3)$$

where,  $P(\omega)$  and  $Q(\omega)$  represent the Fourier transforms of the excitation  $p(t)$  and the response  $q(t)$  respectively.

Solving the Eq. (2.3) with respect to  $Q(\omega)$ , it can be concluded that the response Fourier transform function directly depends on the excitation and on a complex function  $H(\omega)$  equal to:

$$H(\omega) = \frac{Q(\omega)}{P(\omega)} \quad (2.4)$$

Finally, the desired solution  $q(t)$  is given by the inverse Fourier transform of  $Q(\omega)$ , given by:

$$q(t) = \frac{1}{2\pi} \int_{-\infty}^{+\infty} H(\omega) P(\omega) e^{j\omega t} d\omega \quad (2.5)$$

For a system with  $n$  degrees of freedom, the equations of motion are traditionally expressed in time domain, and for general MDOF system, the following set of linear, second order differential equations expressed in matrix form are provided

$$[M]\{\ddot{q}(t)\} + [C]\{\dot{q}(t)\} + [K]\{q(t)\} = \{p(t)\} \quad (2.6)$$

Where  $\{\ddot{q}(t)\}$  is the vector of acceleration;  $\{\dot{q}(t)\}$  is the vector of the velocity and  $\{q(t)\}$  the displacement vector.  $[M]$ ,  $[C]$  and  $[K]$  define the

mass, damping and stiffness matrices, respectively;  $\{p(t)\}$  is the generalized force vector. As a result, the complete solution is obtained by superposition of eigensolutions.

This is a standard formulation of the dynamic problem reported in several structural dynamics and modal analysis books (e.g. Chopra 2001, Ewins 2000, Heylen et al 1998). The matrix differential equation of Equation 4.4 becomes a set of linear algebraic equations by applying the Fourier transform:

$$(-\omega^2[M] + cj\omega[C] + [K])\{Q(\omega)\} = \{P(\omega)\} \quad (2.7)$$

where  $\{Q(\omega)\}$  and  $\{P(\omega)\}$  are the Fourier transforms of  $\{q(t)\}$  and  $\{p(t)\}$ , respectively;  $j$  is the imaginary unit. A linear time-invariant system can be, therefore, represented through its FRF, which is given by the ratio between the Fourier transforms of the output and the input. Finally, the total response of the MDOF system in the original geometric coordinates is obtained by the superposition of all the  $n = (1, 2, \dots, N)$  modal contributions (Figure 2.3).

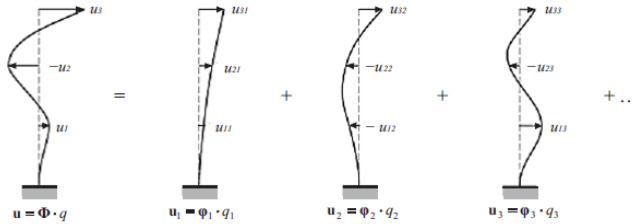


Figure 2.3. Total response as superposition of modal components (Clough & Penzien, 1993)

### 2.3 METHODS FOR OPERATIONAL MODAL ANALYSIS (OMA)

The Operational Modal Analysis (OMA) defines the class of modal identification methods based on response measurements only.

The excitation is either transient (impact hammer testing), random, burst-random or sinusoidal (shaker testing). The advanced signal processing tools used in operational modal analysis techniques allow the inherent properties of a mechanical structure (resonance frequencies, damping ratios, mode patterns) to be determined by only measuring the response of the structure without using an artificial excitation. This technique has been successfully used in civil engineering structures (buildings, bridges, platforms, towers) where the natural excitation of the wind is used to extract modal parameters. This discipline has been systematized in the last two decades but early applications can be traced back to the beginning of modal testing in the Sixties (Rainieri, Fabbrocino, & Cosenza, 2007).

The first applications of OMA were mainly based on the analysis of PSDs and the identification of Operational Deflection Shapes (ODSs). An ODS represents the deflection of a structure at a particular frequency under a generic input and it is usually the result of the contribution of different modes. In early 1990s different number of methods working in time domain were developed as the Natural Excitation Techniques (NExT) and applied in combination with correlation functions, leading to the so-called output-only modal testing. Furthermore, at the end of the Nineties new effective output-only modal identification techniques, such as the Frequency Domain Decomposition (FDD) and the Stochastic Subspace Identification (SSI), became available, overcoming the limitations of the previous techniques in dealing with closely spaced modes and noise. OMA is based on the following assumptions:

- Linearity: the systems response given by the combination of inputs is equal to the same combination of the corresponding outputs;
- Stationarity: the dynamic characteristics of the structure do not change over time; thus, the factors of the differential equations governing the dynamic response of the structure are independent of time;
- Observability: the sensor layout has been defined to see the modes of interest.

## Chapter 2 - Vibration based of dynamic identification: background and open issues

---

The OMA methods can be classified depending on the advantages and limitations related to specific assumptions and data processing procedures. Each criterion points out a specific aspect common to different analysis methods and it is helpful to guide the user towards the choice of the favourite or most appropriate analysis method. The attention is focused on the domain of implementation. In fact, the OMA methods based on the analysis of response time histories or correlation functions are referred to as time domain methods, while the methods based on spectral density functions are referred to as frequency domain methods. The PSD function of the excitation is considered constant.

### **2.3.1 Frequency Domain Decomposition method**

The basic method for output-only modal parameter identification is the Basic Frequency Domain (BFD) method, also known as the Peak-Picking method. The name of the method is given so due to the fact that the modes are identified by picking the peaks in the Power Spectral Density (PSD) plots.

The FDD method, presented by Brincker et al. (2000), can be visualized as an extension of the PP method, which assumes that resonant frequencies are well spaced in frequency and the contribution of other modes in the vicinity of that resonant frequency is null. This method was originally applied to FRFs and known as Complex Mode Indicator Function (CMIF) to point out its ability to detect multiple roots and,



therefore, the possibility to count the number of dominant modes at a certain frequency (Shih et al. 1988). A theoretical formulation of the method is based on the modal expansion of the structural response:

$$\{q(t)\} = [\Phi]\{P(t)\} \quad (2.8)$$

where  $[\Phi]$  is the modal matrix and  $\{P(t)\}$  the vector of modal coordinates. From Eq. (2.8) the correlation matrix of the responses can be computed:

$$[R_{qq}(\tau)] = E[\{q(t + \tau)\}\{q(t)\}^T] = [\Phi][R_{pp}(\tau)][\Phi]^T \quad (2.9)$$

The PSD matrix can be obtained from Equation (2.9) by taking the Fourier transform:

$$[G_{qq}(\omega)] = [\Phi][G_{pp}(\omega)][\Phi]^H \quad (2.10)$$

The PSD matrix of the modal coordinates is diagonal if they are uncorrelated. The superscript H denotes the conjugate transpose and the following relation can be established for the matrix  $\Phi$ .

Considering that the SVD of the PSD matrix at a certain frequency  $\omega$  leads to the following factorization:

$$[G_{qq}(\omega)] = [U][\Sigma][V]^H \quad (2.11)$$

Where  $[U]$  and  $[V]$  are the unitary matrices holding the left and right singular vectors and  $[\Sigma]$  is the matrix of singular values for a

Hermitian and positive definite matrix, such as the PSD matrix, it follows that  $[U] = [V]$  and the decomposition of Equation (2.11) can be rewritten as:

$$[G_{qq}(\omega)] = [U][\Sigma][U]^H \quad (2.12)$$

The comparison between Equation (2.10) and Equation (2.12) suggests that it is possible to identify a one-to-one relationship between singular vectors and mode shapes; moreover, the singular values are related to the modal responses and they can be used to define the spectra of equivalent SDOF systems characterized by the same modal parameters as the modes contributing to the response of the MDOF system under investigation. Assuming that only one mode is dominant at the frequency  $\omega$ , and that the selected frequency is associated to the peak of resonance of the  $k^{\text{th}}$  mode, the PSD matrix approximates to a rank one matrix with only one term on the right side of Eq. (2.10):

$$[G_{qq}(\omega)] = \{u_1\}\{u_1\}^H, \quad \omega \rightarrow \omega_k \quad (2.13)$$

In this contest, the first singular vector  $\{u_1\}$  represents an estimate of the mode shape of the  $k^{\text{th}}$  mode and the corresponding singular value  $\sigma_1$  belongs to the auto PSD function of the equivalent SDOF system corresponding to the mode of interest. The FDD method was improved by Brincker et al. (2001) with the Enhanced FDD (EFDD) method. Basically, the first step of the EFDD is equal to the FDD

method but the estimation of frequency values and damping coefficients are calculated by the application of inverse FFT of each spectral density function for each mode shape.

The comparison of the mode shape estimates  $\{\widehat{\phi}_k\}$  peak with the singular vectors associated to the frequency lines around the peak leads to the identification of the singular values whose singular vectors show a correlation with  $\{\widehat{\phi}_k\}$  higher than a user-defined threshold.

The Modal Assurance Criterion (MAC) is used as a measure of the correlation between two modal vectors. (Allemang and Brown 1982).

Details are shown in the following section.

### **2.3.2 Stochastic Subspace Identification Method**

The time domain methods and, in particular, the Stochastic Subspace Identification (SSI) method (Figure 2.4) deals directly with time series processing (DD-SSI), driven stochastic subspace identification).

The Data-Driven Stochastic Subspace Identification (DD-SSI) method allows the estimation of the states directly from the experimental data by applying robust numerical techniques, such as SVD and QR decomposition (Rainieri & Fabbrocino, 2014).

On the other hand, the implementation is not as friendly as the FDD method, and more processing time is needed during parameter estimation. The mathematical model has parameters that can be adjusted to minimise the deviation between the predicted system response and the measured system response.

## Chapter 2 - Vibration based of dynamic identification: background and open issues

---

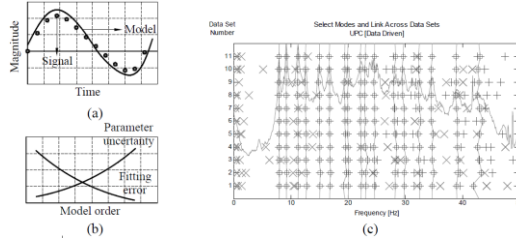


Figure 2.4. Stochastic Subspace Identification method: (a) model calibration; (b) model parameter estimation dilemma; and (c) data driven with the poles selection through the several test setups (Ramos 2007)

The main objective of the SSI method is the identification of the state matrix  $A$  and the output matrix  $C$ , see Eq.(2.38), which contain the information about the resonant frequencies, mode shapes vectors and damping coefficients.

$$X_{k+1} = Ax_k + w_k \quad (2.14)$$

$$y_k = Cx_k + v_k$$

where  $w_k$  is defined as the process noise resulted from input perturbations and modelling inaccuracy and  $v_k$  is measured noise due to transducers and data acquisition disturbances. For further reading about State-Space Formulation, the reader is referred to Peeters (2000). The DD-SSI method as well as the FDD method are implemented, in the software ARTeMIS (SVS, 2018) that has been used in the applications described below.

## **2.4 SOME REMARKS ON THE DYNAMICS OF HERITAGE STRUCTURES**

The experimental modal analysis is more importance as a valuable tool for the execution of accurate structural analysis, and to obtain useful information in the assessment of the structural behaviour of existing buildings. In this context, the purpose of the monitoring does not consist only the identification of sudden or progressive damages, but also evaluating their performance under operational conditions or during some particular environmental conditions such as earthquakes. The use of dynamic identification techniques and monitoring systems is increasingly common tools in the structural analysis. The indirect and non-destructive assessment is suitable for historical buildings and monuments; in line with the principles of conservation and protection of the architectural heritage and to identify the dynamic response of the structure (fundamental natural frequencies, mode shapes and damping coefficients). The experimental identification tests combined with the numerical investigations can be considered as effective tools for the knowledge path of the historical buildings. In this framework, the objective of the dynamic tests in operational conditions is the reduction of the modelling uncertainties, in terms of the mechanical properties and which supports the setting of a reliable numerical model. In the case of historical structures, more attention on the opportunities provided by Operational Modal Analysis (OMA) is paid recently. OMA can be defined as the modal testing procedure that

## Chapter 2 - Vibration based of dynamic identification: background and open issues

---

allows the experimental estimation of the modal parameters of the structure from measurements of the ambient vibration response only. The idea behind OMA is to take benefit of the natural and freely available excitation due to operational loads and ambient forces (wind, traffic, micro-tremors, etc.) to replace the artificial excitation. In this context, OMA is very attractive because tests are cheap and fast when compared with the EMA procedures, and the benefit is that the test are easily conducted even in the operational condition of the structure.

Moreover, the identified modal parameters are representative of the actual behaviour of the structure in its operational conditions as, they refer to the levels of vibrations. On the other hand, the main limit of the application is identified by a low ratio between signal and noise, thus, requires very sensitive, low-noise sensors and a high-performance measurement chain. The OMA procedures as well as the EMA allow to evaluate the structural dynamic parameter as: natural frequencies, vibration modes and damping ratios. However, the random and not measured input in OMA, does not allow to define the effective modal mass corresponding to the principal modal shapes. For this reason, the numerical models and sensitivity analyses, can support the assessment of the adequacy of a measurement chain for the specific OMA application, in terms of frequencies and mass distribution representative of the real structure.

During the last few years a large effort in the development of experimental and numerical studies on reinforced-concrete structures

is observed, which highlights the potential of this investigation tools. Details, and more advanced procedures can be found in the literature as well as in the recent design codes and guidelines (e.g. Eurocode 8, NTC 2018). While in the case of heritage structures, adopting proceedings for preserving a heritage demand a deeper knowledge on the structural behaviour due to heterogeneity and complexity of their structural systems. In this case, its characteristics are mostly provided by case-by-case approaches; often with repeated dynamic tests and structural health monitoring (SHM) schemes. Recent reports have elaborated some simplified dynamic monitoring procedures for different structural typology such as Churches, Towers and Palaces (Boscato et al. 2016).

A possible classification of the structures as per the function of the dynamic parameters is particularly difficult for the historical masonry structures. The uncertainties such as the geometry, structural details, unique configurations, heterogeneity of the material, and the plano-volumetric irregularities make this evaluation a complex task. However, Modern instruments and software packages for the architectural and structural representation, are effective options to assist the assessment process of Architectural Complex (AC). The FE modal analysis applications show the possibility to identify the main characteristics of the dynamic response. The modal parameter estimates provided by FE models are often not fully reliable, due to inaccuracies related to discretization and model setting. As a result, the

numerical model is typically not representative of the actual dynamic behaviour of the structure and a correction is needed to make it more adherent to the experimental observations as describe above. An interesting contribution as reported by Boscato et al. (2016) that comprises several numerical analyses to highlights a possible classification for different structural typology as a function of frequencies and modal mass participating, it was readapted as shown in Figure 2.5 and Figure 2.6. The comparison of the numerical data of the main modal shapes in each case, in terms of frequency and the effective modal mass, allows the definition of the main dynamic response and the relative parameters for the all typology investigated. Through the processing of this data, it was possible to remarks some important aspect which can support effective and reliable procedures for performance assessment of historical structures in seismic areas. In the case of churches (Figure 2.5a) the greater percentage of the effective modal mass is in correspondence to the longitudinal modes (10% 50%) is, related to the response in the plan (Y-direction). The other considerable percentage, below the 10% of effective modal mass, is related to the response that involves the macro elements in the out-of-plane direction (X-direction). The results underline the local behavioural amplitude of this structural typology also if we refer the total modes contribution evaluated (Figure 2.5b,c,d).



## Chapter 2 - Vibration based of dynamic identification: background and open issues

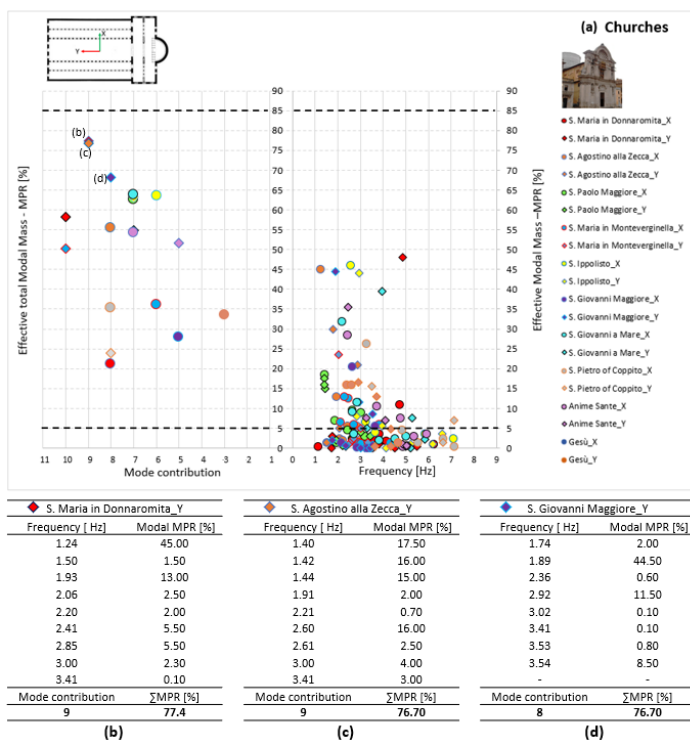


Figure 2.5. a) Distribution of the main modal shapes of some churches in the field of frequency and active modal mass participating; Mode contribution in terms of mass participating : b) S. Maria in Donnaromita, c) S. Agostino alla Zecca, d) S. Giovanni Maggiore. Adapted to Boscato et al 2016

In the case of palaces and masonry building that present as structural aggregates (Figure 2.6), the high participating mass dispersion, already current in the first modes, can be associated with the marked local behaviour of such particular structural typologies.

## Chapter 2 - Vibration based of dynamic identification: background and open issues

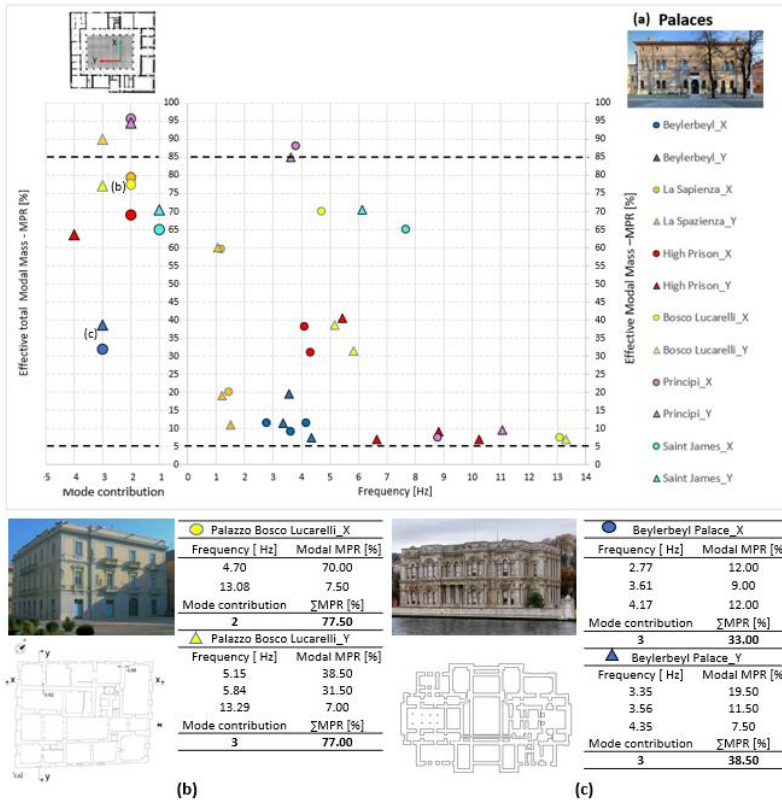


Figure 2.6. a) Distribution of the main modal shapes of some palaces in the field of frequency and active modal mass participating; Mode contribution in terms of participating mass; b) Palazzo Bosco Lucarelli; c) Beylerbeyi Palace. (Adapted from Boscato et al 2016)

Therefore, the evaluation of global dynamic response in such cases demands consideration of the contribution of the higher modes.

In addition, fundamental modal shapes do not necessarily characterize the dynamics of the whole structure, so that local mechanisms, for instance out-of-plane overturning of walls, can represent the key features of the structure subjected to seismic actions. The coexistence of local and global mechanisms and their interaction represents one of the most relevant issues for the architectural complex (AC).

In fact, in the case of the structural complex (Figure 2.6c), for the structural unit (SU) or the AC, existence of overall dynamic response associated with the SU and the its interactions with the other structural units should be considered (Aras, Krstevska et al. 2011). In fact, in the case of the structural complex, for the structural unit (SU) or the AC, existence of overall dynamic response associated with the SU and the its interactions with the other structural units should be considered. Interactions in such case essentially depend on the types of connections among the different parts and the state of conservations of such connections. Nevertheless, it is interesting to note that a meaningful relationship between the local mode and the activation of the local mechanism can be observed.

On the contrary, the masonry buildings which, for the geometry, the structural details and the horizontal diaphragms, present a marked "box" behaviour (Figure 2.6b), the first two modal shapes can be representative of the global dynamic behaviour of the structure (translational mode in X and Y direction), with a high participating mass ratio respectively (greater than 85%). The possibility of suffering

## Chapter 2 - Vibration based of dynamic identification: background and open issues

local seismic mechanisms involve only a fraction of the total mass. In this case a global scale approach is appropriate in the field of seismic assessment (Ceroni, Pecce et al. 2012). For the buildings with predominantly vertical development, the first two modes are characterized by coupling the flexural modes associated with frequencies ranging 0.6 to 1.5 Hz. The third mode is typically torsional mode with a low percentage of participating mass, which is often connected with the local damages. In existing literature, for the towers, there are some approaches employed to classify the dynamic behaviour with respect to different parameters such as: slenderness of the structure; type of connection between the masonry walls; the presence of low annexes that are able to provide a meaningful horizontal constraint, among others (Figure 2.7).

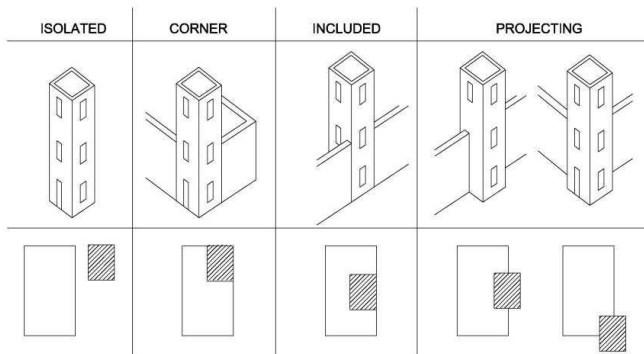


Figure 2.7. Different structural configuration of Bell Tower

## Chapter 2 - Vibration based of dynamic identification: background and open issues

The reliable connection as the high slenderness, for example, guarantees a cantilever beam behaviour with a stiffness that involves the whole section in plan. In this framework also the linear models, with the owed cautions, can provide useful and reliable information about the dynamic analysis of towers, particularly of the modal analysis.

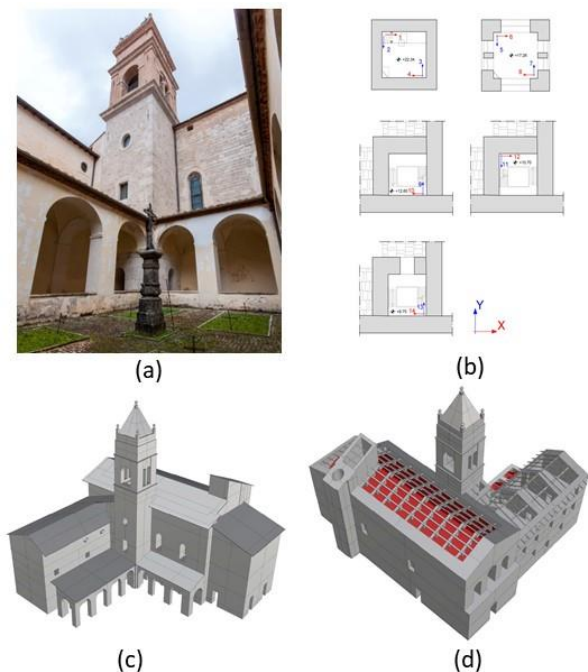


Figure 2.8. a) Bell Tower view of the San Bartolomeo church; b) layout of the sensor at each floor; c-d) 3D model of the church aggregate

## Chapter 2 - Vibration based of dynamic identification: background and open issues

---

This topic is discussed with reference to the case study of the Bell Tower of the San Bartolomeo church (Figure 2.8), one of the AC inside the Carthusian Monastery (Certosa) of Trisulti in Collepardo (Frosinone). In this context, ambient vibrations tests were carried out to provided reference values of the modal parameters useful for the validation of the numerical FEM model and to consider the influence of the annex interaction (the interested reader can refer to Fanelli (2014) for a more complete discussion about the refinement of the numerical model of the church and the dynamic tests on the bell-tower).

The results of the sensitivity analysis, aimed to consider the uncertainties of the artefact (mechanical properties of masonry, structural details, connection between the walls, presence of lower nearby structures acting such as horizontal restraints), show again a high participating mass distribution for the first modes that involves the structural masses in the flexural and torsional modes of the Bell Tower with a higher frequency value in comparison with the existing literature for the presence of annex (Figure 2.9a). Local modes of different macro-elements of the AC are recorded below 10% of participating mass.

The analysis underlines that it is useful in determining the accuracy of dynamic response, considering all the modes characterized by a Participating Mass Ratio (PMR) greater than 5% or, alternatively, a number of modes characterized by a total PMR grate than 85%. This

rule provides also a guide to select the number modes to be considered in model refinement.

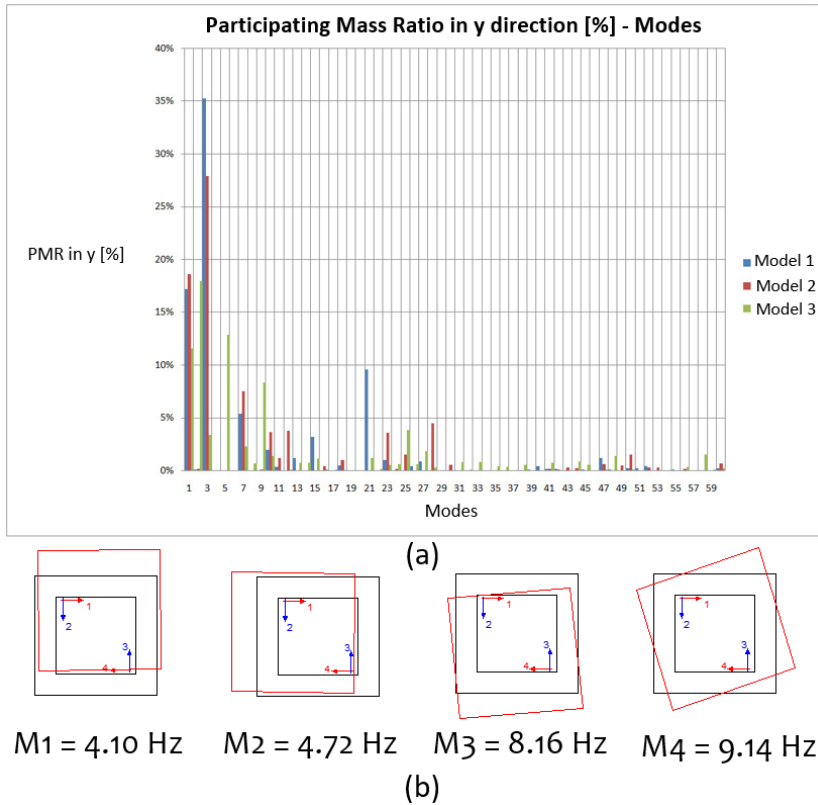


Figure 2.9. a) Graph of PMR in y [%]; b) experimental mode and frequency values of the Bell Tower

Other important aspect, that should not be underestimate in the dynamic tests, is the influence of the pre-existing damage. For the

## Chapter 2 - Vibration based of dynamic identification: background and open issues

---

historical masonry structures, the damage is often represented by an extensively propagated crack patterns, slow deterioration and degradation of the materials, and other phenomena that can change the original characteristics/capacity of the structural materials.

As discussed previously, the modal parameters are evaluated on a linear elastic model, thus, in the case of ultimate resistance condition of the materials, their reliability in the assessment is often limited.

The case study presented for the masonry Tower of the Osservatorio Vesuviano (<http://www.ov.ingv.it/ov/it/museo/sede-storica.html>) located in Ercolano (Napoli), it is particularly interesting in this perspective. The experimental tests were performed by the team of S2X s.r.l, spin-off company of the University of Molise, in the context of the structural assessment of the structure, under the responsibility of Pro. Maria Rosaria Pecce from the University of Sannio.

The Output-only modal identification tests were made to obtain information regarding the local flexural modes (out-of-plane) and global modes of the tower under operational conditions. The figure below shows the sensors layout for the vibration tests. Due to particular state of the damage of the tower (

Figure 2.11. a) Damage survey of the Osservatorio Vesuviano Tower; b) damage detail on vaulted

), it is difficult to assess the occurrence of the global modes. However, to underline as expected, the potential activation of local mechanisms.



## Chapter 2 - Vibration based of dynamic identification: background and open issues

The only value of frequency and damping obtained by sufficient consistency from the different records, is related to the individual response of each walls.

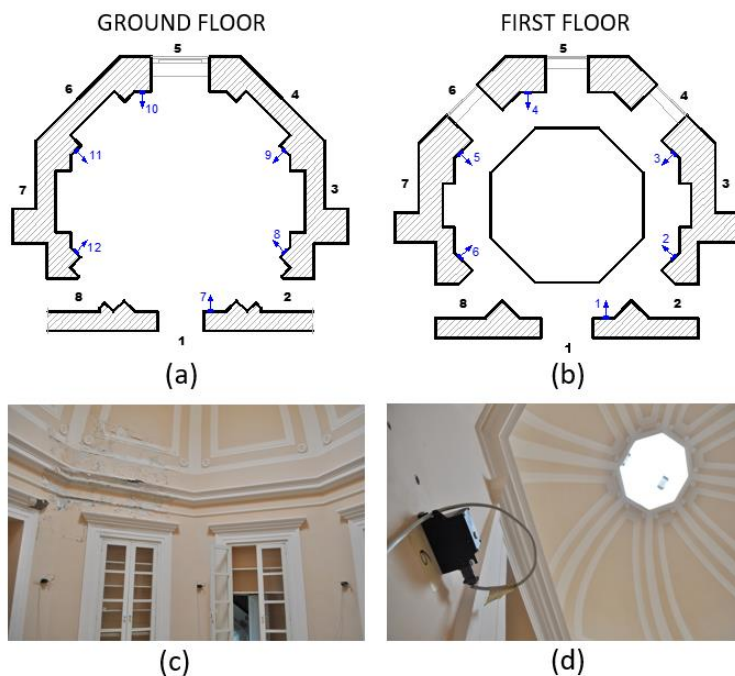


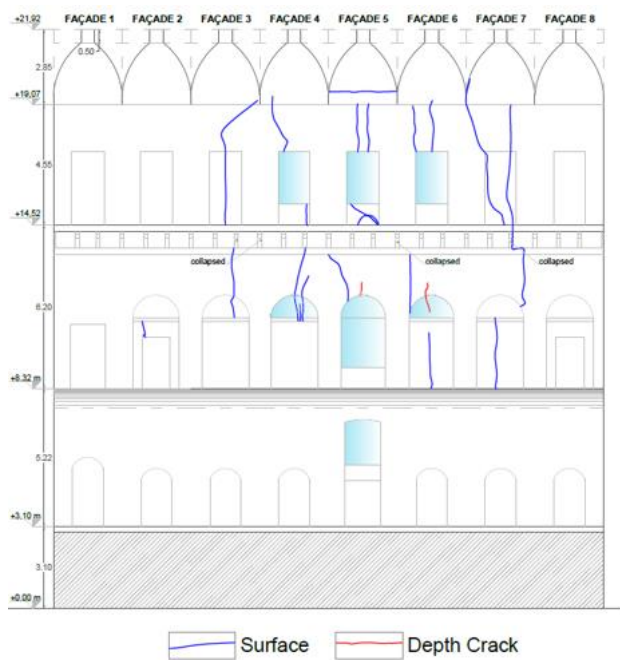
Figure 2.10. Layout of the accelerometers at each floor of the Tower

Natural frequencies and damping ratios are summarized in Table 2.1.

Mode	$f$ [Hz]	$\xi$ [%]
I	3.29	9.7

Table 2.1. Experimental values

## Chapter 2 - Vibration based of dynamic identification: background and open issues



(a)



(b)

Figure 2.11. a) Damage survey of the Osservatorio Vesuviano Tower; b) damage detail on vaulted

This frequency is also a unique value connected with a higher coherence (close to unity). In order to remark the uncertainty and difficulty in the data processing, it is worth noting that the damping values associated with the three peak frequencies ( candidates to represent the possible structural modes) identify in the frequency range 0-10 Hz; they are in the order of 5-10%. One of the possible causes can be related with a non-linear response of the structure already for low vibration levels.

The cases illustrated above provide important indications, confirming the need of developing effective and reliable procedures for performance assessment of historical structures in seismic areas.

The main aspects emerged in the different cases analysed show potentiality and limit of the dynamic identification techniques of existing structures.

The dynamic response of the AC or parts of that (SU), can be defined by the dynamic behaviour of the structure. Further possibility is to combine the numerical and experimental results in order to relate the obtained mode shapes with the global or local mechanisms expected.

The theme certainly provides great interest points, highlighting great innovation elements , which require to continue both experimental and methodological research.

## **2.5 AN OVERVIEW OF EXPERIMENTAL**

### **SUBSTRUCTURING TECHNIQUES**

Seismic prevention requires the definition of appropriate analysis procedures to deal with the several uncertainties related to design of interventions in architectural heritage. Some of those uncertainties stem from the unique structural schemes, the aging of materials and hidden damage or defects. Thus, developing reliable numerical models for seismic assessment of architectural heritage is definitely challenging. One of the most investigated tasks concerns the discrimination between global behaviour and local response of the architectural complex. However, the structural models commonly used in the civil engineering are often incapable of predicting these local dynamic effects and their interaction with the global dynamics effects due to their geometric simplification. Therefore, a need exists for more detailed structural dynamic analysis tools, without losing versatility and generality. The dynamic substructuring approach shows great potential for use in different fields, such as wind turbine engineering, aerospace engineering, automotive engineering, industrial machinery. Dynamic substructuring is a method to obtain the structural dynamic behaviour of complex structures by dividing them into some, smaller structural units (or simpler substructures) of which the dynamic behaviour is easier to evaluate. By using component model reduction techniques, the number of degrees of freedom (DOF) of the substructure models are significantly reduced.

---

An accurate and compact set of equations of motion describing the global dynamic behaviour is obtained after assembly of these component models.

### **2.5.1 The substructuring approach to dynamic analysis**

The dynamics behaviour of the global structure is obtained by assembling the dynamic models of the components. The development of this technique came two decades after the simulation concept developed from the theoretical basis established by the fine element method (FEM), which can be connected with the publication of a set of scientific papers by Hrennikoff (1941) and Courant (1943). The method is developed for analysing complex structural systems through interconnected components for the first time. The displacement is expressed in generalized coordinates, that are defined by displacement modes. The scientific pillars of the finite element model reduction and dynamic substructuring can be traced back to the works of Hurty (1960) and Gladwell (1964); this method became known as Component Mode Synthesis (CMS) back then. Others fundamental contributions, following the CSM methods, were introduced soon after: Craig and Bampton in 1968, Mac Neal in 1971 and Rubin in 1975. The potential of the Dynamic substructuring (DS) appeared very quickly in the structural dynamic analysis and gained importance rapidly in the engineering field. The enhancement of analysis techniques and the increase of computational capabilities of measurement software

## Chapter 2 - Vibration based of dynamic identification: background and open issues

---

programs, allowed the use of the measurements in the substructuring analyses. From the 1980's onwards, DS appeared to be a very common tools in the assessment of structural dynamic behaviour, and experimental substructuring caught the attention of the researchers. (e.g. D. de Klerk et. al, 2006).

The substructuring method applied to dynamic analysis allows to divide a complex problem into several smaller and simpler substructures in order to find a solution. Moreover, the numerical substructure models can be combined with the experimental measurements, in order to calibrate and validate the adopted assumptions for the global structural assessment. The main issue in setting the numerical model is related to the definition of the boundary conditions, since, the structural unit is not isolated. In this framework, it is possible to consider two domains in which dynamic substructuring can be applied:

- The time domain, where the structural properties in terms of mass, stiffness and damping are used.
- The frequency domain where frequency response functions (FRFs) of the macroelements are assembled.

In addition, inside the time domain one can identify two different methods:

- The "Physical" substructures, where one describes the structural units considering geometric distributions of mass,

damping and stiffness in terms of  $M$ ,  $C$  and  $K$  matrices respectively and the associated displacement ( $u$ ). The equations of motion for the substructure  $s$  in the global structure are computed as:

$$M^{(s)}\ddot{u}^{(s)} + C^{(s)}\dot{u}^{(s)} + K^{(s)}u^{(s)} = p^{(s)} + g^{(s)} \quad (2.15)$$

Where  $p^{(s)}$  are the applied external forces and  $g^{(s)}$  are the connecting forces between the interface

- The "modal" substructures are described in terms of generalized mass, damping and stiffness matrices with the associated set of generalized DOF ( $q$ ). In this case the equation of motion is given by:

$$\tilde{M}^{(s)}\ddot{q}^{(s)} + \tilde{C}^{(s)}\dot{q}^{(s)} + \tilde{K}^{(s)}q^{(s)} = \tilde{p}^{(s)} + \tilde{g}^{(s)} \quad (2.16)$$

In such situation is possible identify two different interfaces, the first where the remains displacements of the interface in the new set of DOF:

$$q = \begin{bmatrix} \eta \\ u_b \end{bmatrix} \quad (2.17.)$$

and the second where all physical DOF are lost and the new set of DOF contains only modal amplitudes and interface forces:

$$q = \begin{bmatrix} \eta \\ g_b \end{bmatrix} \quad (2.18.)$$

This can deliver three possible assembly cases :

**1 - Displacements method** (Figure 2.12), where combine the interface displacements ( $u_b \leftrightarrow u_b$ ). In this case the components have the original set of interfaces DOF ( $u_b$ ). The compatibility condition, given that the interface DOF are defined in terms of displacements, can be satisfied by assembling the interface displacements between the interface. To comply the equilibrium conditions, an additional interface force field ( $g_b$ ) is considered.

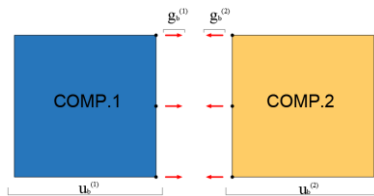


Figure 2.12. Assembly using interface displacements (adapted from van der Valk. 2010)

**2 - Forces methods**), where interface forces can be combined ( $g_b \leftrightarrow g_b$ ). Here the assembling substructures is that both sets of interface DOF consist of only interface forces ( $g^{(s)}_b$ ) as show in the Figure 2.13. In this case the equilibrium condition can be satisfied by assembling the interface forces ( $g_b$ ) between the interface. For the compatibility



conditions, another equation in terms of interface displacements ( $u^{(s)}_b$ ) is considered.

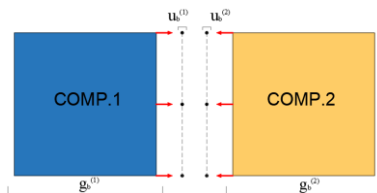


Figure 2.13. Assembly using interface forces (adapted from van der Valk. 2010)

3 - Mixed method, where combine interface displacements to interface forces ( $u_b \leftrightarrow g_b$ ). The procedure combines the first two methods shown above. In this context, since both interface DOF describe different physical quantities, it is not possible merge directly both structural components. In Figure 2.14 for the component 1, the interface DOF are in terms of displacements and for the component 2 are in terms of forces.

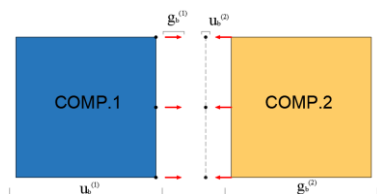


Figure 2.14. Mixed interface method (adapted from van der Valk. 2010)

Thus, to satisfy the equilibrium condition an additional interface force set is introduced for the component 1. While, to satisfy the compatibility

conditions, an additional interface displacement sets are considered for the component 2. In such a context the equations 2.15 and 2.16 gives a set of equations.

$$\begin{cases} M^{(1)}\ddot{u}^{(1)} + C^{(1)}\dot{u}^{(1)} + K^{(1)}u^{(1)} = p^{(1)} + g^{(1)} \\ \tilde{M}^{(2)}\ddot{q}^{(2)} + \tilde{C}^{(2)}\dot{q}^{(2)} + \tilde{K}^{(2)}q^{(2)} = \tilde{p}^{(2)} + \tilde{g}^{(2)} \end{cases} \quad (2.19)$$

The subscript  $b$  denotes coupling (boundary) degrees of freedom.

These methods are also applicable to structures with light damping. Independently of whether components are defined in the frequency or time domain, two important conditions must be satisfied when assembling the components:

1. Compatibility condition: where the interface displacements of both sets must be the same.
2. Equilibrium condition: the internal forces between the interface must be equal in magnitude and opposite in direction, to satisfy the equilibrium.

More details of assembly and reduce methods can be found in the M.Sc. thesis of P.L.C van der Valk (2010).

### **2.5.2 The Modal Assurance Criterion (MAC) in the dynamic substructuring**

As a result of the reduction and assembly procedures described in the previous sections, the assembled system is obtained. There are numerous analyses one can perform on this assembled system, one of

this is developed to identify which substructure modes are dominant in the global dynamic behaviour. This allows to identify eventually the correlation between modes; through the MAC method (which will be described in section 2.5.3) that compare for instance, the experimental results obtained with the numerical models. In the field of dynamic substructuring, from the MAC method derives the Substructure Modal Assurance Criterion (SUMAC) presented in the section 2.5.4.

### 2.5.3 Modal Assurance Criterion (MAC)

The Modal Assurance Criterion (Allemang and Brown 1982) is a vector correlation index frequently used in experimental dynamics to quantify the similarity of mode shapes represents the most popular index to quantify the correlation between mode shapes, but it also shows some limitations, for instance the experimentally estimated mode shapes. Given two mode shape vectors under comparison, the experimentally estimated mode shape  $\{\hat{f}_i\}$  and the numerically predicted mode shape  $\{\hat{f}_j\}$ , the MAC is computed as follows

$$MAC(\{\Phi_i\}; \{\Phi_j\}) = \frac{|\{\Phi_i\}^T \{\Phi_j\}|^2}{(\{\Phi_i\}^T \{\Phi_j\})(\{\Phi_j\}^T \{\Phi_i\})} \quad (2.20)$$

The MAC index is basically a squared, linear regression correlation coefficient which provides a measure of the consistency (degree of linearity) between the two vectors under comparison. The MAC values

are bounded between 0 and 1, representing inconsistent and perfectly consistent correspondence between the two vectors, respectively.

Even if the MAC between analytical and experimental mode shapes is generally used for verification and updating of finite element models, it is worth noting that it provides only a measure of consistency between the vectors but it does not ensure validity. For instance, when the experimental mode shapes are measured at few locations, the incomplete information can lead to a MAC value near unity with the corresponding analytical mode shape, but the consistency between the two vectors does not ensure that the analytical mode shape is correct.

#### 2.5.4 Substructure Modal Assurance Criterion (SUMAC)

As described in the previous sections, The MAC approach, is a well know method to compute the correlation between modes (i.e. numerical and experimental results). This method can be also a valid tool to understand the correlation between the substructure modes (reduction method) and the global system modes. When the mode shapes under comparison are the part of the global mode shape  $\Phi^{(s)}_g$  that acts on the DOF of substructure, and the local mode shape  $\Phi^{(s)}_i$  of the substructure (uncoupled); the MAC equation can be rewritten as follows:

$$SUMAC = \frac{|\{\Phi^{(s)}_g\}^T \{\Phi^{(s)}_g\}|^2}{(\{\Phi^{(s)}_i\}^T \{\Phi^{(s)}_j\}) (\{\Phi^{(s)}_j\}^T \{\Phi^{(s)}_i\})} \quad (2.21)$$

$\Phi^{(s)}_g$  is extracted by localization of the global mode shape  $\Phi_g$  using the Boolean matrix L as follow:

$$L\phi_g = \begin{bmatrix} \phi_g^{(1)} \\ \phi_g^{(2)} \\ \vdots \\ \phi_g^{(n)} \end{bmatrix} \quad (2.22)$$

Through this formulation, the participation of certain component to the global mode shape can be calculated and will automatically have the same length as the uncoupled mode shapes of the component. In this way a MAC value is possible to be evaluated using the extracted part from the expanded global mode shape or the uncoupled mode shape. MAC values excess of 0.8÷0.9 are accepted as indicators of high local mode contribution to the global mode shape, while values less than 0.1÷0.2 denote a poor mode contribution to the global mode shape. Moreover, better MAC consistency denotes how the precision of the local mode will have an important influence on the accuracy of the global mode. At the same time eventually, significant errors of the dominant component modes will define significant errors in the global dynamic behaviour. In such a context the SUMAC index can be seen as a valid tool in the definition of the substructure modes which are dominant in the global dynamic behaviour.

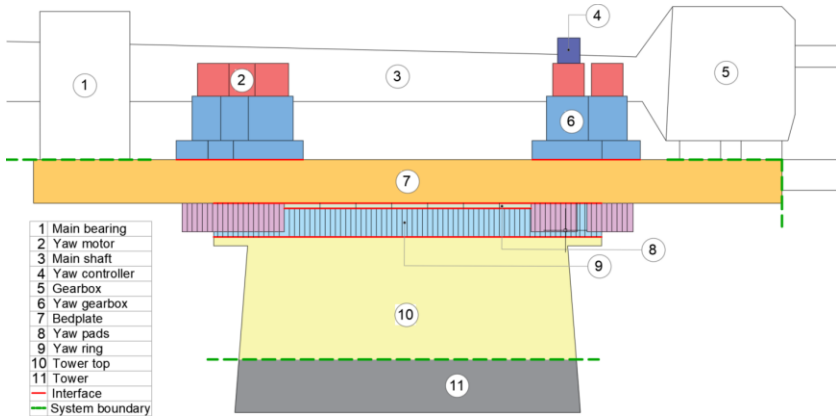


Figure 2.15. Yaw system of a 2.3. MW Siemens wind turbine adapted from P.L.C van der Valk (2010)

Some applications presented in literature, in the field of dynamic substructuring, demonstrate the promising applicative perspectives for this index. In the field of wind turbine systems (Figure 2.15), different DS analysis are proposed using the component models of the yaw system, an important part of these modern wind turbine and an interesting case for the different model reduction approach as indicated earlier.

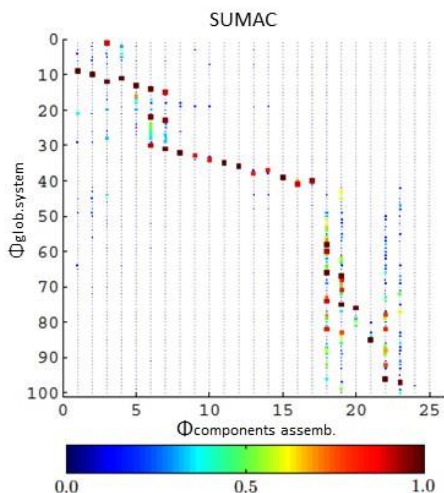


Figure 2.16. SUMAC of the models from the total assembly and he modes of the component assembly adapted from van der Valk (2010)

In this framework, the SUMAC index is computed using the modes of the global yaw system and modes of the assembly components. The Figure 2.16 shows the SUMAC matrix correlation between the global mode shapes and the mode shapes of the components assembly. In particular visualize the effects on the mode shapes , caused by mounting the yaw gearboxes onto the bedplate.

The highs values of the SUMAC matrix, defined with red blocks, denote a high correlation between the component and the other part (For instance, mode 14 define an interaction between the gearboxes and the rest of the assembled system). This allow to identify the gearbox modes in the set of global modes.





# Chapter 3

## MODEL UPDATING VS. DAMAGE ASSESSMENT

### 3.1 INTRODUCTION

Protection of architectural heritage requires a deeper analysis of the structures through a path of knowledge—the geometry, the construction details, the material properties—and also with the use of appropriate computational models. The aim is to assess the state of conservation of the structures to detect any critical situations with respect to the exceptional events such as earthquakes and natural hazards, which have seriously affected the cultural heritage in recent years (Boscato et al. 2016). Vibration-based damage identification methods (VBDIMs) supported by continuous structural health monitoring are probably the best tool available to evaluate the structural condition of non-conventional systems and to catch the onset of damage at the earliest possible stage.

The evaluation of the structural conditions is needed to plan cost-effective remedial measures, before the extension of damage leads the systems to stop operation, requiring expensive in-depth interventions.

## **3.2 CLASSIFICATION OF VIBRATION-BASED DAMAGE**

### **IDENTIFICATION METHODS**

The field of damage identification is very broad and it contains different analysis depending on the case and the criteria. The first distinction regarding the damage identification methods, is between global and local methods. The classification is based on changes of vibration characteristics of structures, whereas, the latter is based on visual inspections and localized experimental tests.

Another distinction with respect to the effect of damage in these methods can be divided in Linear or Nonlinear depending on which type of behaviour is assumed after the damage occurrence. Linear methods can be further distinguished in modal-based and non-modal-based, depending on whether or not changes in modal parameters are used to infer the damage. A further distinction is between model-based and non-model-based methods. Figure 3.1 summarizes most of the methods present in existing literature. In the following sections, focus is paid on the spectrum drive damage identification method

Further information about Vibration based Method and the related tests are given in M.G. Masciotta (2015)

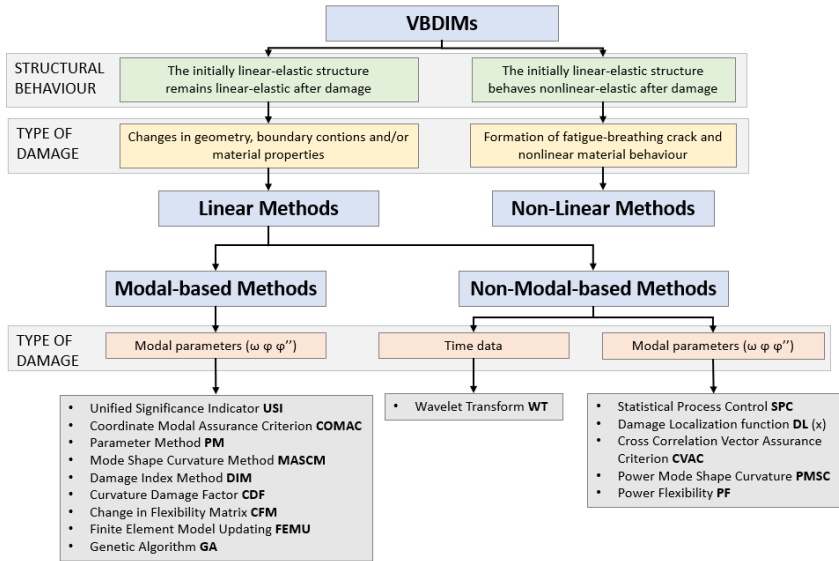


Figure 3.1. Classification of Vibration-based Damage Identification Methods by (M.G. Masciotta, 2015)

### 3.3 SPECTRUM DRIVEN DAMAGE IDENTIFICATION METHOD

The dynamic identification procedures and structural monitoring offer accurate global structural data and above all the dynamic assessment of the actual behaviour of a structure. Use of monitoring systems is progressively common in the structural conservations field, with different purposes, i.e., the evaluation of the dynamic response to assess the structural integrity or to identify the dynamic parameters for model updating procedure. In post-earthquake situations, it is an important method for the identification of damage and for the assessment of the efficacy of the safety intervention.

The main scope of this study is the evaluation of a robust spectral-based algorithm able to detect, locate and assess the structural damage, suitable for both output-only and input-output dynamic identification techniques, independently of the excitation sources, and applicable to any type of structure.

### 3.3.1 Basic theory

In stochastic environment, the response  $X(t)$  of a system to dynamic loading  $F(t)$  can be defined as unidimensional multivariate stochastic vector process whose elements are the time-dependent nodal response processes. In this context, the dynamic characterisation of a given structural system can be performed by the use of normal spectral analysis methods based on the eigenvalue decomposition of the PSD response matrix  $S_x(\omega)$  according to the following equation:

$$S_x(\omega) = \Psi_X(\omega)\Lambda_X(\omega)\Psi_X^H(\omega) \quad (3.1)$$

Where  $\Lambda_X(\omega)$  is a diagonal matrix containing frequency-dependent eigenvalues  $\Lambda_X(\omega) = \text{diag}\{\lambda_1(\omega), \lambda_2(\omega) \dots \dots \lambda_j(\omega), \dots \lambda_i(\omega)\}$  in decreasing order,  $\Psi_X(\omega)$  is a complex matrix including mutually orthogonal eigenvectors as columns and  $\Psi_X^H(\omega)$  denotes the conjugate transpose of  $\Psi_X(\omega)$ . Each eigenvalue  $\lambda_i(\omega)$  is proportional to the energy of a certain vibration mode, whereas each eigenvector  $\psi_i(\omega)$  is a mode shape estimation corresponding to certain eigenvalue.

A complete description of the fundamentals of stochastic dynamics and spectral analysis is not pursued in this study and for this purpose the reader is referred the book (L.H. Yam, Y.J.Yan, Z.Weii, 2004)

The first step of the spectral damage analysis consists in the estimation of the global dynamic properties of the structure under investigation, i.e. frequency and damping coefficient.

In order to upgrade the spectral analysis and move to higher levels of damage identification, coordinate-dependent parameters must be considered in the procedure. For this purpose, the second step of the method involves the analysis of the complex eigenvectors obtained from the PSD matrix decomposition. Each eigenvector mode shape  $\Psi_X(\omega)$  estimation corresponding to a certain eigenvalue, thus it depends on the nodal coordinates of the system and can provide spatial information concerning the damage. The number of eigenvectors equals the rank of the matrix, or rather the number of independent measured DOFs. The comparison between spectral modes belonging to different scenarios may be used to locate the damage, real eigenvalues are combined with complex eigenvectors through the following expression:

$$\Delta_{\Psi} = \sum_{j=1}^n \left\| \left[ \sum_{i=1}^m \left[ \Psi_j^d(\omega_i) \sqrt{\lambda_j^d(\omega_i)} \right] - \left[ \sum_{i=1}^m \left[ \Psi_j^u(\omega_i) \sqrt{\lambda_j^u(\omega_i)} \right] \right] \right\| \quad (3.2)$$

where  $\Psi(\omega)$  denotes the eigenvector;  $\lambda(\omega)$  indicates the corresponding non-zero eigenvalue, m specifies the frequency range, n represents the

### Chapter 3 - Model updating vs. damage assessment

---

mode number and upper scripts d and u stand for damaged and undamaged conditions, respectively.

Basically, the index relies on the difference between spectral modes belonging to different structural conditions. If only a single damage scenario is available, the index is univocally computed by comparing the DS with the RS; whereas in case of multiple damage scenarios, the index can be calculated either by comparing each DS with the RS (absolute index) or by comparing the current DS with the previous DS (relative index). If the aim is to catch the progressive evolution of damage up to the last scenario, a relative comparison between DSs is more appropriate.

## Chapter 4

# A MAC BASED APPROACH: DYNAMIC IDENTIFICATION OF THE STRUCTURAL BEHAVIOUR

### 4.1 THE ROLE OF THE DYNAMIC IDENTIFICATION

#### 4.1.1 Introduction

The problem of the characterization of the reference unit/component for the evaluation of seismic performance of masonry buildings is fully within the approach of the regulatory framework, not only in the case of historic constructions but also in the case of the traditional masonry building stock in many historical sites in the big cities, towns and villages in Italy. It is obvious that historical buildings are integral part of the built environment and thus deserve to be preserved (Lagomarsino & Cattari, 2015).

## Chapter 4 - A MAC based approach: dynamic identification of the structural behaviour

---

Apart from this, the high vulnerability of historic masonry buildings to seismic actions needs to be considered, mainly due to the lack of proper connections between the various structural elements (masonry walls, wooden beams in the floors and wooden beams on the roof). These conditions often lead to overturning collapse of the perimeter walls under seismic excitation. Simplified limit state analysis methods are often used for safety analysis and design of strengthening interventions (Direttiva 2011).

The preservation of the historical city centres in seismic areas, therefore, requires a strategic plan and a suitable methodology that includes a rational approach of multidisciplinary knowledge discrimination between local and global response, therefore, represents a key step in seismic performance assessment of existing buildings, and strongly influences the significance of non-linear static procedures (Cattari, et al. 2015).

In spite of the peculiarities of existing masonry buildings in aggregates, National and International codes and guidelines do not provide exhaustive recommendations to rationally distinguish the local from the global response. The present Chapter investigates the possibility of applying a well-known tool in experimental modal analysis to define the nature of a mode. The proposed procedure is applied to different explanatory case studies, pointing out how the proposed methodology can guide towards the selection of the more appropriate analysis procedure.



#### **4.1.2 Masonry buildings in aggregates**

Aggregate constructions are common in historical city centres throughout the world. It is customary the coexistence of several and subsequent stratifications and modifications, sometimes incongruous and due to multiple factors, too. The progressive transformation of existing urban neighbourhood is synthesized in the aggregate itself. That is the result of an articulated, but not unified, source due to structural alterations, e.g. incremental construction and extensions which are sometimes structurally related to the pre-existing structures, otherwise partially separated by structural joints or adherent walls.

The potential interactions due to the structural contiguity within the aggregates is one of the main factors influencing the seismic response and damage mechanisms.

Design codes do not exhaustively define the analysis approach to use in these cases. Moreover, in the literature several papers addressed these issues aiming at assessing the response of masonry building aggregates. For instance, some Authors (Luigia Binda & Saisi, 2005) proposed a general methodology for seismic vulnerability assessment and protection of historical masonry buildings based on state-of-the-art research carried out in Italy in the field of cultural heritage restoration and conservation.

A general approach to seismic safety assessment should analyse the building within the aggregate, but this approach requires extensive analyses of the entire architectural complex. As a consequence, an

## Chapter 4 - A MAC based approach: dynamic identification of the structural behaviour

appropriate structural modelling (spatial scale, structural scheme and type of analysis) should start by classifying the investigated building into one of the following structural typologies :

- Structures which tend to an isolated building behaviour (Figure 4.1a);
- Structures that have a global configuration behaviour; so, it is reasonable to analyse global as well as local collapse mechanisms considering the potential interactions due to the structural contiguity within the aggregates (Figure 4.1 b);
- Structures characterized by a complex interaction among the buildings, with a meaningful local behaviour and whose overall response can be obtained by evaluating the local collapse mechanisms of all building elements (Figure 4.1c,d).

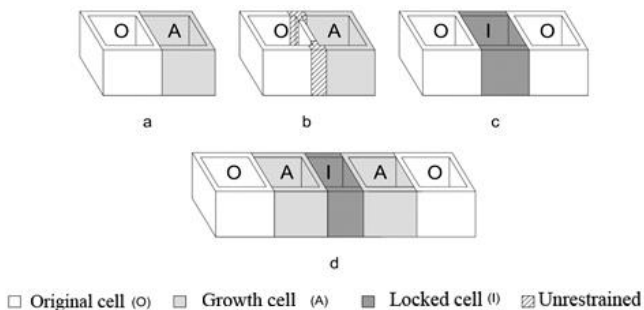


Figure 4.1. Classification of the type of behaviour of the existing masonry building

If the studied structure does not behave as an isolated building, the preliminary analysis should focus on those unique features that are peculiar of the aggregate itself, as suggested by (Carocci, 2012).

Eventual interactions between various structural units have to be identified. The first stage of analysis relies on information about the aggregation processes, layout of voids, alignments of façades with the pathways of roads, extensions, rotations, intersections, sliding of the axes of the original walls and filled wall cells, the position of the plots in the tiles, disassembly and tapering of walls in order to determine weak areas in the stress transmission path (NTC 2018). As a second stage of analysis, relevant macro-elements have to be identified based on some insight in the static and dynamic behaviour of the building. This can be achieved by either very complex numerical approaches (Luis F. Ramos & Lourenço, 2004) or experimental dynamic tests (Augusti et al. 2001).

Seismic analysis of structures can be carried out according to different methodologies either in the linear or in the non-linear field ( Elnashai and Di Sarno 2015). Simplified methodologies of structural analysis based on the application of a distribution of quasi-static forces, which depends on the dynamics of the structure, can be also used in this case. The structural analysis is carried out in the elastic field (Elastic Static Analysis, ESA), so it can be reasonably applied to the design of new structures, but it has some drawbacks and limitations in the analysis of the existing buildings. Accurate simulation of the seismic response of

## Chapter 4 - A MAC based approach: dynamic identification of the structural behaviour

---

the structure by means of Non-Linear Dynamic Analysis (NLDA) requires an exhaustive knowledge of the cyclic response of materials and structural components that can be integrated in the non-linear constitutive models implemented in analysis codes. It is easy to recognize that such an approach can be unsuitable for general applications, not only due to the high level of the procedure's complexity but also due to the need of field investigations aimed at assessing the actual properties of materials and components.

The Response Spectrum Analysis (RSA) is a linear dynamics method of analysis which measures the contributions of each modes of vibration. Combination of responses of the most relevant modes of vibration allows computing the maximum seismic response of the structure in the elastic field according to a probabilistic combination procedure.

The above considerations remark that the complexity of analyses increases with the complexity of the structure from a geometric and mechanical point of view. Furthermore, irregularities in plan and elevation and presence of flexible floors make the analyses even more challenging: in fact, the structural response is less dependent on the fundamental modes, while local mechanisms may arise.

It is possible to identify two categories of architectural complexes. The first includes all those structures historically affected by interventions that have led to the presence of significant percentages of stiff floors connected to the masonry. For this class of buildings, the participating mass ratios associated with the fundamental modes are appreciable

and not far from the limits for the application of non-linear static analysis methods. The second category consists of structures characterized by very small values of participating mass ratios, suggesting the existence of local vibration modes.

In the former case, a global “box-like” behaviour can be observed; in the latter, subdivision of the building into subassemblies of relevant structural elements (macro-elements) that can be extracted and analysed separately from the rest of the complex, and analysis of local mechanisms according to the kinematic approach are recommended.

An effective support to the analysis of historical structures comes from Operational Modal Analysis – OMA – (Rainieri and Fabbrocino 2014) and model updating techniques (Friswell and Mottershead 1995) which have been proved to be valuable tools for indirect non-invasive structural assessment. However, an extensive experimental analysis of large architectural complexes is definitely expensive and sometimes infeasible. Nevertheless, some tools traditionally used in the context of experimental modal analysis (Boscato et al. 2016) can be profitably used also to compare the results of numerical analyses and check the effectiveness of sub-structuring.

#### **4.1.3 An approach to discriminate global or local mode**

The dynamic sub-structuring concept is not completely new: several applications are already present, mainly in the mechanical field. Application of dynamic sub-structuring can be considered as a viable

## Chapter 4 - A MAC based approach: dynamic identification of the structural behaviour

---

way to obtain the structural dynamic behaviour of a large and complex structure by dividing the structures into smaller parts so that it is easy to determine the behaviour of the whole structure without neglecting the boundary conditions due to the interaction in the sub-parts (De Klerk et al. 2008). The dynamic behaviour of the whole structure is obtained afterwards by assembling the dynamic models of the components. In this scenario, modal analysis plays a fundamental role. the Modal Assurance Criterion – MAC (Allemang & Brown, 1982) can be used to identify local components and subsystems.

The proposed approach to the division in structural units is based on a vector correlation analysis of selected modal displacement fields based on a well-established index for mode shape comparison traditionally used in experimental modal analysis. In particular, it is often used in finite element model updating to evaluate the correlation between experimental and numerical mode shapes (Russo 2013).

From the mathematical viewpoint, given two vectors  $\{f_i\}$  and  $\{f_j\}$ , the MAC is computed as follows:

$$MAC(\{\Phi_i\}; \{\Phi_j\}) = \frac{|\{\Phi_i\}^T \{\Phi_j\}|^2}{(\{\Phi_i\}^T \{\Phi_i\})(\{\Phi_j\}^T \{\Phi_j\})} \quad (4.1)$$

The MAC index represents a squared, linear regression correlation coefficient and it provides a measure of the consistency (degree of linearity) between the two vectors of interest. A scalar value is

Chapter 4 - A MAC based approach: dynamic identification of the structural behaviour

obtained in the closed interval between 0 and 1, where a value of 1 or very close to 1 value indicates correlated mode shapes, whereas a value close to zero means that there is no match between the compared modes (mode shape vectors are almost orthogonal). MAC values in excess of 0.8-0.9 are usually accepted as indicators of good consistency, while values less than 0.1-0.2 are considered as indicators of null consistency. These limit values for the MAC must not be regarded in absolute terms, since there are some applications that demand high levels of consistency and some others that can accept lower MAC values, depending on the final objectives of the analysis.

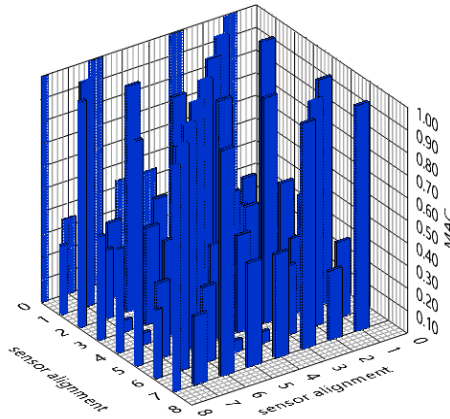


Figure 4.2. Sample MAC matrix

When multiple vectors are compared in couples, a MAC matrix is usually computed and graphically represented as in Figure 4.2.

A mathematical explanation of a high MAC value is identified by two vectors that have the same direction in an N-dimensional space regardless of their amplitudes. From this, it can be seen that incomplete information can give rise to high MAC values even if the vectors under comparison are not very similar. In addition, the MAC is sensitive to large differences between the corresponding components of the vectors under comparison, but it is basically insensitive to small changes and small magnitudes of the modal displacements. These shortcomings have to be taken into account when it is used for the selection of structural units according to the herein described approach.

## **4.2 A NOVEL USE OF THE MAC: ASSESSMENT OF THE METHOD**

The MAC matrix depends on the characteristics of the modes. Thus, it can be conveniently used as a tool to distinguish between global and local modes and as an operational function to identify sub-structures that can be analysed separately.

In order to identify macro-elements in a large architectural complex, the modal displacement fields associated to the selected verticals are compared.

The vertical alignments concept consists on the selection of simulated alignments identified long the macro-elements of the structure. In the case of the numerical models, they are represented by "virtual sensors" distributed throughout the model and able to comparing the modal



displacement fields associated to these verticals for a given mode. In the same way, in the field of experimental vibration tests, the distribution of the sensors (single or a couples) provides the vertical alignment definition as described in the Chapter 5 for the experimental case study.

The degrees of freedom in each vertical are characterized by the same elevation as the corresponding vector components in the others. The dimension of the vectors under comparison depends on the modelling assumptions and the eventual reduction of the number of vector components to reduce the computational efforts. Moreover, it is fundamental to ensure the correspondence of the position of the elements in the vectors under comparison. In other words, since at a given elevation degrees of freedom along the  $x$  as well as the  $y$  direction are considered, the corresponding values of the modal displacements must be ordered in the same way, that is to say, for a given elevation, modal displacements in the same direction must be considered.

Assuming that a sufficient number of virtual sensors have been considered, the computation of the MAC matrix from the modal displacement fields associated to the selected verticals provides a clear indication about the nature of the considered mode. In fact, if it is a global bending mode, all the vectors under comparison are very similar each other and all the elements of the MAC matrix show large values (close to 1).

## Chapter 4 - A MAC based approach: dynamic identification of the structural behaviour

---

On the contrary, in the case of a local mode, the MAC will be large and close to 1 only when the comparison affects verticals belonging to the same macro-element. Analysing the spatial distribution of highly correlated verticals in the case of local modes the associated macro-elements can be identified. A threshold to discriminate highly correlated verticals must be set. A value of 0.9 is adopted in the present case. The process above described has been implemented for validation with reference to a numerical model of an aggregate masonry building and applied afterwards to the analysis of a real case study (Chapter 5).

### **4.2.1 Explanatory numerical cases: Regular masonry structure**

A proper assessment of complex masonry buildings generally cannot disregard the definition of the reference structural units and of a number of them acting as aggregates depending on basic structural characteristics and geometric configuration. The herein analysed explanatory case, albeit not exhaustive of all the observed configurations, is conceived as representative of structures located in many historical centres of Italian villages (Marcari & Fabbrocino, 2008). The main objective of computational analysis is the study of mode shapes and other relevant dynamic properties in terms of natural frequencies and participating mass ratios, taking into account some uncertainties related to the knowledge of the connections between the various parts of the building.

Figure 4.3 shows the simple explanatory geometry of the aggregate, whose views is reported in detail below.

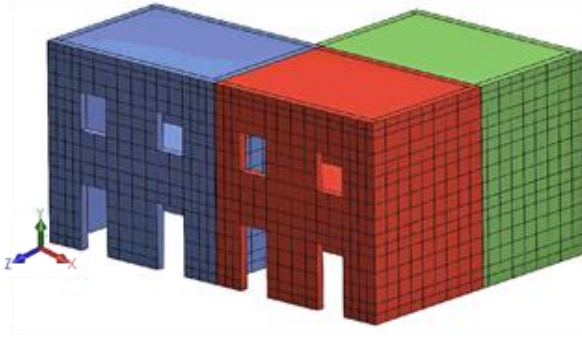


Figure 4.3. 3D Model of the aggregate

The masses have been defined according to the dimensions of the structural elements and the physical properties of materials (reinforced concrete for the floors, masonry for the walls).

A fine mesh of three-dimensional elements has been considered in the analyses. Once the models have been set, modal analyses have been carried out in order to obtain mode shapes and modal participating mass ratios of the first twenty modes. In particular, the modal displacements have been extracted for a subset of degrees of freedom.

To compare the global behaviour of the different buildings, the same masonry type has been used for all models.

An example of the arrangement of sensors (checkpoints) is summarized below (Figure 4.4).

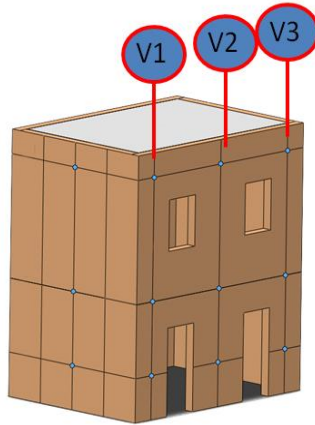


Figure 4.4. Location of virtual sensors

Starting from the basic configuration of the isolated building, which has a regular distribution of the openings and is characterized by rigid planes, a further variation has been defined in order to investigate the effects of the interactions among the original cells and the surrounding added structural units depending on the different grade of floor connections.

To compare the global behaviour of the different buildings, the same masonry type has been used for all models. reports the matrix of the numerical tests performed in this study (Table 4.1).

The structural modelling and the analysis have been performed with the FE software SOLIDWORKS Ver. 2016.

MODEL		a	b	c
1	A	Restrained Floor		
	B	Unrestrained Floor		
2	A	Restrained Floor	Restrained Floor	
	B	Restrained Floor	Unrestrained Floor	
3	A	Restrained Floor	Restrained Floor	Restrained Floor
	B	Restrained Floor	Unrestrained Floor	Restrained Floor

Table 4.1. Matrix of the numerical simulation

Furthermore, definition of the quality of the data with editing the size parameters of vertical and "virtual sensors" on the numerical model can be interpreted as optimization in the next phase of the experimental analysis. In the next paragraphs, in detail, different configuration for the alignments and number per alignments of virtual sensors are presented

#### 4.2.2 Single Cell

The starting point of the analysis is reported by the simple buildings reported in Figure 4.6, which is represented a distinct original cell from the architectural complex. Furthermore, it is a two-story masonry building with masonry in stone blocks and horizontal structures made up of reinforced concrete slabs.

The examined structure is a one-bay two-story 3D solid masonry building with vertical structures made of 25 cm thick at each floor (Figure 4.5 a), linearly elastic, homogeneous, 16 nodes to elements be seen and is perfectly constrained at the base.

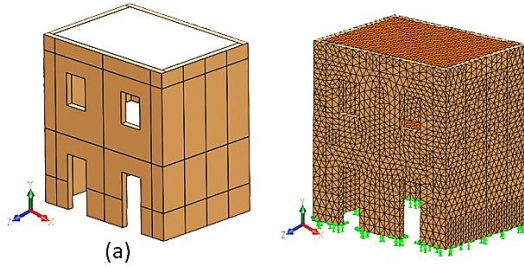


Figure 4.5. a) 3D Model of the isolated building; b) Finite mesh view

The numerical model consists of solid, 16 node elements, with linear elastic and homogeneous materials and is perfectly constrained at the base. The global coordinate system has been identified based on the orientation of the walls: the x-axis corresponds to the direction of the longitudinal walls with openings, while the z-axis is parallel to the transverse walls. The main façade is composed by a symmetric distribution of the openings' basic information about the fine mesh of three-dimensional elements are reported in Figure 4.5 b. The masonry is characterized by the following mechanical properties (Circolare 617 2009): elastic modulus  $E = 2400 \text{ N/mm}^2$ , shear modulus  $G = 780 \text{ N/mm}^2$ , specific weight  $\rho = 22 \text{ kN/m}^3$ .

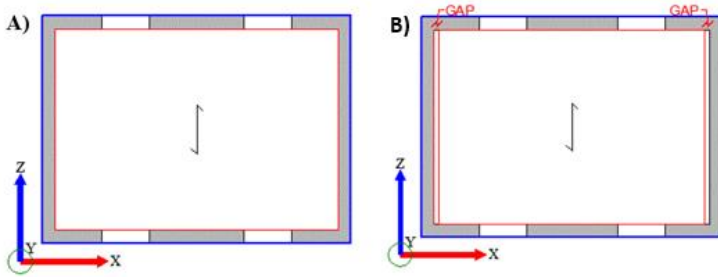


Figure 4.6. Model 1: schematic plan view of the aggregate reference basic cell with restrained floor (A), and unrestrained floor (B)

The role of the axial stiffness of the floors is assessed by considering two conditions, rigid and a restrained floor (Figure 4.6 a), and rigid and weakly restrained floor (Figure 4.6 b). In the latter case, there is a 0.02 m gap between the floors and the walls to simulate the absence of connections between floors and vertical walls in the direction parallel to the beams of the floor. The process of the numerical analysis consists of a two-step: in the first one modal displacement is extracted for a subset of degrees of freedom of the vertical alignments defined. In the subsequent phase, data are processed in order to obtain the MAC matrix value. The choice of position for virtual sensors have been based on the definition equivalent frame for the different alignments of masonry walls along the two directions (Figure 4.7). For the models has been defined an experimental matrix calculation ( Table 4.2).

Chapter 4 - A MAC based approach: dynamic identification of the structural behaviour

---

This is based on the number of alignments and sensors for each alignment, in order to assess the effects of these and with the aimed to been found an optimal configuration for the dynamic monitoring.

Number of alignments	Number of sensors			Model	
	4	8	16	M.1.A	M.1.B
8	4	8	16	M.1.A	M.1.B
16	4	8	16	M.1.A	M.1.B
40	4	8	16	M.1.A	M.1.B

Table 4.2. Single cell: numerical simulation of virtual sensors

In Figure 4.7 an example of the incremental sensors analysis is reported. In this case has been used 16 vertical alignments and the number of the sensors by the vertical was changed.

Modal analyses have been carried out in order to get model shapes and the main dynamic parameters of the first twenty modes.



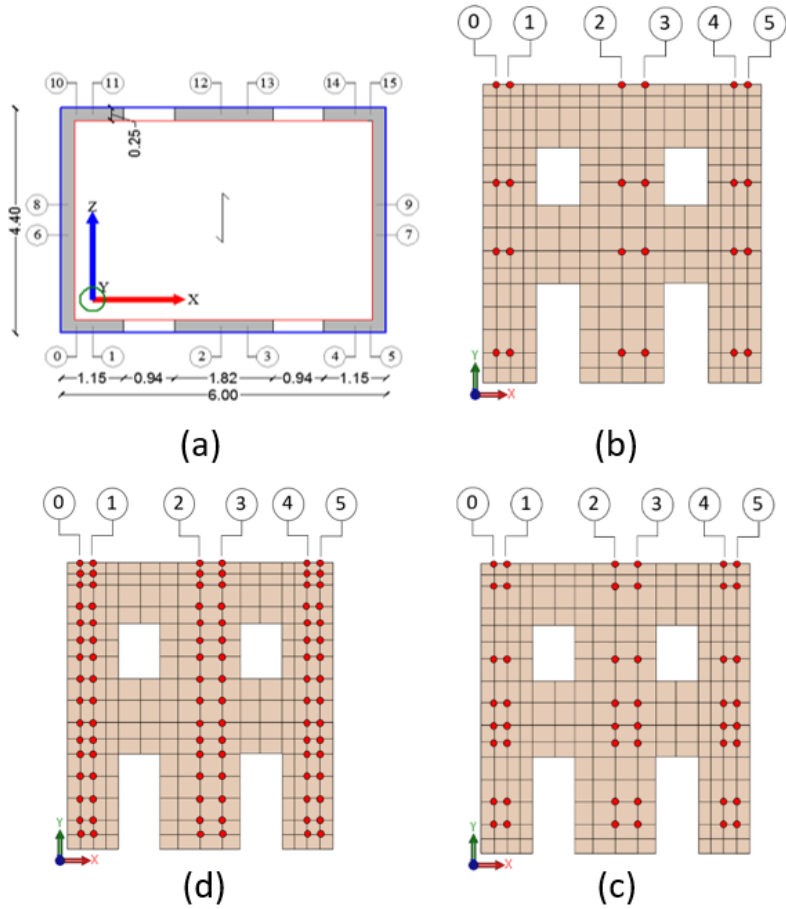


Figure 4.7. Single cell: set of virtual sensor: a) view in plan of the verticals (16 alignments), the number of the sensors increase (b), (c), (d)

Chapter 4 - A MAC based approach: dynamic identification of the structural behaviour

Mode	Model - M.1.A			Model - M.1.B		
	Freq.	Type*	PMR	Freq	Type*	PMR
[-]	[Hz]	[-]	[%]	[Hz]	[-]	[%]
1	9.71	T-X	83.00	8.92	T-X	76.99
2	9.91	T-Z	73.00	9.67	T-Z	71.66
3	15.80	R-Y	81.82	13.35	T-X	1.2e-06
4	19.60	T-Z	10e-04	15.41	R-Y	81.87
5	21.05	T-X	6.0e-03	16.39	T-X	6.83
6	24.13	T-X	1.9e-06	18.52	T-X	2.131
7	25.04	T-X	1.97	19.25	T-X	1.1e-04
8	26.20	T-X	5.9	19.75	T-Z	2.7e-06
9	29.32	T-Z	3.6	20.93	T-Z	6.1e-02
10	27.90	T-Z	13	23.31	T-Z	16.10

Table 4.3. Modal analysis results: modal shape definition codes: T-X=Translational along X axis; T-Z=Translational along Z; R-Y=Rotational in Y axis.

The results of modal analyses are summarized in Table 4.3, which shows relevant dynamic parameters (primary direction in the case of flexural modes, axis of rotation in the case of torsional modes, natural frequency, Participating Mass Ratio - PMR). The modes for the two isolated building models (M.1.A - Modal analysis for rigid and restrained floor; M.1.B - Modal analysis for rigid and unrestrained floor) are defined. The number of mode cases developed ensured that a total of 84% of mass participation was accounted for. A relevant remark is the regularity of the mode shapes and the highest participating mass calculated is equal to 83.00% in the X axis and 73.00% in Y axis as expected for the regularity of the artefact. Moreover the configuration

## Chapter 4 - A MAC based approach: dynamic identification of the structural behaviour

with unrestrained floor determine a weakly reduces the participating mass equal to 7.25% in the X axis and 1.85% in the Y axis.

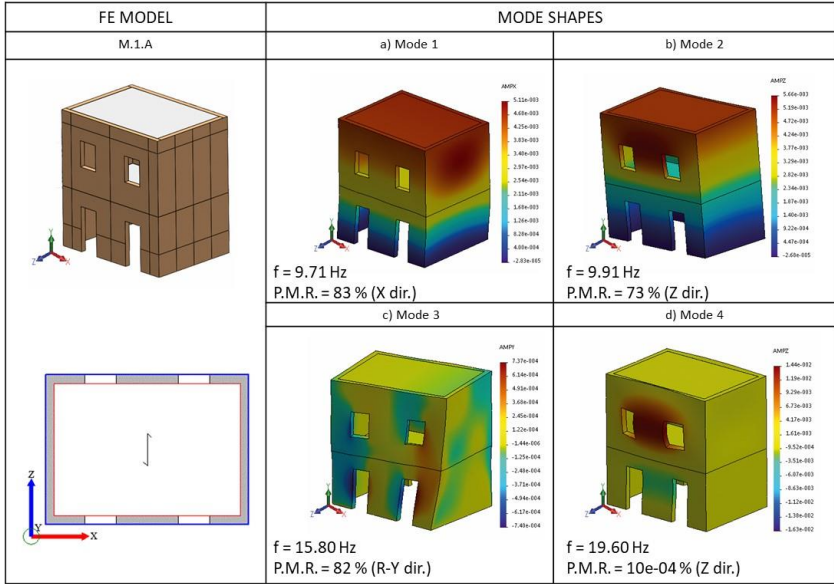


Figure 4.8. M.1.A: modal analysis results for rigid and restrained floor

Observing Figure 4.8 and Figure 4.9, in both configurations it is clear that the predominant transversal modes of vibration of the building, that are very close in terms of frequency and participating mass, show a global mode behaviour. Is equal for the torsional mode where in the M.1.B there is a decrease of about 2.45 % in frequency.

## Chapter 4 - A MAC based approach: dynamic identification of the structural behaviour

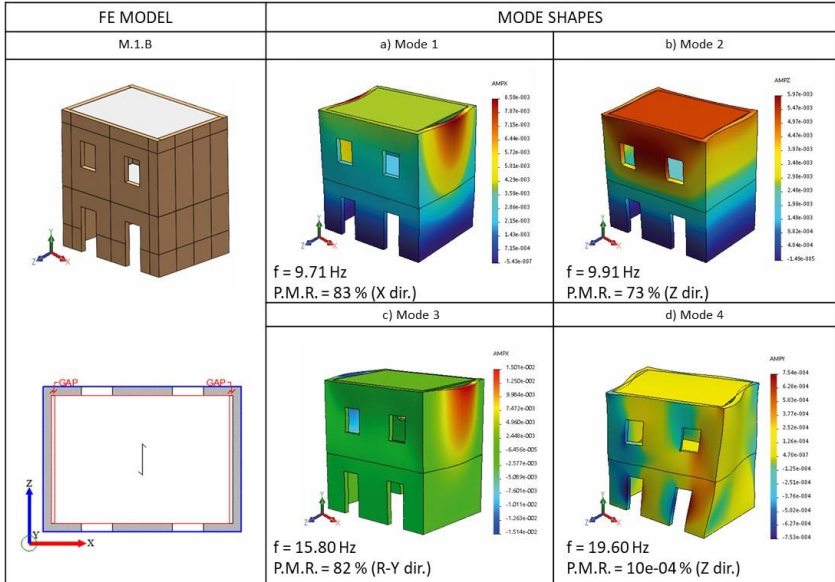


Figure 4.9. M.1.B: modal analysis results for rigid and restrained floor

The low participating masses are representative of the local modes. In the M.1.B configuration the local mode is localized in the third mode (Figure 4.9c) where the facades, free from the floor, moves at frequency of 13.35 Hz in the X direction. To confirm as the poor quality of the connection is one of the elements that define a local behaviour of the structure.

The MAC procedure has been carried out for each deformed shapes evaluated as related to the selected verticals. The results of the

Chapter 4 - A MAC based approach: dynamic identification of the structural behaviour

assessment for the models M.1.A and M.1.B is shown by the schematically in Figure 4.10 and Figure 4.11.

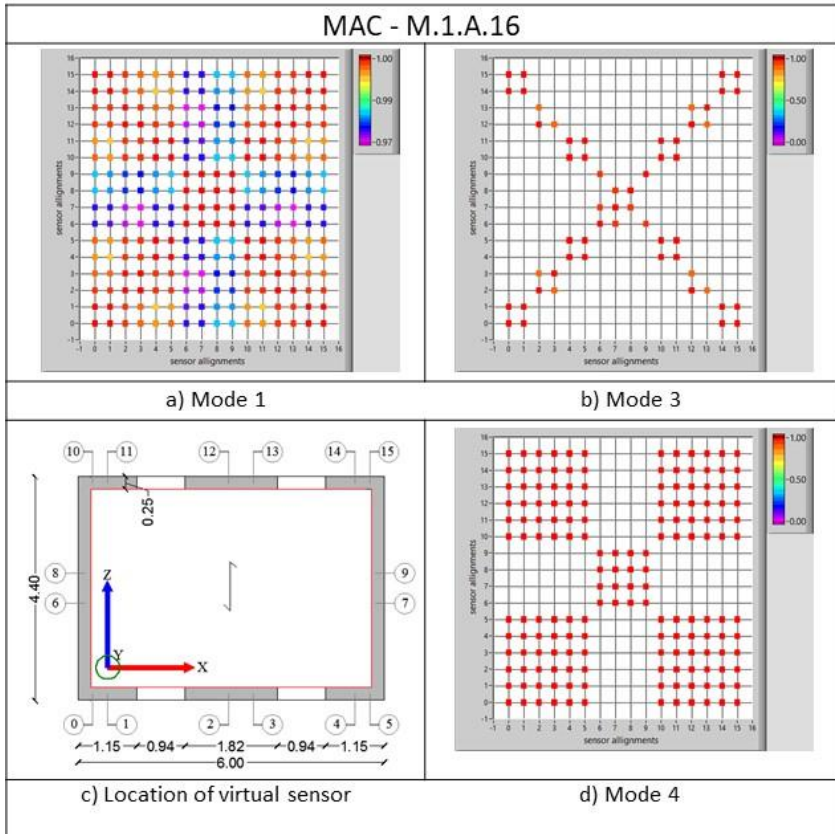


Figure 4.10. Results M.1.A.16: the MAC matrix associated with the global modes a-b) and local mode d); c) schematic plan view of the virtual alignments

Chapter 4 - A MAC based approach: dynamic identification of the structural behaviour

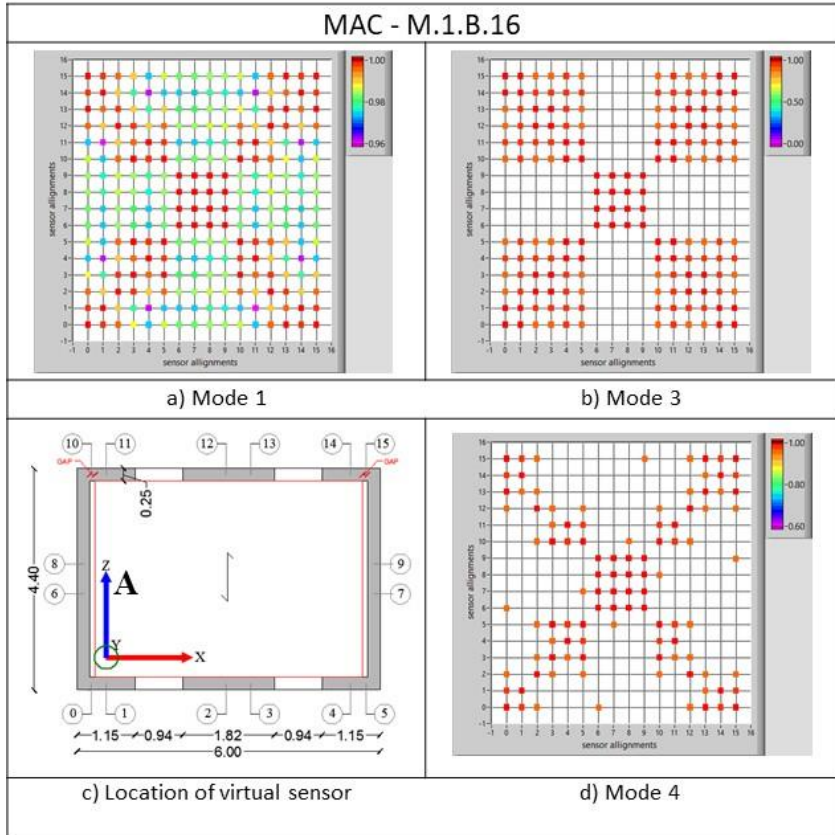


Figure 4.11. Results M.1.B.16: the MAC matrix associated with the global modes a-b) and local mode d); c) schematic plan view of the virtual alignments

The MAC matrices plots for the global and local modes assume as reference the chosen value of 0.9, so to represent a high level of correlation amongst the verticals. On the contrary, the absence of points in the MAC matrix identify a poor correlation between the

selected alignments. Eight virtual sensor alignments were considered, with 16 verticals for the box model.

The results show in the case of principal global modes, the histograms, highlight as much values always exceed the threshold specified (Figure 4.10a). Conversely, the results of local modes (Figure 4.10d) are characterized to a limited number of verticals with higher value of the threshold. The trend is analogous for the model characterized by the presence of rigid and restrained floor (M.1.A.16) as well as for the model characterized by rigid and unrestrained floor (M.1.B.16).

Torsion modes are characterized by a cross structure of the MAC matrix in the both models. The absence of the connection between the walls and the horizontal structures in the M.1.B. define the higher values of the histogram (Figure 4.9 d) also between the adjacent verticals (e.g. Vert. 0 and Vert 6 or Vert.5 and Vert.7).

For sake of generality, it is worth noting that the presence of large scatters in terms of stiffness among components of structures may lead to modes characterised by substructures affected by negligible displacements and as a contrast others that clearly move. Assuming that all the values of the "motionless" block are not equal to zero, as generally happens in the modal analyses, the discrimination process can be made according to a double level of assessment, consisting of the MAC index and the computation of the norm of the vector of the vertical alignments defined. The latter is defined as follows - let the vector of an n-dimensional vector

$$[\phi_i] = \begin{bmatrix} \phi_1 \\ \phi_2 \\ \vdots \\ \phi_n \end{bmatrix} \quad (4.2)$$

the general vector norm  $\|\phi\|$ , is defined as the length or magnitude of the vector and can be calculated using the formula:

$$\|\bar{\phi}\| = \sqrt{\phi_1^2 + \phi_2^2 + \dots + \phi_n^2} \quad (4.3)$$

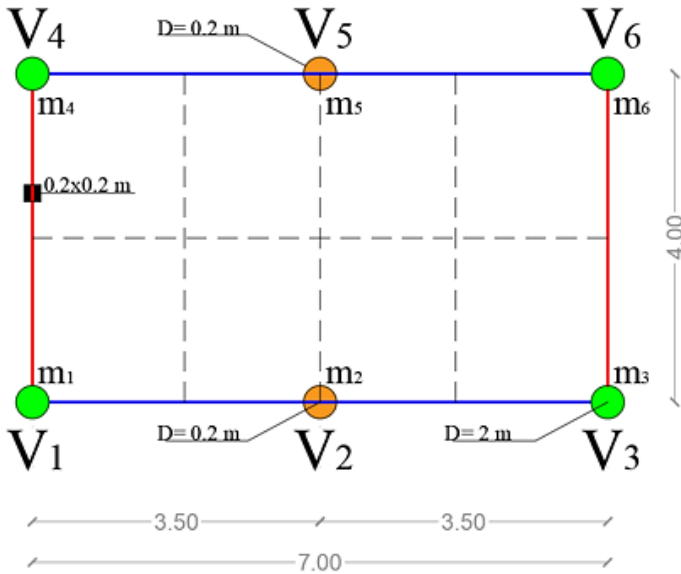


Figure 4.12. Plan view of the reference numerical model



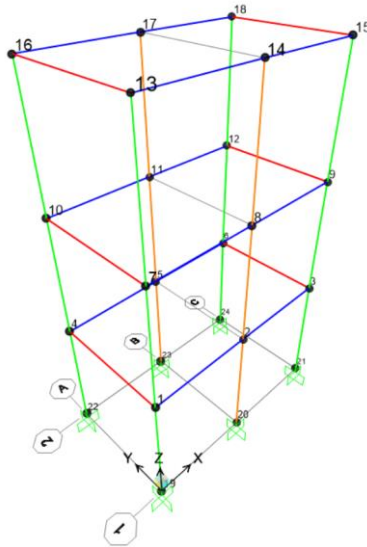
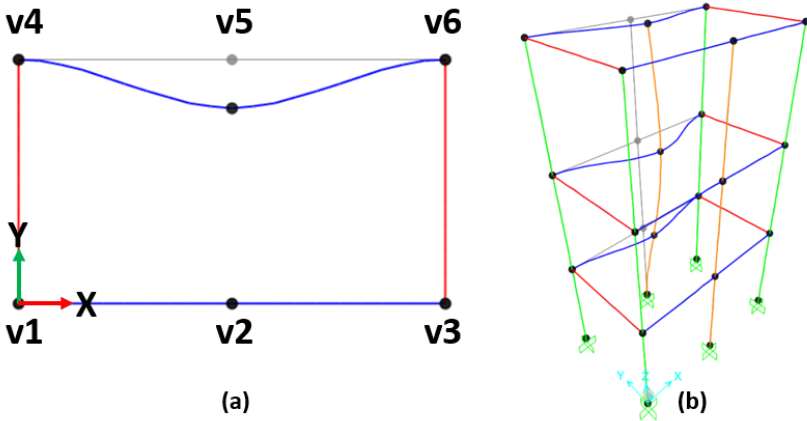


Figure 4.13. 3D View of the reference numerical model

As an explanatory case of this condition, a simple frame model of a multi-storey table (Figure 4.13) is shown, with two vertical alignments (v2 and v5) made of a circular full section of 0.20 m diameter and the other alignments (v1,v3,v4,v6) with a circular section of 2 m diameter, in such a way to define a rigidity ratio a thousand times greater. The beams are dimensioned with a very high stiffness for those in the Y direction, and low bending rigidity for those in the X direction. The masses have been redistributed in the vertical nodes of each alignment,

Chapter 4 - A MAC based approach: dynamic identification of the structural behaviour

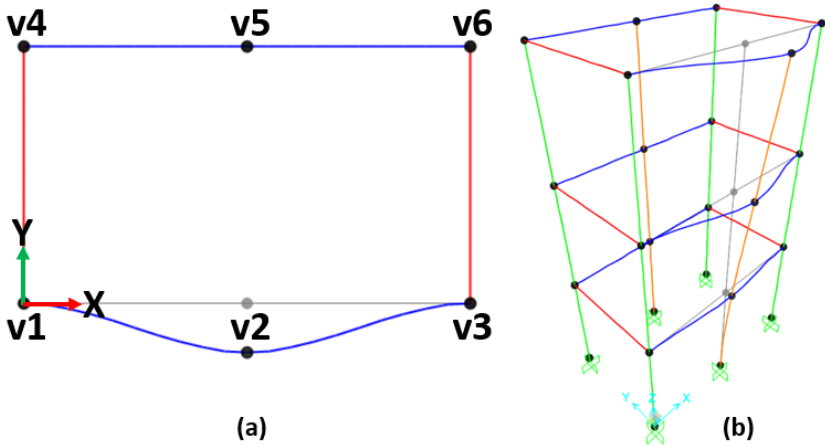
so as to reproduce a typical condition of a masonry building without horizontal rigid diaphragm.



MAC - Mode 1						
	v1	v2	v3	v4	v5	v6
v1	1.00	0.80	0.38	0.63	0.74	0.94
v2	0.80	1.00	0.80	0.93	0.84	0.93
v3	0.38	0.80	1.00	0.94	0.74	0.63
v4	0.63	0.93	0.94	1.00	0.90	0.84
v5	0.74	0.84	0.74	0.90	1.00	0.90
v6	0.94	0.93	0.63	0.84	0.90	1.00
Vector Norm	7.55E-06	9.13E-06	7.55E-06	1.63E-05	2.29E-01	1.63E-05

(c)

Figure 4.14. Results multi-storey table mode 1: a) deformed shape view in plan; b) 3D view of mode shape; c) the MAC matrix associated with the first mode and vector norm values.

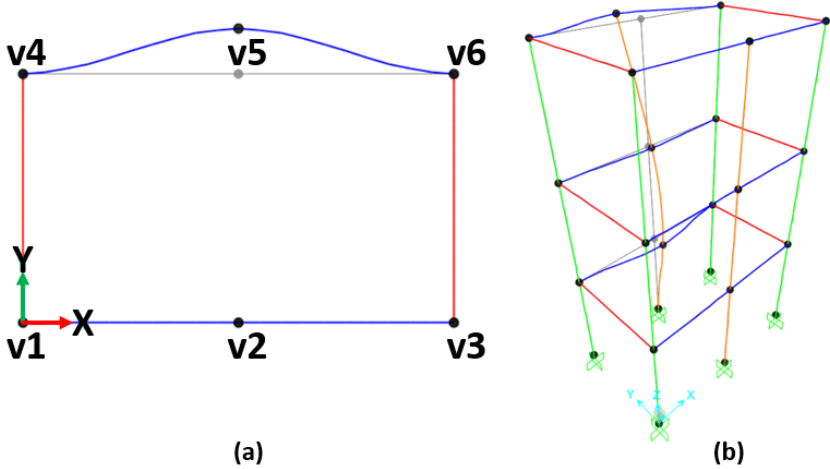


MAC - Mode 2						
	v1	v2	v3	v4	v5	v6
v1	1.00	0.93	0.86	0.64	0.22	0.94
v2	0.93	1.00	0.93	0.78	0.38	0.78
v3	0.86	0.93	1.00	0.94	0.22	0.64
v4	0.64	0.78	0.94	1.00	0.16	0.38
v5	0.22	0.38	0.22	0.16	1.00	0.16
v6	0.94	0.78	0.64	0.38	0.16	1.00

Vector Norm	2.28E-05	3.01E-01	2.28E-05	1.02E-05	3.94E-04	1.02E-05
-------------	----------	----------	----------	----------	----------	----------

(c)

Figure 4.15. Results multi-storey table mode 2: a) deformed shape view in plan; b) 3D view of mode shape; c) the MAC matrix associated with the first mode and vector norm values.



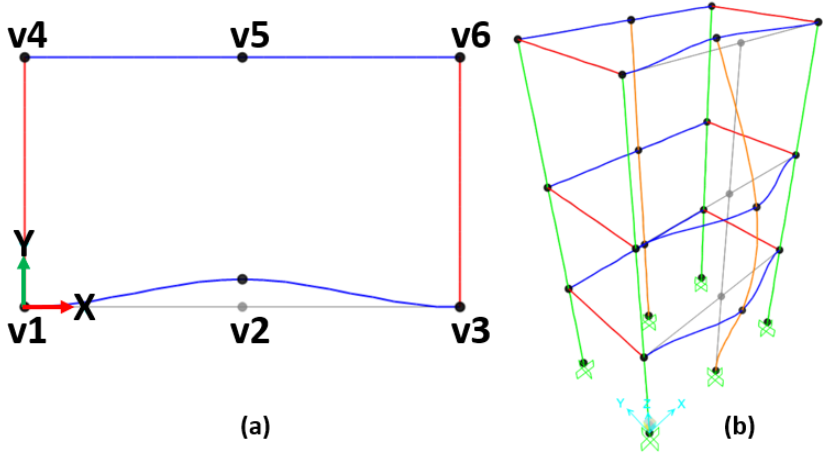
MAC - Mode 3						
	v1	v2	v3	v4	v5	v6
v1	1.00	0.79	0.39	0.60	0.21	0.88
v2	0.79	1.00	0.79	0.96	0.40	0.96
v3	0.39	0.79	1.00	0.88	0.21	0.60
v4	0.60	0.96	0.88	1.00	0.48	0.86
v5	0.21	0.40	0.21	0.48	1.00	0.48
v6	0.88	0.96	0.60	0.86	0.48	1.00

Vector Norm	4.23E-06	4.49E-04	4.23E-06	9.68E-06	2.65E-01	9.68E-06
-------------	----------	----------	----------	----------	----------	----------

(c)

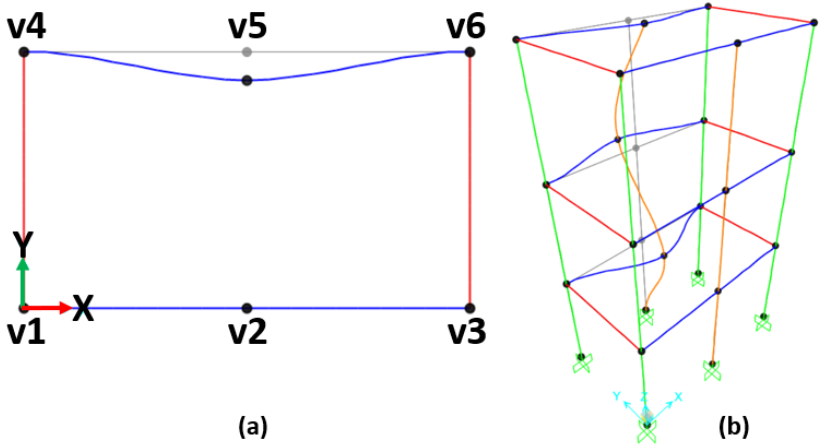
Figure 4.16. Results multi-storey table mode 3: a) deformed shape view in plan; b) 3D view of mode shape; c) the MAC matrix associated with the first mode and vector norm values.



MAC - Mode 4						
	v1	v2	v3	v4	v5	v6
v1	1.00	0.55	0.90	0.50	0.26	0.72
v2	0.55	1.00	0.55	0.10	0.01	0.10
v3	0.90	0.55	1.00	0.72	0.26	0.50
v4	0.50	0.10	0.72	1.00	0.58	0.39
v5	0.26	0.01	0.26	0.58	1.00	0.58
v6	0.72	0.10	0.50	0.39	0.58	1.00
Vector Norm	5.88E-06	3.01E-01	5.88E-06	2.15E-06	9.16E-07	2.15E-06

(c)

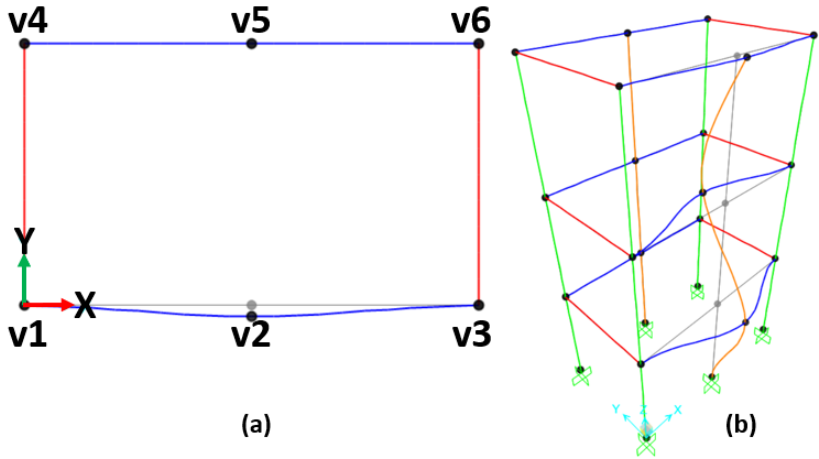
Figure 4.17. Results multi-storey table mode 4: a) deformed shape view in plan; b) 3D view of mode shape; c) the MAC matrix associated with the first mode and vector norm values



MAC - Mode 5						
	v1	v2	v3	v4	v5	v6
v1	1.00	0.77	0.39	0.57	0.05	0.83
v2	0.77	1.00	0.77	0.72	0.01	0.72
v3	0.39	0.77	1.00	0.83	0.05	0.57
v4	0.57	0.72	0.83	1.00	0.30	0.87
v5	0.05	0.01	0.05	0.30	1.00	0.30
v6	0.83	0.72	0.57	0.87	0.30	1.00

Vector Norm	1.57E-06	6.48E-07	1.57E-06	3.71E-06	2.25E-01	3.71E-06
-------------	----------	----------	----------	----------	----------	----------

Figure 4.18. Results multi-storey table mode 5: a) deformed shape view in plan; b) 3D view of mode shape; c) the MAC matrix associated with the first mode and vector norm values

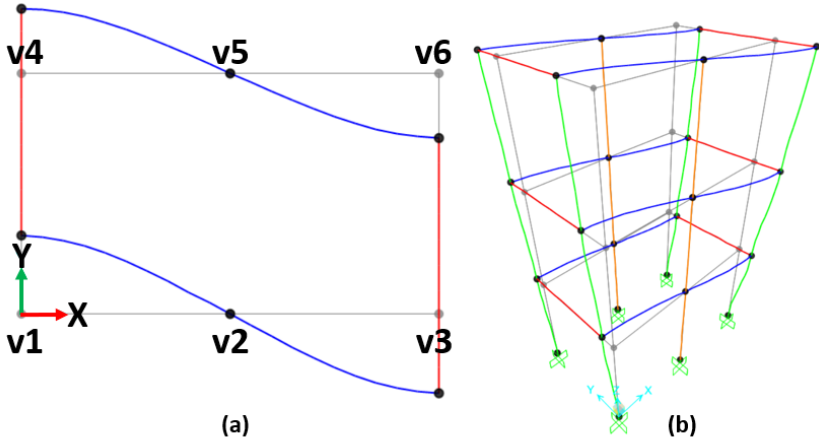


MAC - Mode 6						
	v1	v2	v3	v4	v5	v6
v1	1.00	0.73	0.96	0.32	0.46	0.43
v2	0.73	1.00	0.73	0.05	0.12	0.05
v3	0.96	0.73	1.00	0.43	0.46	0.32
v4	0.32	0.05	0.43	1.00	0.72	0.39
v5	0.46	0.12	0.46	0.72	1.00	0.72
v6	0.43	0.05	0.32	0.39	0.72	1.00

Vector Norm	2.42E-06	3.01E-01	2.42E-06	5.86E-07	6.18E-08	5.86E-07
-------------	----------	----------	----------	----------	----------	----------

(c)

Figure 4.19. Results multi-storey table mode 6: a) deformed shape view in plan; b) 3D view of mode shape; c) the MAC matrix associated with the first mode and vector norm values



MAC - Mode 7						
	v1	v2	v3	v4	v5	v6
v1	1.00	0.77	0.39	0.57	0.05	0.83
v2	0.77	1.00	0.77	0.72	0.01	0.72
v3	0.39	0.77	1.00	0.83	0.05	0.57
v4	0.57	0.72	0.83	1.00	0.30	0.87
v5	0.05	0.01	0.05	0.30	1.00	0.30
v6	0.83	0.72	0.57	0.87	0.30	1.00
Vector Norm	1.57E-06	6.48E-07	1.57E-06	3.71E-06	<b>2.25E-01</b>	3.71E-06

(c)

Figure 4.20. Results multi-storey table mode 7: a) deformed shape view in plan; b) 3D view of mode shape; c) the MAC matrix associated with the first mode and vector norm values

In particular, the alignments 1,3,4 and 6 have a uniform mass distribution, while the alignment 5 has a mass twice greater than the alignment 2. The results of the assessment for the model is shown by



the tables below. The results of the assessment for the model is shown by the schematically from Figure 4.14 to Figure 4.20 reported above. For each modes the MAC matrix and the norm of the vectors were evaluated.

From the results proposed here, it is clear, how a vibration modes process also allows the management of singular cases like this, allowing the discrimination of the parts subject to local ways in a given global system.

### 4.2.3 Double Cell

A correct approach for evaluate the performance of building aggregates should include the analysis of double cell in order to investigate the effects of the interaction among the original cells and the added structural units.

The geometrical and mechanical characteristics of the numerical structural mode follow the outlines of the single unit described previously. The behavior of masonry aggregates was studied by using the use of the same numerical process showed for obtain the MAC matrix of single cell. The position of the verticals and the number of virtual sensors per alignments have been defined as in the Table 4.4.

The structural model has been fully connected along the X direction (Figure 4.21), and the middle transversal walls are modelled as continuous (assuming a good quality of the walls connection) in both configurations.

Number of alignments	Number of sensors			Model	
15	4	8	16	M.2.A	M.2.B
30	4	8	16	M.2.A	M.2.B
72	4	8	16	M.2.A	M.2B

Table 4.4. Double cell: numerical simulation of virtual sensors

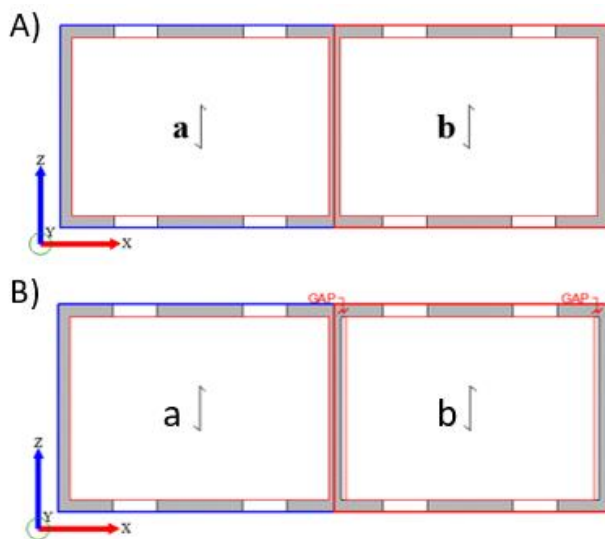


Figure 4.21. Double cell: geometry modelling with restrained floor (A); and unrestrained floor with 0.02 m gap (B) configuration

The main outcomes of the modal analyses are summarized in the following Table 4.5. In particular, are reported the main results of the modal analyses carried out on the double cells without gap (M.2.A) and with gap (M.2.B). The Figure 4.22 show the distribution of the alignments, with an incremental analysis that consider the vertical alignments and the sensors number per vertical.

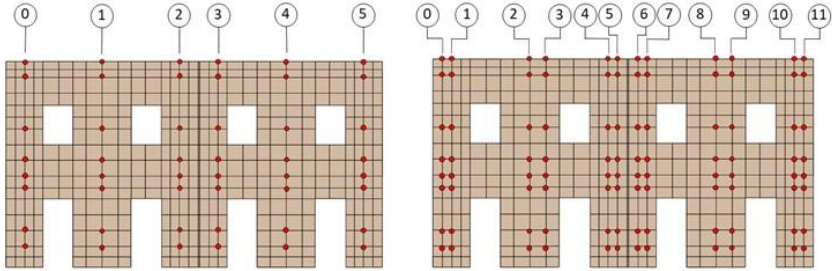


Figure 4.22. Double cell: set of virtual sensor: the number of the sensors and the vertical increase.

Figure 4.23 and Figure 4.24, instead, show explicative results of the deformed shape analysis carried out on the 3D aggregate model characterized with the restrained and unrestrained floor. In these cases, eight virtual sensor alignments were considered, with 30 verticals for the building aggregates in line. The deformed shapes of the double cell model for the flexural mode does not present any difference between the two configuration (Figure 4.23a and Figure 4.24). The only difference that emerges is the torsional mode higher in the first configuration compared with the unrestrained floor (Figure 4.23d and Figure 4.24d). The dispersion of the mode shapes (in terms of mass participation) highlights the presence of local modes.

Chapter 4 - A MAC based approach: dynamic identification of the structural behaviour

Mode	Model - M.2.A			Model - M.2.B		
	Freq.	Type*	PMR	Freq	Type*	PMR
[-]	[Hz]	[-]	[%]	[Hz]	[-]	[%]
1	9.43	T-Z	70.00	9.23	T-Z	69.41
2	10.36	T-X	79.04	9.68	T-X	77.87
3	13.66	R-Y	21.67	13.41	R-Y	78.34
4	19.62	T-X	2.24e-02	15.13	T-X	2.30
5	19.73	T-Z	7.97e-04	19.41	T-X	3.10e-02
6	20.79	R-Y	4.09	19.75	T-X	7.35e-02
7	21.40	T-Z	5.79	20.44	R-Y	3.74
8	23.45	T-X	1.53e-06	21.27	T-Z	8.5
9	24.42	T-X	7.9e-01	23.43	T-Z	12.28
10	25.61	T-Z	11.3	23.86	T-X	4.51

Table 4.5. Summary of the results : Modal shape definition codes: T-X=Translational along X axis; T-Z=Translational along Z; R-Y=Rotational in Y axis.

The MAC results (Figure 4.25, Figure 4.26), does not show differences with the single unit case in the flexural global modes (Figure 4.25a,c ) as so as in the local modes (Figure 4.25d) for the first configuration. In the M.2.B is worth noting that modelling features are well reflected by the form of the MAC matrix, especially for the local modes. The histogram shown one more a matrix blocks distribution, but with a smaller number of verticals with a high degree of correlation.

This is consistent with the nature that local modes the play a more relevant role whenever restraints between elements is poorer influencing the number of modes affected by significant PMR.

# Chapter 4 - A MAC based approach: dynamic identification of the structural behaviour

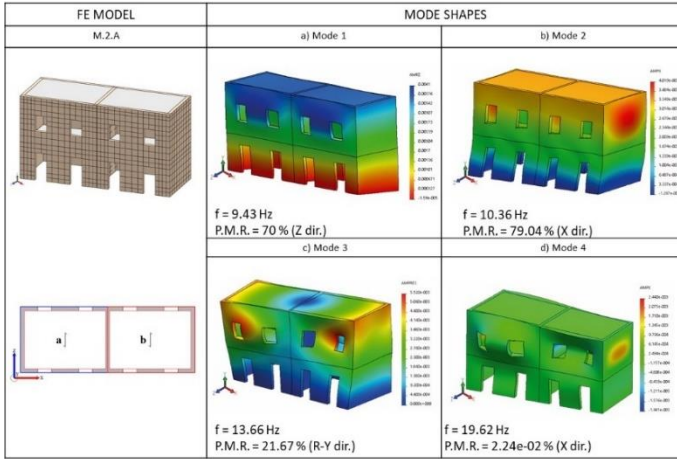


Figure 4.23. M.2.A: modal analysis results for rigid and restrained floor (a) and rigid and unrestrained floor (b)

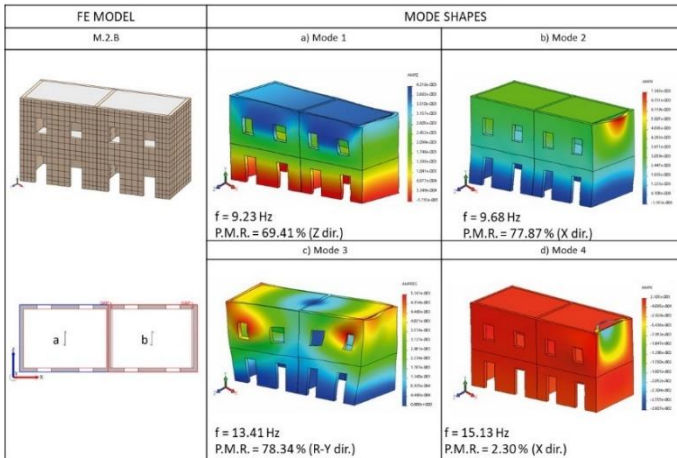


Figure 4.24. M.2.B: model analysis results for rigid and restrained floor (a) and rigid and unrestrained floor (b)

## Chapter 4 - A MAC based approach: dynamic identification of the structural behaviour

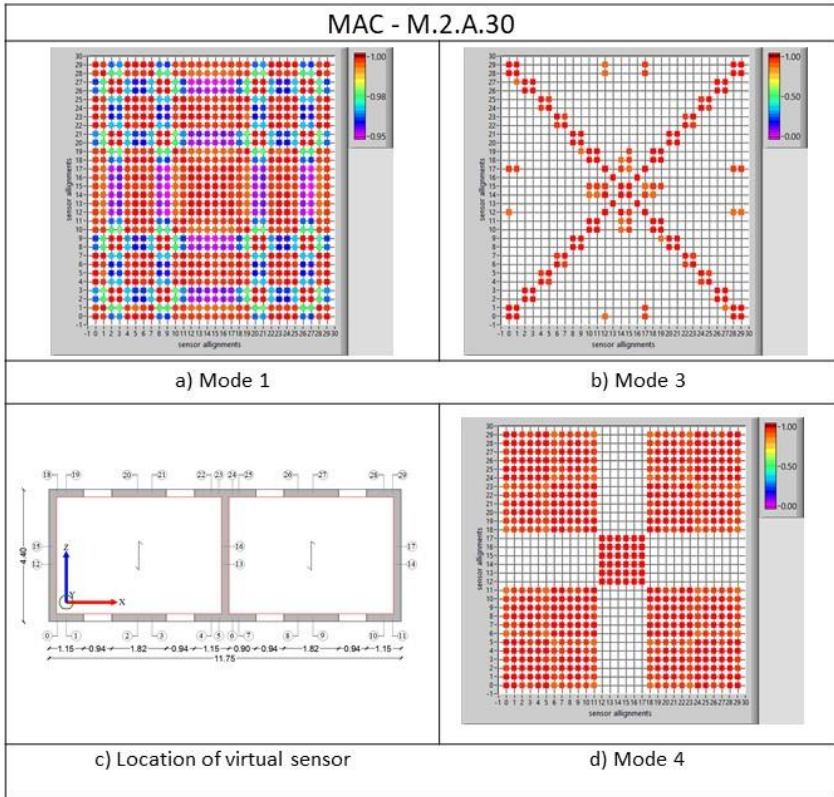


Figure 4.25. Results M.2.A.30: the MAC matrix associated with the global modes a-b) and local mode d); c) schematic plan view of the virtual alignments

## Chapter 4 - A MAC based approach: dynamic identification of the structural behaviour

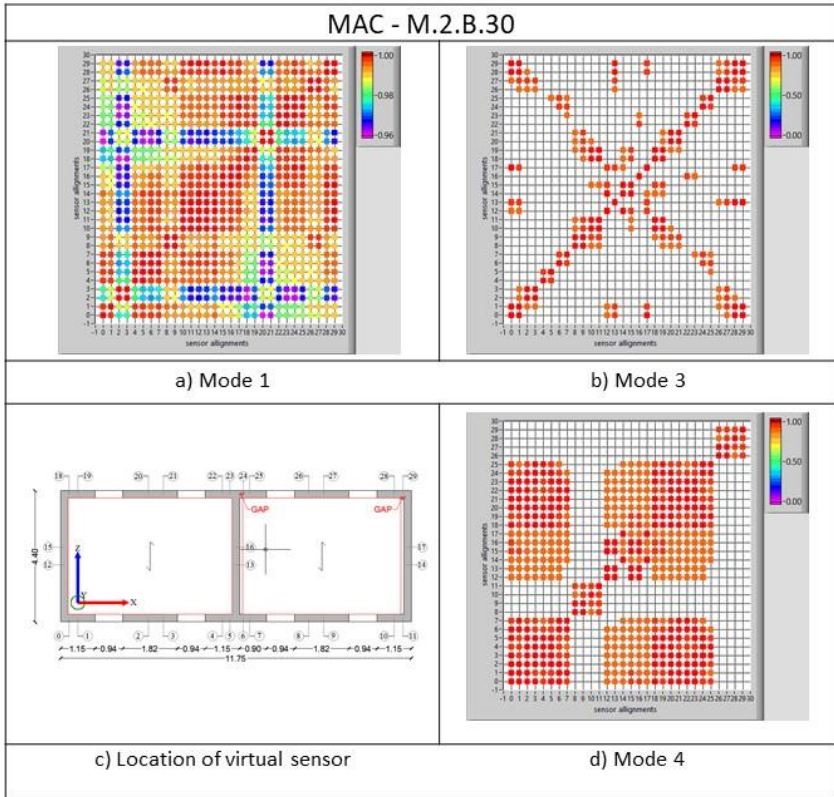


Figure 4.26. Figure 4.27. Results M.2.B.30: the MAC matrix associated with the global modes a-b) and local mode d); c) schematic plan view of the virtual alignments



#### 4.2.4 L-Shaped aggregate

In order to evaluate the seismic behaviour and the response of aggregate buildings, another additional configuration has been considered. In particular, the base structural unit has been modelled with a L-shaped geometry (Figure 4.29), always are considering the two boundary condition of horizontal structures.

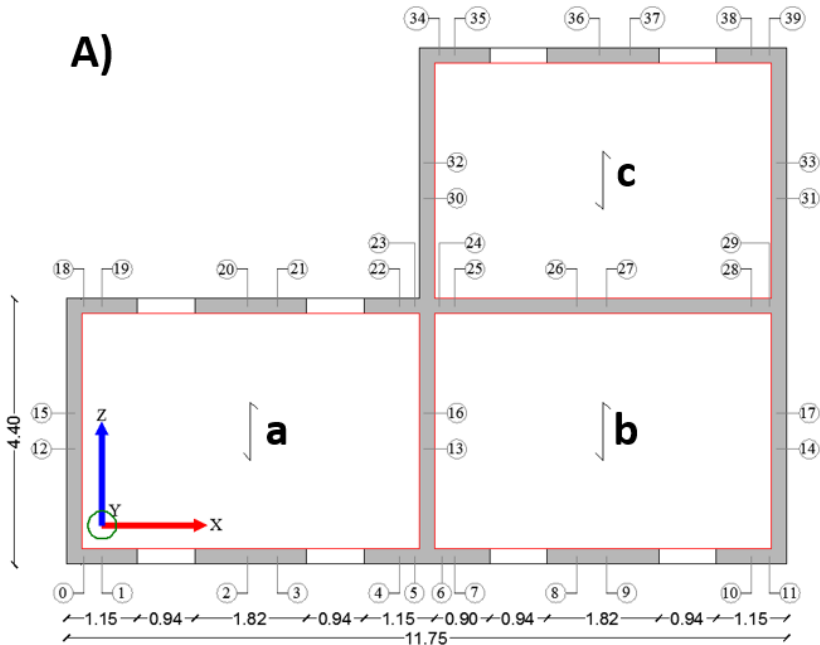


Figure 4.28.a) L-Shape aggregate: schematic plan view of the aggregate with restrained floor (A).

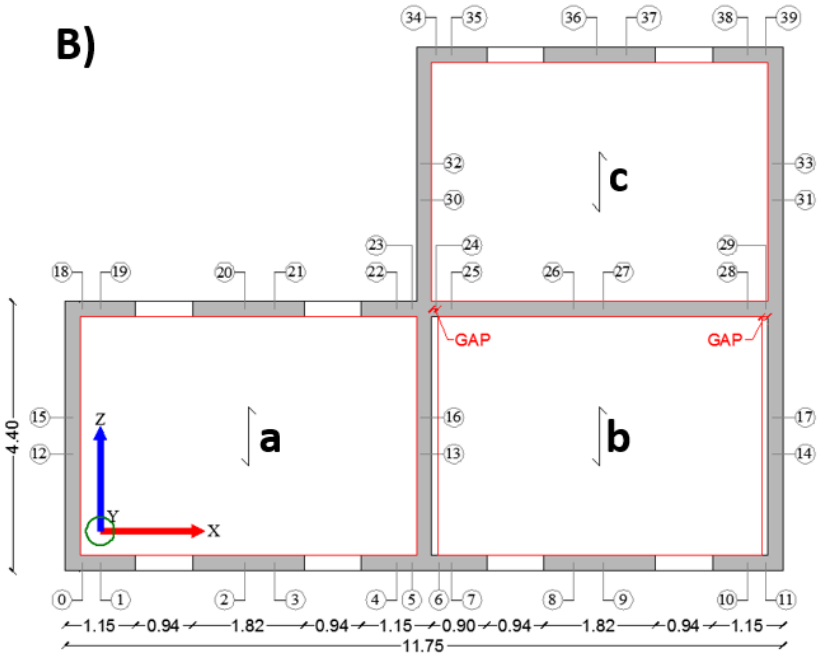


Figure 4.29.b) L-Shape aggregate: schematic plan view of the aggregate with unrestrained floor - application of a 0.02 m gap - (B).

The whole masonry structure has been discretized by means of 3D solid elements (Figure 4.30) and the mechanical properties are considered as in previous cases.

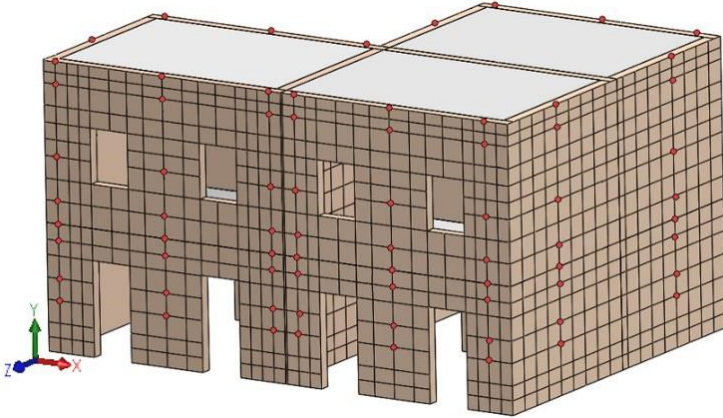


Figure 4.30. L-Shape aggregate: set of virtual sensor alignments

Virtual sensors have been therefore defined with the same one concept shown before and synthesized in Table 4.6.

Number of alignments	Number of sensors			Model	
	4	8	16	M.3.A	M.3.B
20	4	8	16	M.3.A	M.3.B
40	4	8	16	M.3.A	M.3.B
80	4	8	16	M.3.A	M.3.B

Table 4.6 L-Shape aggregate: numerical simulation of virtual sensors

For the aggregate model, eight virtual sensor alignments were considered, with 40 vertical. The modal results among of the two configuration is reported in Table 4.7, while the deformed shapes for the global and local modes is displayed in Figure 4.31 and Figure 4.32.

Chapter 4 - A MAC based approach: dynamic identification of the structural behaviour

The observation of the results shows clearly the influence of the unrestrained floor ( M.3.B) as the decrement of the frequencies and the increment of the local mass mode activated. In addition, for the M.3.B it is observed the dispersion of the mode shapes associated to local modes.

Mode	Model - M.3.A			Model - M.3.B		
	Freq.	Type*	PMR	Freq	Type*	PMR
[-]	[Hz]	[-]	[%]	[Hz]	[-]	[%]
1	9.78	T-X	77.48	9.37	T-X	77.31
2	11.14	T-Z	67.68	11.05	T-Z	67.27
3	13.60	R-Y	70.46	13.28	R-Y	69.12
4	19.61	T-Z	7.34e-03	15.68	T-Z	6.80
5	19.77	T-X	1.07e-02	19.34	T-X	3.36e-02
6	20.19	T-Z	1.56	19.72	T-Z	3.90e-02
7	21.04	R-Y	7.62	19.87	T-Z	1.18e-01
8	23.42	T-Z	3.83	20.91	T-Z	9.21e-01
9	23.61	T-X	5.60e-02	22.95	T-Z	3.01e-01
10	24.19	R-Y	2.06	23.37	R-Y	1.78e-01

Table 4.7. Results : Modal shape definition codes: T-X=Translational along X axis; T-Z=Translational along Z; R-Y=Rotational in Y axis

Since the PMR is basically the same in the analysed models (Table 4.7), it is clear that the proposed approach allows to distinguish the case of a large activated mass with small modal displacements from that of a small mass activated with significant modal displacements.

## Chapter 4 - A MAC based approach: dynamic identification of the structural behaviour

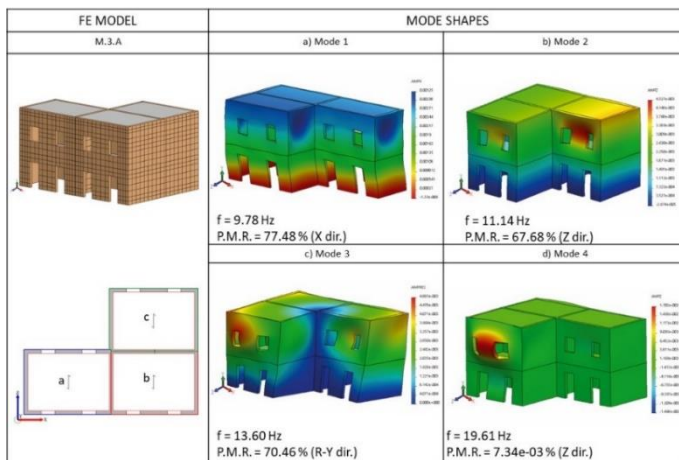


Figure 4.31. Results for building aggregate: M.3.A- Modal analysis with rigid and restrained floor;

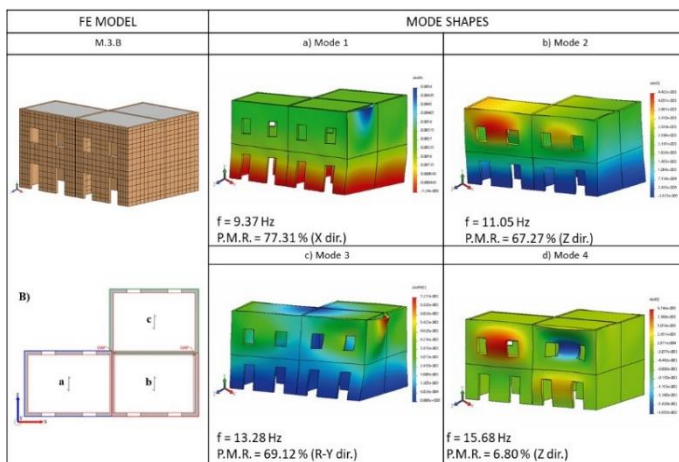


Figure 4.32. Results for building aggregate: M.3.B- Modal analysis with rigid and unrestrained floor;

## Chapter 4 - A MAC based approach: dynamic identification of the structural behaviour

---

The comparison between the MAC index values related to the numerical models examined with reference to the L-shape aggregate (M.3.A and M.3.B) of building is shown in Figure 4.33 and Figure 4.34.

In order to define a local and global mode selection procedure, the results obtained from MAC matrix configurations over a given threshold appear to provide reliable results not only in the base configuration, but also in the aggregate model. The MAC matrix among all couples of alignments shows a distinct structure depending on the nature of the mode. In fact, for global bending modes, the MAC matrix is a full matrix with almost all values close to 1 (Figure 4.33a). In the case of torsion mode and isolated building, the largest MAC values are located along the main diagonal and the main anti-diagonal when the number of alignments is set to a minimum. When this number increases, the largest MAC values are located not only along the above-mentioned diagonals but also along a few nearby diagonals (Figure 4.33b). As a result, torsion modes are always characterized by a cross structure of the MAC matrix that can be eventually cross banded in the presence of a redundant number of alignments. Within the substructuring analysis process, the results of spatial distribution of vertices that produce large MAC values (greater than 0.9) provide convenient data to quantify the similarity of mode shapes, making possible to determine the portion of structure that can be modelled as a macro-element or structural unit of large aggregate complexes. It's important in this framework, as seen in the section 2.5.1, to consider

Chapter 4 - A MAC based approach: dynamic identification of the structural behaviour

the definition of the boundary conditions, since, the structural units is not isolated.

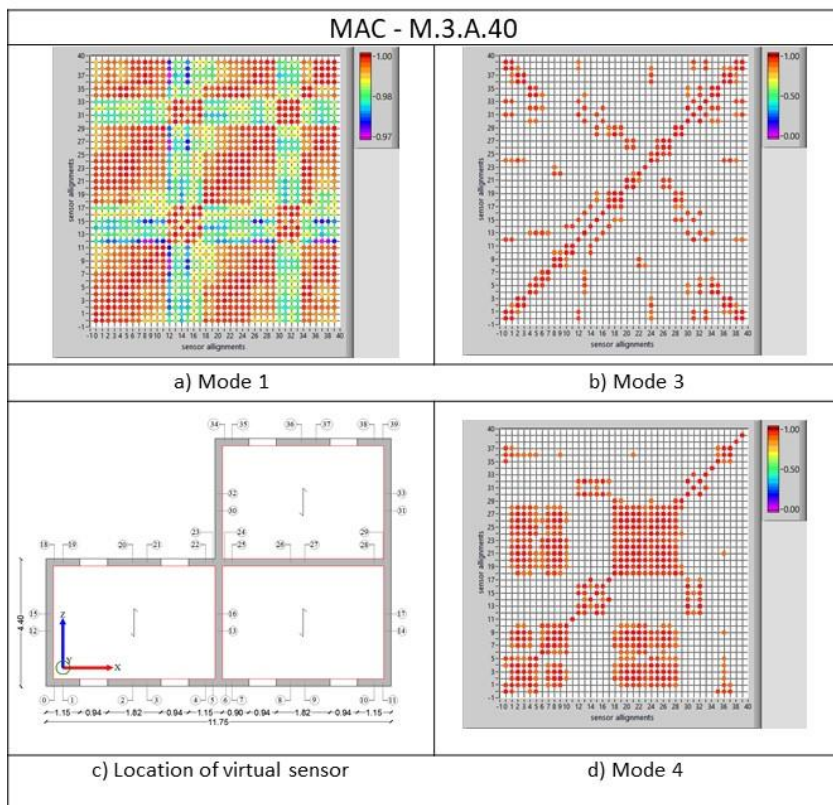


Figure 4.33. Results: M.3.A.40: the MAC matrix associated with global mode a-b) and local modes d)

Chapter 4 - A MAC based approach: dynamic identification of the structural behaviour

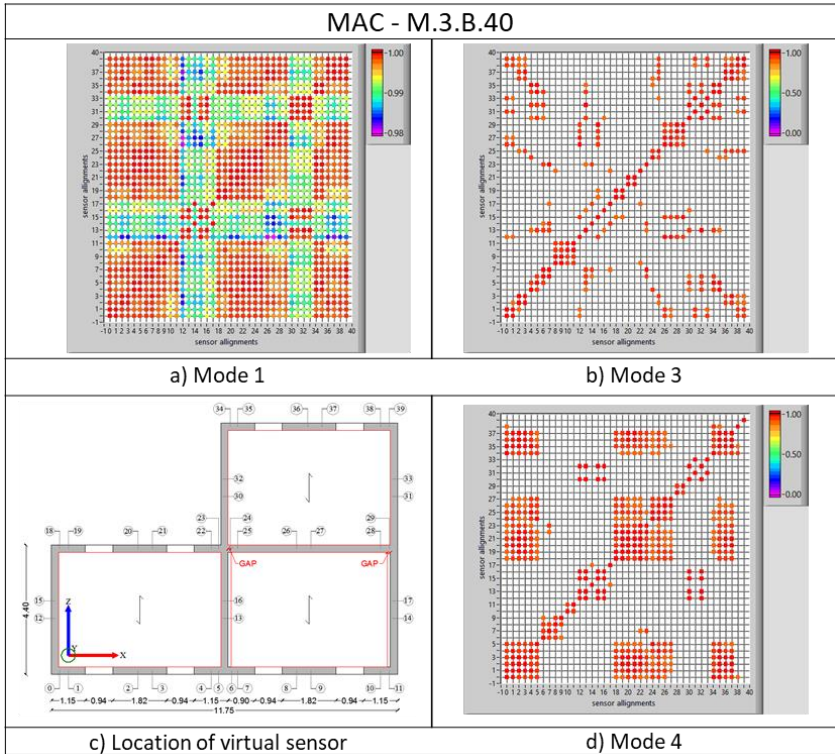


Figure 4.34. Results: M.3.B.40: the MAC matrix associated with global mode a-b) and local modes c)



#### **4.2.5 Monitoring strategies**

The possibility of applying the simplified procedures for the dynamic identification of the different structural typologies is, therefore, strategic to obtain useful information to apply the design criteria and the structural verifications in the seismic field.

Advantages and limitations of MAC was discussed in this section in light of its perspective application to the seismic analysis of architectural complexes.

Considering the above shown for the three case studies, single sensor or a couple of sensors have been examined as the monitoring system scheme for the extraction of dynamic parameters and for a correct MAC index assessment.

To evaluate the local mode, in terms of MAC index, the ideal distribution of the sensors provides for the installation of a couple of sensors per alignments (Figure 4.35b). The configuration with a single sensor, if on the one hand reduce the number of sensors, from the other can yield high MAC values (Figure 4.35d) even if the vectors under comparison are actually not very similar (missing values of modal displacements associated to a number of dynamic degrees of freedom). For these reasons, considering the distribution long the height of the walls, a minimum layout with a couple of sensors per vertical to adopt in a Structural Health Monitoring system, for the aggregate buildings masonry it is proposed.

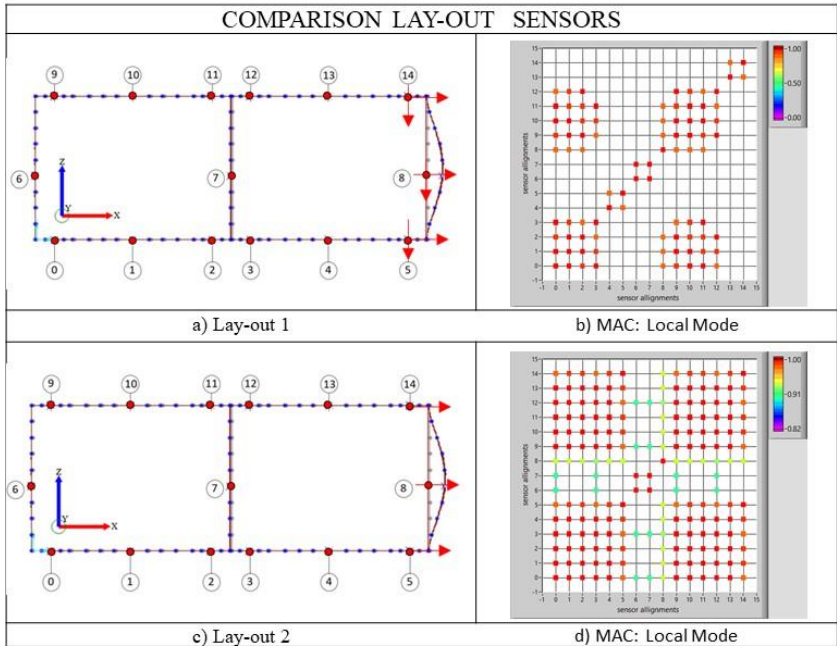


Figure 4.35. a) Schemes in plan of the sensors distribution b) results in terms of MAC index

### 4.3 FINAL REMARKS

This Chapter reviewed some aspects related to seismic modelling of masonry building aggregates typically encountered in Italian historical city. In particular, attention has been focused on the potentialities of the MAC index to serve as a tool in the assessment of the dynamic response of existing buildings, in particular the aggregate structures. In fact, either the separation of the architectural complex in structural

units or the distinction between local and global response can be considered as major outcomes of this study. A simplified assessment procedure for isolated building masonry has been implemented, first, considering different levels of connection between floors and walls, obtaining results in agreement with the expectations for box-shaped buildings. The procedure has been further validated afterwards by analysing aggregates of buildings, obtaining encouraging results.

The proposed technique allowed characterizing the nature of the modes even in the case of aggregate structures. Each structural unit is identifiable from the analysis of the spatial distribution of MAC computed between modal displacements associated to selected alignments of nodes.

The illustrated procedure appears effective in its simplicity.



## Chapter 5

# FIELD VALIDATION ON AN ITALIAN MASONRY BUILDING

### 5.1 INTRODUCTION

This Chapter present the experimental identification carried out in the context of the Agreement for an experimental project with the University of Molise and the Regional Command of the Guardia di Finanza (Italian Finance Police) in the framework of novel procedures for the seismic assessment of existing masonry buildings.

The focus of this study is based on a well-established vector correlation index - Modal Assurance Criterion (MAC), frequently used in the field of experimental modal analysis.

Results of application of the novel approach to explanatory case study are reported, pointing out how a rational methodology can guide towards the selection of the most appropriate analysis procedure. The operational modal analysis OMA using output-only technique has

been carried out to identify the modal characteristics through poly-reference.

## **5.2 KNOWLEDGE PATH OF THE STRUCTURE**

### **5.2.1 Knowledge path**

The knowledge path can be reconduct to manifold activities in order to make a final judgment on the safety and seismic knowledge, referring to the existing masonry buildings.

These activities can be described as a knowledge path that show different evaluation levels. Starting point is the identification of the buildings, in relation of the areas seismic risk with the urban context. In this context a basic information of the structure is collected which may affect the risk level. Following stage is the definition of the assets within a defined class for the seismic performance assessment. Within this context, the knowledge of the state of art represent the early stage of the assessment, basically point to comply with both prevention and reparation objectives.

Thus, the historical analysis and the in-situ investigation can represent a main tool for a qualitative approach sufficient to obtain a clear picture of the building safety. Last but not least, the monitoring plan, in order to follow the evolution of the degradation and damage phenomena over time and thus ensure the conservation of assets over the years.

### 5.2.2 Historical evolution

The building built since 1950 (Figure 5.1), has undergone few changes during the nineteenth century. In fact, the Palace of domanial own from 1953, was built above the remains of an old artefact masonry of the 1920's.

*“In 1925 the Corpo Reale of Genio Civile built on a wreck of the ex-National 2th road stretch no. 49, on behalf and with funds from the Ministry of Public Works. For the purpose of the work already mentioned, a masonry shed of external dimensions 15.00x5.80 m destined as a shelter for the workers and as a materials storage for the Corpo Reale of Genio Civile was built - Office of Campobasso”.*

During the period (1938 - 1941) it was turned into a public office with annex garage to service by the Genio Civile. On March 1951 an evaluation was carried out for the extension and restructure of the building. This document contains important news for more understanding the structural evolution of the artefact. In fact, the valuation is presented as a preliminary project of the structure, where the geometrical and structural details are described:

*“Along the State road no. 87, at the entrance of the Campobasso city, it existed for about 25 years, a masonry shack, by the State owned. The time, the inadequate foundations, the lack of maintenance and some indirect and slight consequence of military causes, have caused a gradual deterioration of it, by profoundly changing its stability. [...] the extension project, compatible with the total area and need to solve in the best way all the needs of the various offices not yet considered, has been attached. Thus, the building will have two*

## Chapter 5 - Field validation on an Italian masonry building

*new upper floor, in addition to the ground floor with a total area equal to 162 square feet. On the ground floor two distinct garages, separate by the stairwell has been obtained. The first floor has been organized with two small housing and the necessary services for the civil residences. On the last floor some spaces have been defined in accordance to the needs of the public offices."*



Figure 5.1. The artefact printing

Moreover, in that document are collected information relating the project of the structural scheme (Figure 5.2), in terms of: foundation typology, kind of material used, horizontal structures, texture and quality of masonry, thickness and profile, as reported below:

*"The plan will quite regular and compact, with overall dimensions 18.32 by 9.12 meters and it is 12.81 meters high.*

*The structural system, of the new building, will by ashlar masonry with a list recourse of clay brick masonry for every 60 cm of height, with hydraulics limestone mortar. Only the transversals walls of the stair, those of spine*



## Chapter 5 - Field validation on an Italian masonry building

walls, as well as the masonry walls of the second floor will be made by clay brick masonry.

Given the characteristic of the soil, are expected deep foundations especially in the Nord-West zone. However, to avoid the excessive depth (in terms of cost and time), the widen of the foundation plan has been considered.

The dimension has been evaluated so that the transmitted unitary load not exceeding the 2 kg/cm<sup>2</sup>. The foundation plans will be made by a proper continuous concrete block with a plinth section.

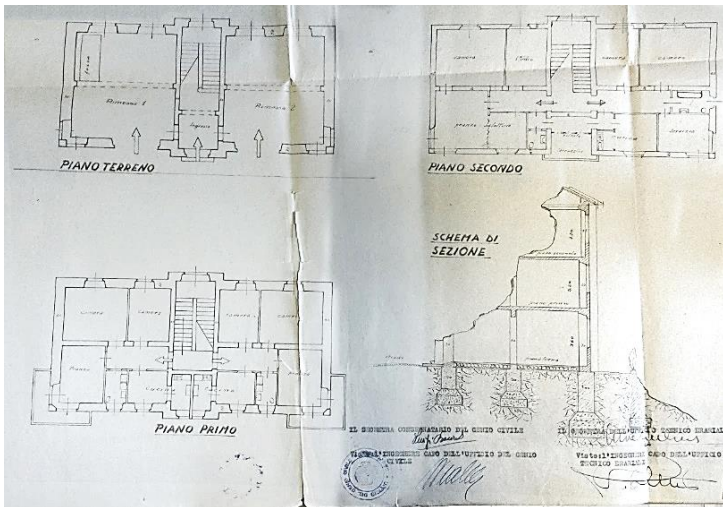


Figure 5.2. Plans and section of the building 1951

Mixed horizontal structures, kind S.A.P floor, with reinforced steel under the concentrated loads of the upper partition walls will be made. These are going to connect with a perimetric reinforced concrete curb from 20 cm of thickness for the first two floors and 15 cm under the cover plan. The roof of the

## Chapter 5 - Field validation on an Italian masonry building

---

*building will be realized by struts, purlins, and wooden beam with a roof tiles cover. [...]"*

The building was completed in June 1952, and from that date the inspection which was carried out only in June '53, as evidenced by the test certificate.

### 5.2.3 Structural assessment

In the path of knowledge, the phases of survey of mechanical and structural characterization of materials are aimed at defining the level of knowledge necessary for interpretation the seismic behaviour. An accurate historical analysis can be enables to limits the extensive investigations campaigns to obtain a clear information of the building safety. Moreover, a combined use of the qualitative approaches (historical and in-situ diagnosis), allow the execution only of non-destructive testing or weakly destructive, for obtained an adequate knowledge of the structural performance, and information on the quality of the materials and structural details.

In order to achieve a clear picture of the structure examined, it was necessary to lead a survey phase. Some parts of the structures were objected study, through non-destructive and weakly destructive surveys. The non-destructive evaluation (NDE) was used to validate the information derived from the historical stage and, for a preliminary assessment, sufficient to define the critical situations that needed a more accurate evaluation. Unfortunately, most of the procedures can give only qualitative results; therefore the results are

## Chapter 5 - Field validation on an Italian masonry building

used as an comparative values between different ND analysis of the same masonry wall.(L. Binda, Saisi, & Tiraboschi, 2000)

Main goal of the weakly destructive tests (WDT) it was to characterize the typology of the masonry for the different levels, the quality of the connection between the walls, presence of adequate structural details between walls and the horizontal structures ( curbs, typology of floor).

The investigation activates has been organized in this way:

- Thermography: An important survey tool to obtain structural information. This investigation tool was used as to support the further qualitative data (historical, geometrical) and to found semi-quantitative information through by further ND tests, in order to complete the knowledge stage. The choice of the points to be investigated has been made in operation of the information retrieved around the origin and the historical evolution of the building
- Endoscopic tests: direct visual inspection of cavities or further inaccessible parts inside the walls and the horizontal structures;
- Slightly destructive testing : To understand the morphology of a masonry wall, direct inspection in order to qualify the state of preservation of stone or brick masonry walls , the presence of multiple leaves and their type of connection (L Binda & Saisi, 1996).

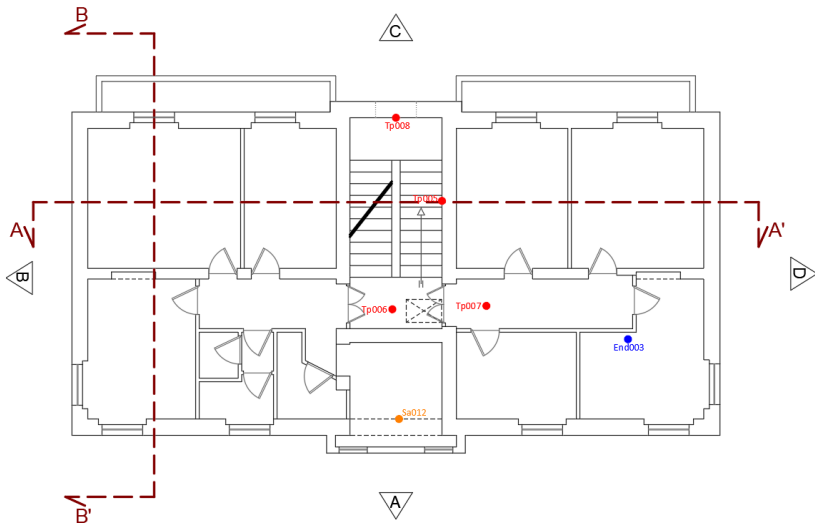


Figure 5.3. Plan of the building in which the relevant investigations are marked

In order to have a clearly knowledge of this stage, a detailed of the in-situ inspection of the building was produced. Figure 5.3 illustrates the building plan, in which the relevant parts investigated with the different technique it has been subjected to, are marked.

The investigation techniques applied are been according to the following code:

- Tp: passive thermography in red;
- End: Endoscopic tests, in blue;
- Sa: slightly destructive testing, in orange.

#### **5.2.4 Description of the structural systems**

The information derived by the geometry relief is associated to the accuracy with which the geometry of the building is represented in the actual spatial configuration, that is enriched by reading and restitution of the cracks described in the salient characteristics that qualify their position, size, and extension.

Results of the geometry relief shows a quite regular and compact plan (Figure 5.4), with overall dimensions 18.32 by 9.12 meters and it is 12.81 meters high. The perimeter wall thickness varies between 0.40 m and 0.75 m at the ground floor, while it is thinner at the upper levels.

During the survey activities conducted on the structural parts of the building, have been identified the weaving of masonry walls for the different levels.



## Chapter 5 - Field validation on an Italian masonry building

Infrared thermography proved itself to be an effective, convenient and economical method used in the conservation field to detect hidden characteristics of building (structural changes, presence of cavities, pre-existing forms, texture of walls, frame of floor, structural abnormalities). The image acquisition module is an instrument that allows to distinguish the temperature distribution on the objects surface (R. Plescu, et al. 2012).

The result is a thermal image in colour scales associating differences in tones at intervals of temperatures of the order of the fraction of a centigrade degree. The fast and accurate diagnostics for the façades and the large monitoring capacity, represented the main advantages of using the thermography for this case study.

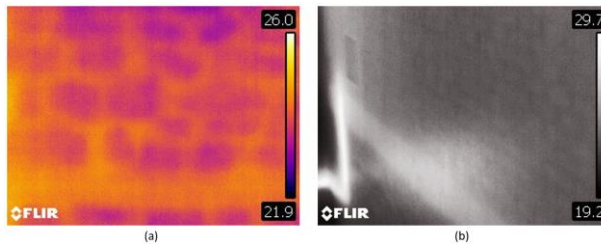


Figure 5.5. Result of thermographic testing of walls: a) ground floor; b) first floor

An infrared thermos camera type FLIR E60bx was used for the relief structures. The camera has the following technical specifications: *IR resolution - 320x240 pixels; Spectral range 7.5-13 m $\mu$ m; FOV - 25 ° $\times$ 19 °; Spatial resolution - 1.36 mrad; Thermal sensitivity <0.045 ° C; Frame rate 60 Hz; Manual focusing; Focal Plane Array (FPA) - Uncooled microbolometer.*

## Chapter 5 - Field validation on an Italian masonry building

---

The passive thermography was used to identify the weaving of masonry (Figure 5.5) and the eventual presence of openings that have been closed respect during the 1953's interventions.

A further confirmation about the type of construction was obtained from the information acquired during the endoscopic and semi-destructive investigations carried out on the walls.

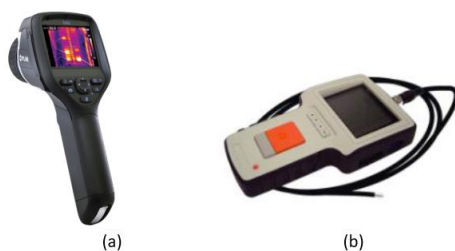


Figure 5.6. a) infrared thermos camera type FLIR E60bx; b) endoscopy

The endoscopy has been allowed a direct inspection of cavities or other inaccessible parts inside the walls. Through this instrumentation, it has been possible the understanding of all wall thickness (single or multiple-leaf walls, internal voids and flaws), with a view to identify the composite material as well as the characteristics of wall section.

The system used has the following features a 3.5" full colour LCD Screen (Figure 5.6), a slim 8.2mm diameter probe with 6 adjustable LED lights, a high performance camera module with crystal clear output. and an integrated 1W CREE flash light for dark area working assistance.



## Chapter 5 - Field validation on an Italian masonry building

Given the presence of different cross-sections and the great influence of the construction technique on masonry behaviour, a direct investigation for understand the morphology and building techniques has been used. The masonry texture, presence of horizontal courses, dimension of the elements and type of connection for the cross walls section, are some of parameters defined.

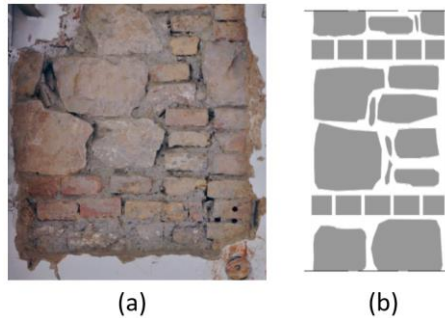


Figure 5.7. Direct investigation: a) front of Masonry Class A3 - Group Ib ; b) cross sections

The analysis allowed to identify two different masonry classes. First and the second level are characterized by *Masonry Class A3 - Group I b* : masonry in compact limestone and mortar of lime and aggregates in limestone; with a homogeneous and undifferentiated texture (Figure 5.7). This class of masonry is characterized by the adjustment of set blocks horizontality at intervals more or less regular in height, and realized through the introduction of elements of particular size "*Ricorsi e listatura*".

## Chapter 5 - Field validation on an Italian masonry building

---

The *Brickwork* characterize the second floor and the attic, by the presence of solid bricks in shape and regular texture (Figure 5.8). The various layers of bricks are connected to each other by layers of mortar.

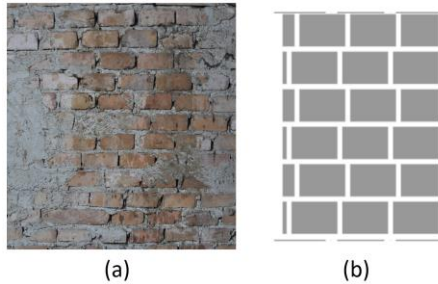


Figure 5.8. Direct investigation: a) front of Brickwork; b) cross section

As regards the horizontal structures, the investigations have been conducted to acquire some parameters like: floor typologies, structural details, geometric aspects, connection quality with walls.

The passive thermography provided an important support to identify the weaving of the floors (Figure 5.9. a). At the same time, the endoscopy test confirmed the assumptions made on the basis of existing literature.

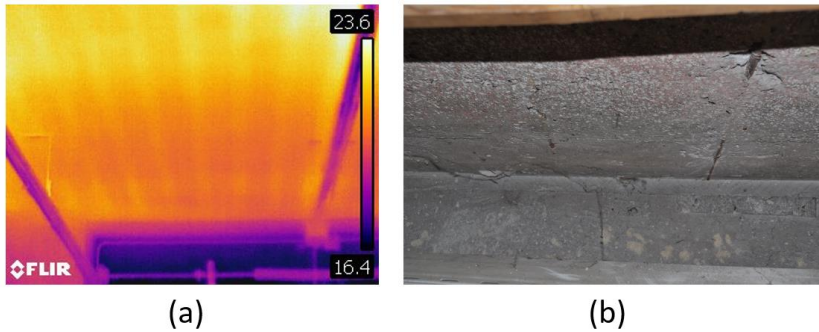


Figure 5.9. a) IR image of weaving floor; b) detail of concrete curb

The building is characterized by S.A.P floor (Figure 5.10) for the first three levels. Introduced in Italy around 1930, and largely employed up to the years '60, today represent a rather common typology for the building heritage.

In that specific case, it is made up beams assembled through installation of reinforcing bars (smooth and from the reduced diameter) in special holes predisposed in the hollow clay block and seals through mortar. The beams among them are approached for the realization of concrete casting completion.

The horizontal structures are effectively connected to perimetric walls with a reinforced concrete curb ( thickness 20 cm) for all levels.

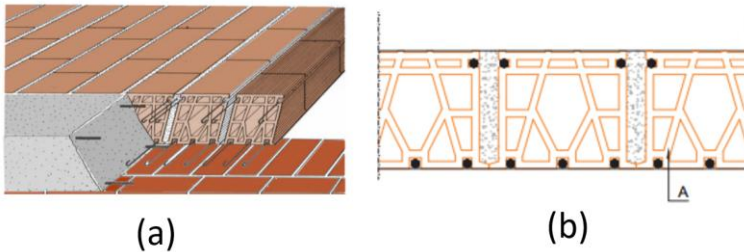


Figure 5.10. a) detail between S.A.P and concrete curb; b) cross section of S.A.P. ([www.leca.it](http://www.leca.it))

While the roof is made by two wooden trusses (Figure 5.11) with 8 m wheelbase and a poor connection to the perimeter walls . The wood beams ( square section 15-20 cm) with the wooden floor define the cover package.



Figure 5.11. View of the wooden trusses

## 5.3 DESCRIPTION OF THE NUMERICAL MODEL

### 5.3.1 Introduction

Numerical analyses are often very complex due to significant uncertainties in the characterization of material properties and structural behaviour. Besides, the reliability of seismic analyses is often jeopardized by the need of defining an appropriate structural and dynamic model.

The unique structural configurations, the old construction techniques and the presence of stratified structural modifications occurred over the centuries make the definition of an appropriate and reliable numerical model very challenging.

The aim of investigation process is the acquisition of clearly knowledge of the artefact for defining a suitable and accurate numerical model. Modern instruments and software packages for the architectural and structural representation are effective options for the analyst, so that detailed modal analyses can be carried out.

Several models, with different theoretical approaches have been available (Lagomarsino & Cattari, 2015). For this case studied the structural model was carried out through the SAP2000® V.15, a software set widely used by practitioners, for seismic assessment of masonry buildings. In the next paragraph, the global modelling used for the preliminary numerical dynamic analysis is described.

### 5.3.2 Equivalent Frame Model

One of the most widespread structural model used by practicing engineer , and suggested also by main national and international is the Equivalent Frame models (EF). In such method masonry wall is discretized by a set of non-linear macroelements (reproducing masonry piers and spandrels), connected by rigid links. The structural macroelements are identified a priori.

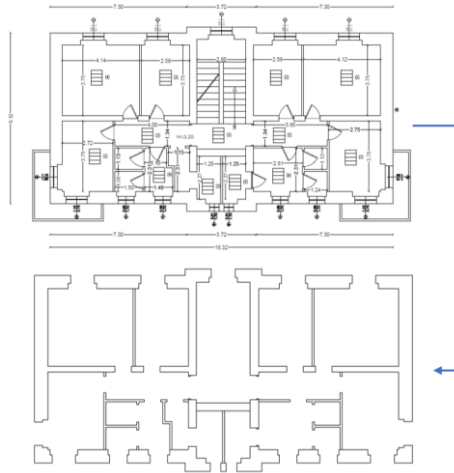


Figure 5.12. Identification of the main structural system

The construction of the undamaged EF model was fundamental to simulate the dynamic and seismic behaviour of the building. For the realization of the model have been adopted a previously phase with a CAD software. Particularly, the available geometric survey of the

## Chapter 5 - Field validation on an Italian masonry building

building has been simplified (Figure 5.12). In this way the geometry is brought back to indication of walls and openings.

Once defined the middle lines to the various levels, they have been overlapped with the purpose to determine an only valid line for everybody levels. Following this, the panels was positioned, in plant and in prospectus, on the line axle of global reference. In this way an alignment of the walls along the vertical one has been obtained. The last step was the definition of the equivalent frame for every wall, getting a simplified 3D geometric model of the building (Figure 5.13).

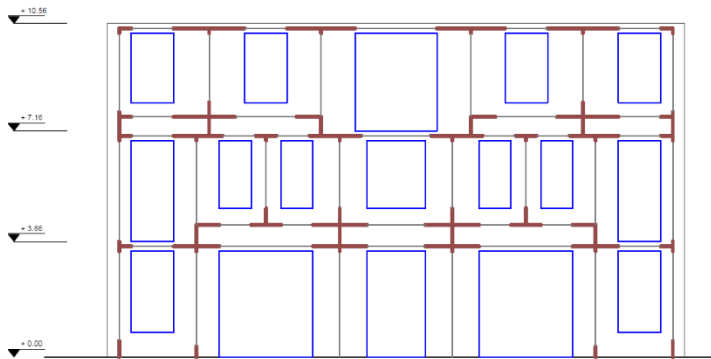


Figure 5.13. Analysed building: drawing of the equivalent frame

The 3D model CAD has been imported directly in SAP2000 for the structural assessment. Every line is recognized in the software as an element frame in the space with six degrees of freedom (three translations and three rotations around the axes ) according to the directions of reference system. Each pier and spandrel beam were defined by frame elements with the equivalent cross section dimension

## Chapter 5 - Field validation on an Italian masonry building

and height. To take the coupling effect between piers and spandrels in account, rigid offsets was assigned at the ends of the frame elements. The rigid length offset of the piers was determined based on an empirical approach proposed by Dolce 1989 Whereas the rigid length of the spandrel beams was defined in according to the method proposed by (Calderoni et al. 2015). Due to the irregularity of the openings, additional rigid elements were introduced to make the connection between the elements that are not aligned.

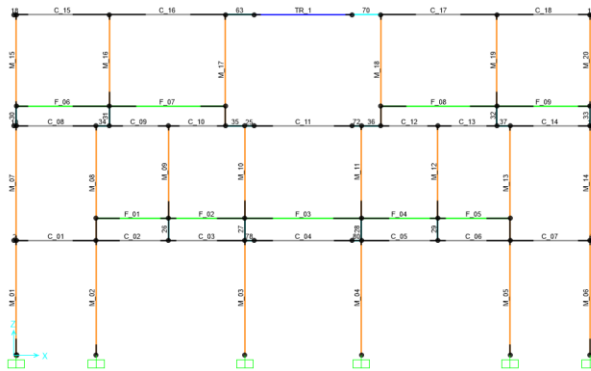


Figure 5.14. SAP modelling: equivalent frame

These elements of the EF model are characterized at the base by perfect constraints and additional rigid elements were introduced to make the connection between the cross section walls for optimize the load distribution. The result of 3D equivalent frame model is presented in Figure 5.15. The model was used to predict the numerical estimation of modal parameters.



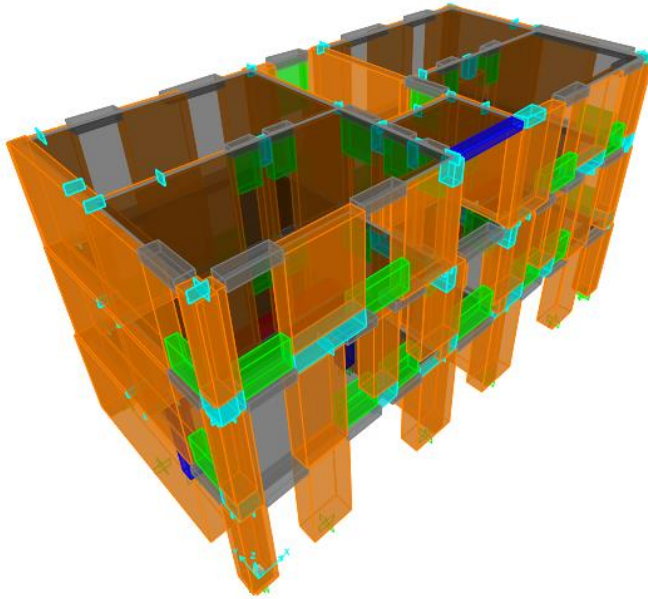


Figure 5.15. Equivalent Frame Model of the building

The model was used to predict the numerical estimation of modal parameters. Moreover, the numerical simulation has been used to predict the location for the reference transducers and the number of points to measure, in order to have enough resolution in the mode shape, as Operational Modal Analysis was chosen for evaluation of dynamic parameters. A modal dynamic analysis has been carried out to estimate all the modes, including the out-of-plane and torsion modes.

## Chapter 5 - Field validation on an Italian masonry building

Table 5.1 and Table 5.2 summarises the parameters adopted for the model. The mechanical properties are derived from the information acquired during the knowledge path. The mechanical properties of the walls have been defined with reference values present in the Italian Code (NTC2018) and to consider the correction coefficients to be applied in the presence of good quality of mortar and presence of courses. The compression strength is considered as  $f_m/1.35$  FC. While, the tensile strength was developed from a ratio of 5% of the compressive strength.

Masonry typology	$f_m$	$\tau_0$	E	G	W
	[MPa]	[MPa]	[MPa]	[MPa]	[kN/m <sup>3</sup> ]
	min-max	min-max	min-max	min-max	min-max
<b>Cut stone masonry, good bond</b>	2.60	0.056	1500	500	
	3.80	0.074	1980	660	21
<b>Full brick masonry with lime mortar</b>	2.40	0.06	1200	400	
	4.00	0.092	1800	600	18

Table 5.1. Reference value for the masonry mechanical parameters

While for the concrete and steel elements has been considered the mechanical properties derived from the norm code of the construction period referred. For the steel bars has been used STIL v1.0 software (Verderame et al. 2011), which allows to perform the search inside a database for the principal mechanical characteristics of the steels. The search is based on the time range, the typology, from the certificates of the steel bars tested. In the time range selected the software show the

Chapter 5 - Field validation on an Italian masonry building  
 yield point stress distribution, strain hardening, as well as the  
 percentage values of use for the different steel categories.

	CLS Rck 300		STEEL FeB22k		
$R_{ck}$	300	[kg/cm <sup>2</sup> ]	$\sigma_{s,amm}$	120000	[kN/m <sup>2</sup> ]
$\sigma_{c,amm}$	9750	[kN/m <sup>2</sup> ]	$\tau_{c0}$	600	[kN/m <sup>2</sup> ]
$E$	31475806,2	[kN/m <sup>2</sup> ]	$\tau_{c1}$	1829	[kN/m <sup>2</sup> ]
			$E$	206000000	[kN/m <sup>2</sup> ]

Table 5.2. Reference value for the concrete and steel mechanical parameters

The assumed constitutive model was heterogeneous, anisotropic and largely influenced by the constitutive materials and constructive system. The masonry behaviour is idealized as a homogenous and isotropic material, characterized by the Young's modulus and the Poisson ratio. The masonry piers and spandrel beams are defined with elastic behaviour, while the nonlinear behaviour is assigned with concentrated plasticity (Simões, et al. 2012). Figure 5.16 shown an example of the distribution of the plastic hinges location in the equivalent frame model of the wall facade.

The horizontal structures is effectively connected to perimetric walls with a reinforced concrete curb ( thickness 20 cm) for all levels, for this reasons a rigid diaphragms was considered in the model.

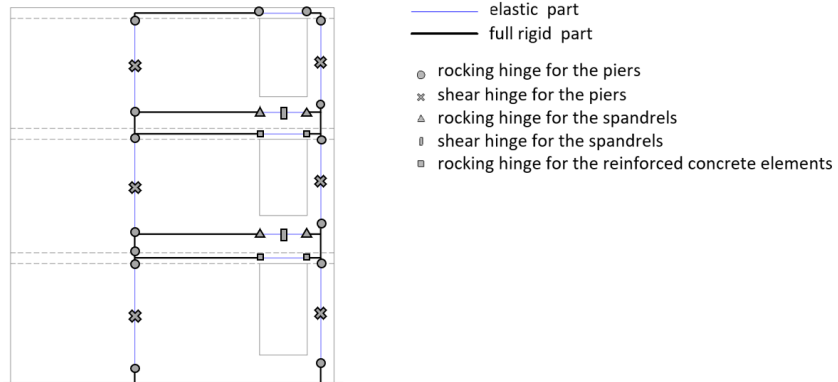


Figure 5.16. Modelling building: plastic hinges' location in the equivalent frame model of the wall façade.

The preliminary model analysis allowed to characterize the seismic behaviour, for the purpose to optimize the design of the experimental dynamic structural monitoring. Global structural systems have been subjected to elastic numerical analysis.

The main significant EF analysis's outcomes are the frequencies and the real modal mass to detect the principal modal shapes.

In this case, the dynamic response is influenced by the modelling condition of the bearing walls and also by the connection degree of the walls and the floor behaviour (rigid or deformable). The first two modal shapes are characterized by flexural modes (Figure 5.17. a, b) and the third by a torsional one (Figure 5.17 c).

The results of the modal dynamic analysis show a homogeneous structural behaviour, as a matter of fact, there is a high participating

Chapter 5 - Field validation on an Italian masonry building  
 mass calculated for the main first modes, equal to 85% in the X direction, 78% in the Y direction and 79% for the torsional mode shape.


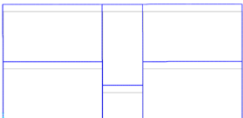

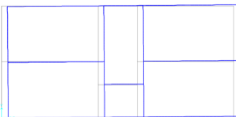

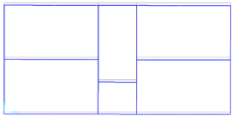
MODE SHAPES		
Mode 1	Mode 2	Mode 3
 <p>f = 5.43 Hz P.M.R. = 85 % (X dir.)</p>	 <p>f = 5.81 Hz P.M.R. = 78 % (Y dir.)</p>	 <p>f = 7.19 Hz P.M.R. = 79 % (RZ dir.)</p>
Mode 4	Mode 5	Mode 6
 <p>f = 14.21 Hz P.M.R. = 9 % (X dir.)</p>	 <p>f = 14.93 Hz P.M.R. = 14 % (Y dir.)</p>	 <p>f = 16.93 Hz P.M.R. = 5 % (Y dir.)</p>

Figure 5.17. Principal mode shapes

## **5.4 DYNAMIC IDENTIFICATION SYSTEM**

This paragraph presents the experimental identification carried out in the context of the Agreement for an experimental project with the University of Molise and the Regional Command of the Guardia di Finanza (Italian Finance Police), in the framework of novel procedures for the seismic assessment of existing masonry buildings.

The operational modal analysis OMA using output-only technique has been carried out to identify the modal characteristics through the stochastic subspace identification techniques were chosen based on the discussion given in Chapter 2. The choice configuration of the sensors depends on the type of monitoring, accuracy, budget compliance, computational burden, durability and ease of use (Gargaro 2018). It's possible considered three different types of monitoring systems: short-term monitoring, periodic monitoring and in-continuous monitoring. The short-term monitoring aims at the identification of the dynamic parameters for the structural characterization, while the period and in-continuous monitoring guarantees in addition the estimation of structural degradation and damage.

### **5.4.1 System identification test**

The dynamic response of the case study has been analysed by means accelerometer sensors, and the monitoring of them was carry out through three different layouts. The dynamic sensors, produced by PCB Piezotronics, are piezoelectric axial accelerometers, with nominal sensitivity of 10 V/g, range interval 0.5 g pk.

## Chapter 5 - Field validation on an Italian masonry building

Different *PCB Piezotronics* accelerometer (Figure 5.18) models has been used for these tests:

- a) Model 393B05: sensitivity 10 V/g, , range interval 0.5 g pk;
- b) Model 393B12: sensitivity 10 V/g, , range interval 0.5 g pk;
- c) Model 393B31: sensitivity 10 V/g, , range interval 0.5 g pk

The sensors have been connected to data acquisition system (DAQ) through coaxial cables to low impedance.

For these sensors coaxial cables of the type RG-58 has been used with BNC connectors for the DAQ connection and MIL-C-5015 for connection to the sensor (Figure 5.19).

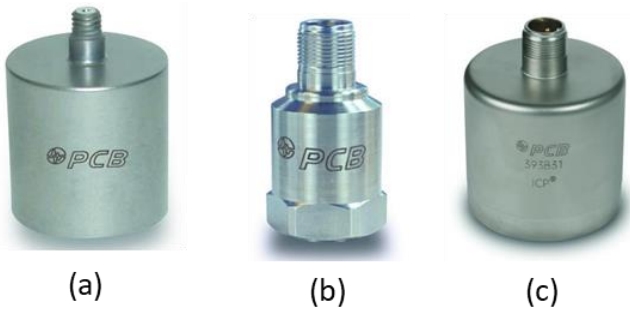


Figure 5.18. PCB models: capacitive accelerometer



Figure 5.19. Coaxial cable for the piezoelectric accelerometers with MIL-C-5015 BNC connection ([www.pcb.com](http://www.pcb.com))

Being the cables very sensitive to the noise, these has been fixed to the structure until to the acquisition system (Figure 5.20), so that to avoid interferences with the other installations present.

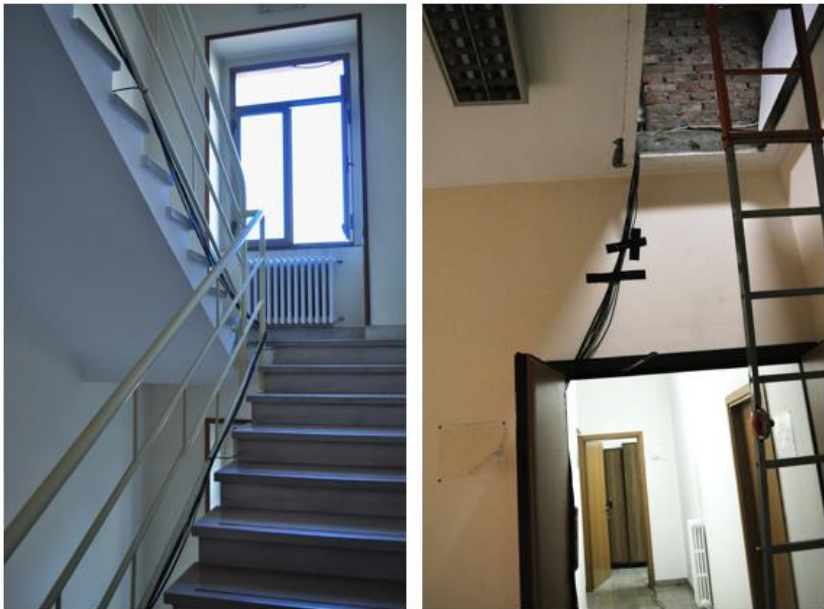


Figure 5.20. The cables system



## Chapter 5 - Field validation on an Italian masonry building

The hardware present four channels installed on a modular controller. The module is ideal for the acquisition of the dynamic signal and is proper for measures of frequency. The four channels in input perform the simultaneous digitization of the signals to maximum frequency of 51.2 kHz for channel and they include filter aliasing. As shown in Figure 5.21, the chassis contain a maximum of 8 modules with the possibility to acquire 32 acceleration measurement.



Figure 5.21. Modular chassis and modules for the acquisition system.

### 5.4.2 Dynamic identification campaign

In order to check the dynamic investigation procedure showed above, an experimental campaign has been conducted by output-only techniques. The number of sensors is limited to improve the stability of signal and to speed up the installation activities.

The accelerometers have been fixed to the structure through interposition of rigid plates (Figure 5.22), so that the frequency range

## Chapter 5 - Field validation on an Italian masonry building

on interest is not biased. Normally the minimum number of sensors for each level is 4, in the mirror position of the corners, so that to be able to also identify the torsional component.

Having available a maximum number of 29 accelerometers (budget compliance) these they have been installed on nine vertical alignments with six sensors per alignments have been positioned for the all building. In addition, 4 sensors (ch1, ch2, ch3, ch4) positioned on the floor has been used for the reference. Therefore, have been carried out three different acquisition , in the first run was used 29 sensors to monitor the global horizontal response and the first three verticals. In the second and third layout respectively was used 16 and 28 sensors.



Figure 5.22. a) View of the installed sensors; b) detail of the sensor with the plate

The acquisitions were of type multirun reconnected by means of process scaling, being focused on the following points of reference

Chapter 5 - Field validation on an Italian masonry building measurement. The Figure 5.23 summarize the positions and correspondence channel sensor of the accelerometers used.

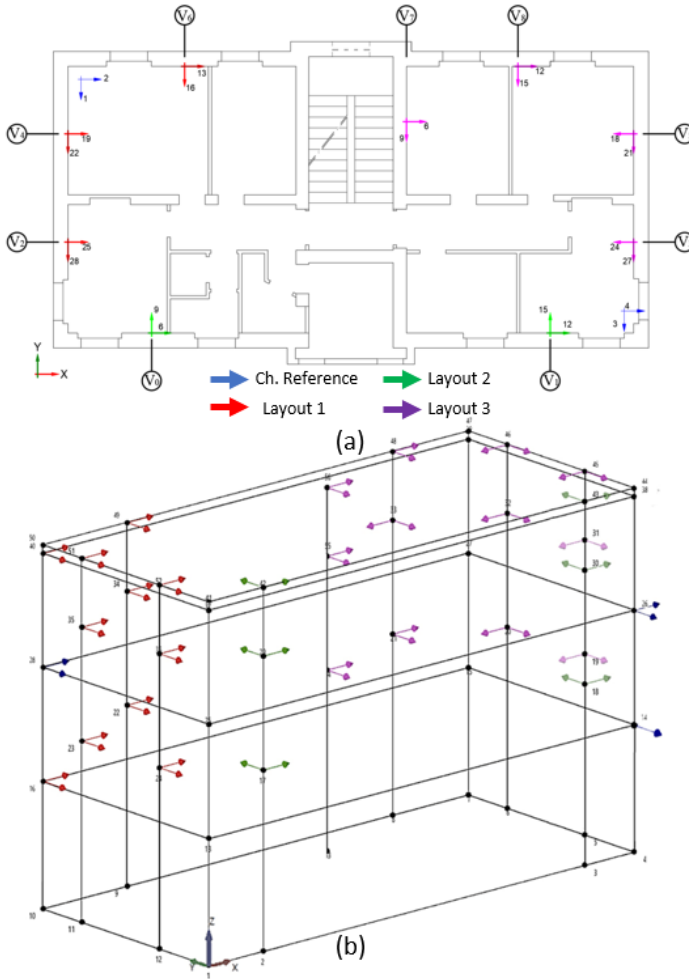


Figure 5.23. Experimental monitoring: a) plan view of the localization of the sensors; b) global view of the verticals

Data acquisition is carried out by a measurement device with 16 bit resolution and on-board anti-aliasing filter. The data acquisition hardware is managed by software developed in LabView environment.

### 5.4.3 Identification of modal parameters

The collected raw data are stored into a local MySQL database. A sampling frequency of 100 Hz is adopted. The acquired data are continuously processed by an innovative fully automated OMA procedure. Data processing was performed using ARTeMIS Modal software (SVS, 2018), in the framework of the research activities carried out by the first author at the University of Minho. After data pre-treatment, the modal parameters of the building has been identified through the Frequency Domain Decomposition (FDD) and Stochastic Subspace Identification (SSI) methods (Brincker et al. 2001) as defined in the Chapter 3.

In all measured degrees of freedom are presented (Figure 5.24) on the test geometry used by the operational modal analysis software ARTeMIS Extractor.

The measurements were conducted using 3 different layout measurement system for 3600 seconds. Most of the relevant natural frequencies of the building are below 10 Hz. Therefore, a decimation of order 50 was applied before the operational modal analysis, reducing the sampling frequency from 100 Hz to 25 Hz.

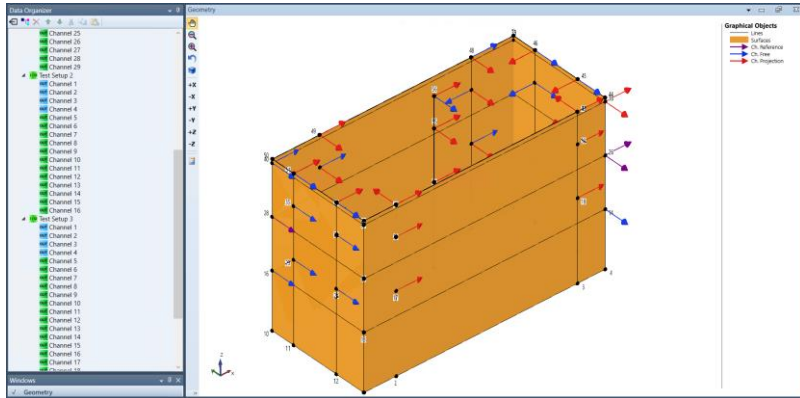


Figure 5.24. The Assign DOF Information Task displaying all sensors of the three test setups. The purple arrows are the reference sensors.

The modal frequencies, and mode shapes were determined by applying both methods, while the damping ratios it was obtained using only the SSI procedure.

The data were later correlated using the Modal Assurance Criterion (MAC) between both sets of results, in order to assess the accuracy of the obtained mode shapes.

In the experimental result shown that only the first five modes can be adequately estimated. Below the one and only Stabilization Diagram is shown.

It displays the Singular Values Decomposition (SVD) of the Spectral Densities of all the Test Setups with an indication of all the global modes based on all Test Setups.

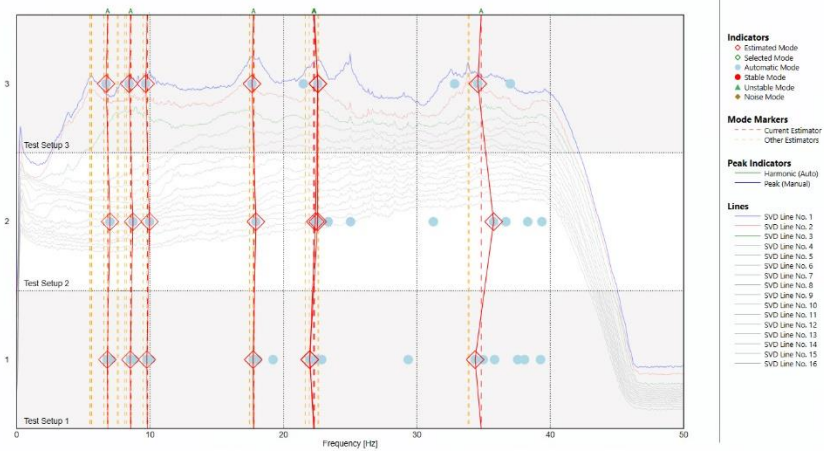


Figure 5.25. Stabilization diagram for SSI techniques from ARTeMIS

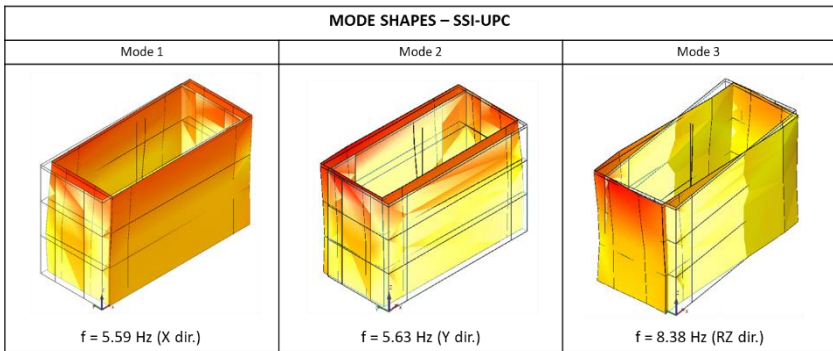


Figure 5.26. Mode shapes of experimental data

The first mode was found at a frequency of 5.59 Hz with a damping of 8.67%, the second mode to 5.63 Hz with a damping of 6.39% and the third mode to 7.92 Hz with a damping of 8.38. It is possible to see in

## Chapter 5 - Field validation on an Italian masonry building

Figure 5.26 that first three modes present, in accord with the predict numerical model, a flexural mode shapes and torsional mode.

The main outcomes of the experimental analyses are summarized in the following table.

FDD			SSI - UPC			MAC
Mode	Type	f [Hz]	f [Hz]	$\xi$ [%]	Complexity [%]	[-]
1	Tran. X	5.52	5.59	8.67	2.52	0.96
2	Tran. Y	5.61	5.63	6.39	0.76	0.99
3	Rot. in Z	7.52	7.92	8.38	1.46	0.97

Table 5.3. Results OMA: natural frequencies (f), damping ( $\xi$ ) and MAC

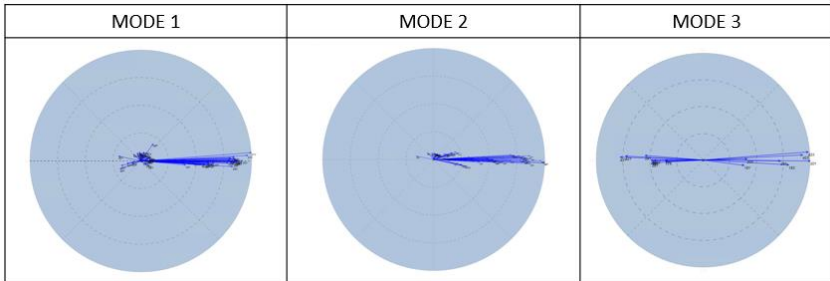


Figure 5.27. The complexity plots for the corresponding mode shapes

The results of the modal frequencies and mode shapes was have been assessed and validated extensively, as shown in Figure 5.27 by the complexity plots. The latter can effectively represent in a graphic way the nature of the modes. In this case, all the modes are real, since the imaginary component is actually low. Conversely, the values of damping, whose calculated value are about 5-6%, are affected by a

## Chapter 5 - Field validation on an Italian masonry building

---

certain bias. Validation of the above-mentioned values estimated by the ARTEMIS software has been made by making the same calculation by means of the ARES® software (acronym for Automated modal paRameter Extraction System, Rainieri & Fabbrocino 2015) and obtaining the same estimate. This circumstance lead recognize that operational conditions and related recorded levels of vibration where not fully satisfactory, leading to basically miss the correct estimation one of the modal reference parameters, like the damping ratio is.

With the aim of updating the numerical model and better define the most relevant mechanical parameters of the structure, in the following the results of a modal analysis of the model are compared with the experimental ones.

The first three eigenfrequencies and mode shapes are used to check the FE model. The horizontal displacement components  $u_x$  and  $u_y$  along the floor measurement points are used for the tuning.

The comparisons show good agreement for the translation mode shape but with more difference for the very sensitive and low signal in torsional mode shape.

This can be related to the presence of a floor with a rigidity lower than the one adopted in the numerical model and eventually a different degree of connection between the cross walls.

Table 5.4 shows x, y translational and torsional mode shapes obtained from the ambient vibration measurements compared with those from the EF model analyses.



Mode	SAP2000	SSI-UPC	error	FDD	error
	[Hz ]	[Hz ]	[%]	[Hz ]	[%]
1	5.43	5.59	2.86	5.52	1.61
2	5.81	5.63	3.20	5.61	3.55
3	7.19	7.92	9.22	7.52	4.17

Table 5.4. Comparison between numerical and experimental values of the natural frequency of the fundamental modes of the building

#### 5.4.4 Assessment of the modal shapes by means the MAC based procedure

According to the procedure illustrated in the Chapter 4 the MAC index has been carried out for each deformed shape evaluated as related to the selected verticals.

The matrix graph shows the MAC results, computed in according to the equation between all couples of vertical alignments of virtual sensors. MAC matrices assume for the evaluated modes as reference the selected threshold value of 0.9. In the case of the first experimental mode, the histogram, highlight as much values always exceed the threshold specified.

In the case of the flexural global mode, the histogram, highlight as much values always exceed the threshold specified (Figure 5.28). In this case the final shape modes were obtained from the merger of the individual measurement previously in the three runs.

Thus, all nine sensors alignments have been considered in the MAC analysis as shown in the histogram (Figure 5.28c). These configurations

## Chapter 5 - Field validation on an Italian masonry building

can be associated to the so-called "box behaviour" with a typical global behaviour of the structure.

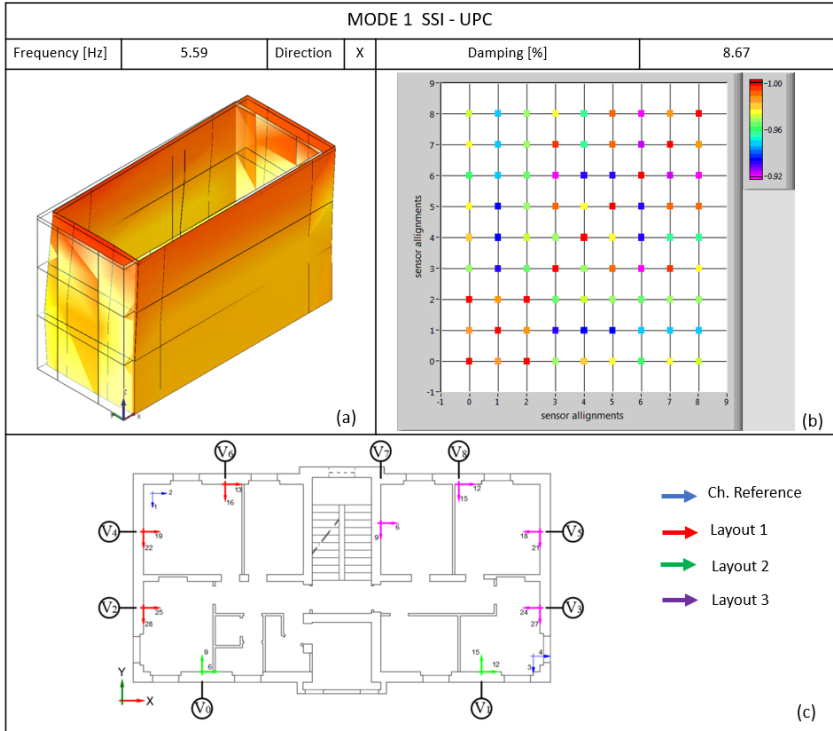


Figure 5.28. Results: a) The shape mode; b) MAC matrix associated with torsional mode; c) Location of the verticals

This means that the building tends to behave as a global unit and the potential collapse can be derives from the in-plane damage of several masonry structural elements.

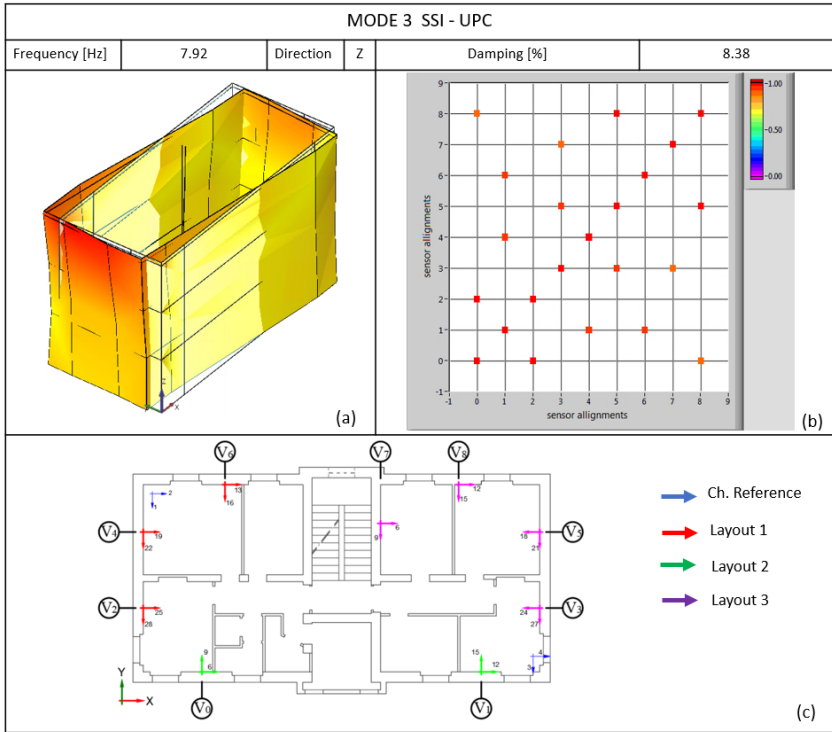


Figure 5.29. Results: a) The shape mode; b) MAC matrix associated with torsional mode; c) Location of the verticals

Also, the torsional mode (Figure 5.29) from the calculation of the cross-power spectra of all sensors has identified, but with the, but reducing the sampling frequency at 25 Hz in order to investigate only a narrow bend frequencies.

In the case of torsion mode and isolated building, as well as shown in the numerical simulation, the largest MAC values are located along the

main diagonal and the main anti-diagonal, point out a box behaviour of the building. However, the histogram results of the spatial distribution vertices that produce large MAC values (greater than 0.9) it's also located between the adjacent verticals (e.g. Vert.0 and Vert.2 or Vert.5 and Vert.8). Such condition underlines the influence of the horizontal structures in the knowledge of the structural behaviour, as well as seen in the numerical simulation.

## 5.5 CLOSING FINAL REMARKS

The present Chapter shown the potential of the dynamic identification as non-destructive tool in the knowledge path of the existing masonry buildings. The use of ambient vibrations as bases of excitation is then mainly effective in the assessment of the dynamic behaviour of the heritage structures, because this procedure suggests a preservation care unlikely nearby with other methods. Attention has been focused on the potentialities of the MAC index to distinguish a global or local response from the analysis of the spatial distribution of MAC computed between modal displacements associated to selected alignments. The procedure it is easy to manage, and it can offer some advantages in the classification of the dynamic behaviour. The case-study of an isolated masonry building is presented to evaluate the method capability. The natural frequencies identification has been performed by using established methods for dynamic identification.

## Chapter 5 - Field validation on an Italian masonry building

Given the global behaviour of the building analysed, classified as structure which tend to an isolated building behaviour, no appreciable local modes have been identified as expected. Encouraging results have been obtained. However, further analyses and other validation of the proposed methodology are needed in view of its extended use as survey tool in the knowledge path.



## Chapter 6

# DAMAGE ASSESSMENT: AN OLD ARCH REPLICA

### 6.1 INTRODUCTION

The evaluation of the structural conditions is needed to plan cost-effective remedial measures, before the extension of damage leads the systems to stop operation, requiring expensive in depth interventions. Nowadays, the availability of inverse approaches contributes to overcome this problem allowing to characterize the 'unknown' parameters of a structure by the identification of its dynamic properties. Moreover, the direct interdependence between dynamic and physical properties makes modal-based methods suitable tools for detecting the structural damage.

For the purpose of this work, damage can be considered as an adverse condition that compromises the structural integrity of a system and affects its performance in terms of load-bearing capacity of the structural elements, materials strength and, stiffness.

## Chapter 6 - Damage assessment: an old arch replica

---

The alterations induced into the system by the damage and the reversibility of the process depend on the severity and size of the damage and last, but not the least, on the number and type of elements involved. The stiffness degradation due to the loss of structural integrity will be reflected in changes of the properties of the system in terms of modal parameters (frequencies, mode shapes and damping ratios). The possibility to easily measure these quantities has been fostering their use as damage indicators in all engineering fields (Abdel Wahab & De Roeck, 1999).

The main scope of this study is the evaluation of a robust spectral-based algorithm able to detect, locate and assess the structural damage, suitable for both output-only and input-output dynamic identification techniques, independently of the excitation sources, and applicable to any type of structure (Masciotta et al. 2016)

To pursue this goal, the procedure will be tackled according to an analytical approach that combines both numerical and experimental activities.

The present Chapter describes the experimental campaign carried out on the masonry arch replica built at UMinho Lab in 2018. The arch model was built in the laboratory where a controlled damage not recoverable (support movement) was applied. The dynamic response of the system was processed based on the spectral output.



## 6.2 ARCH MODEL DESCRIPTION

### 6.2.1 Arch construction description

Two scaled replicas of an ancient masonry arch were built in a semi-circular shape (0.95 m radius, 1.90 m span, 0.44 m. width and 0.05 m thickness, Figure 6.2).

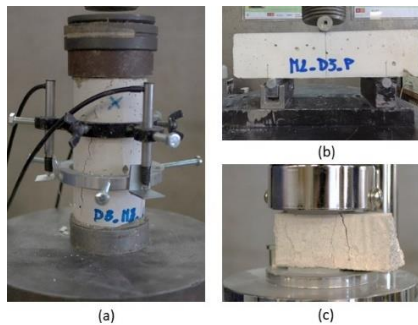


Figure 6.1. a) Mortar Cylinder compression test for Elastic modulus; b) flexural strength test of prism specimen; c) compressive test of prism specimen

They were built by using low compressive strength clay bricks ( from the Northern area of Portugal) with  $100 \times 75 \times 50 \text{ mm}^3$  and were bounded using REABILITA mortar (approximately 5 mm thickness) with low mechanical properties (Elastic modulus  $E_{\text{med}}=3375 \text{ MPa}$ ; compressive strength  $f_{c,\text{med}}=2.02 \text{ MPa}$ ; flexural strength 1.1 MPa), to make the construction compatible with the materials used in historical constructions. All the arches were constructed with 39 brick courses, Figure 6.2 shows a geometrical plan of the model.

## Chapter 6 - Damage assessment: an old arch replica

The abutments, initially, were made of concrete over rectangular steel plates fixed to the laboratory floor. The arches were built, over a wooden mould keeping a constant intrados mortar joint thickness of 10 mm.

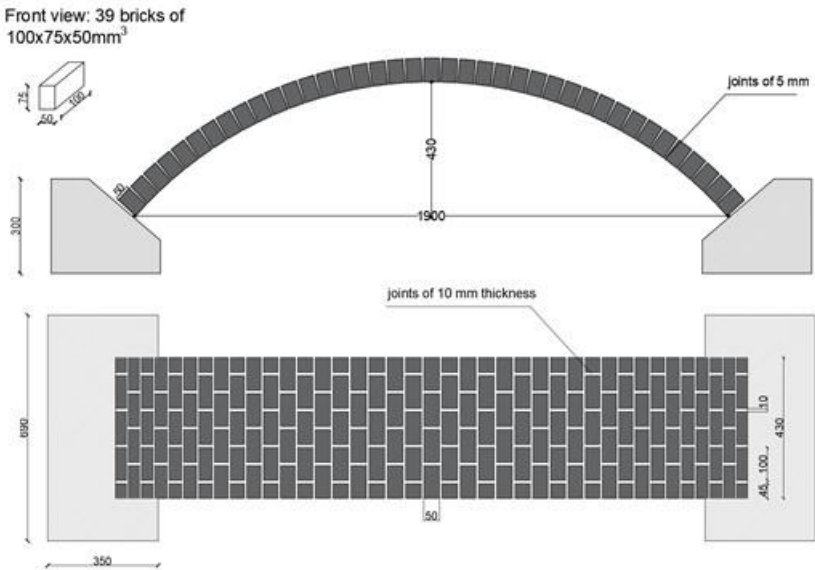


Figure 6.2. Arch geometry

The masonry arch structure was built in two consecutive phases, the first layer of bricks was laid over the formwork starting from the right abutment up to crown perimeter of the arch, as shown in Figure 6.3a. After that, following the same technique starting from the left abutment, in the end the key brick was laid such that the joint thickness could be tuned as shown in Figure 6.3b.

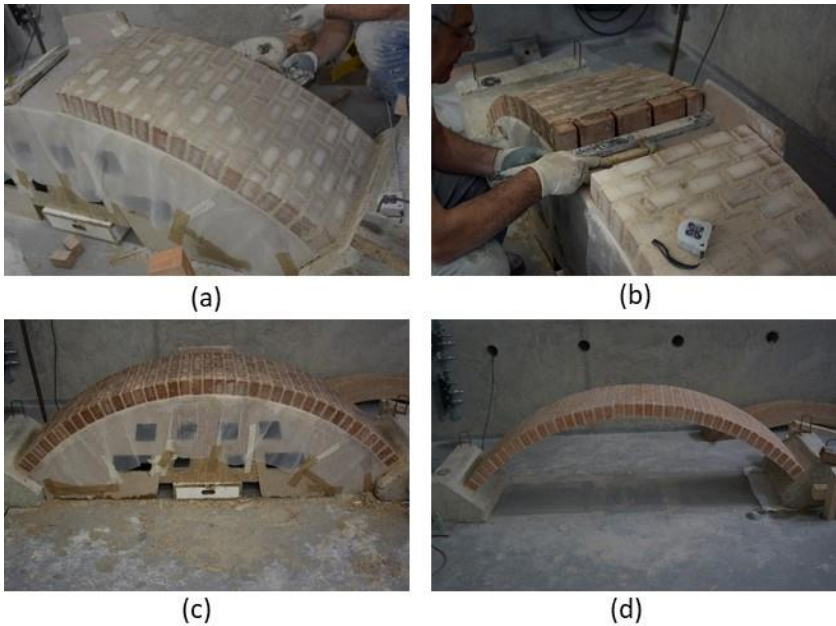


Figure 6.3. Arch model phases in the construction of masonry arches

The demoulding process has been made after one week ( minimum time required)as shown in Figure 6.3d

### 6.2.2 Numerical Model description

The structural modelling and the analysis have been performed with the FE software DIANA Ver. 10.2. This analysis assisted in the design of experimental dynamic tests. The FE modal's outcomes were chosen for the parameter estimation as: the reference and moving sensors definition, the acquisition time and the sampling frequency. All those

parameters are important in order to have enough resolution in the mode shapes.

The arch is composed by masonry units and mortar. The main material characteristics for the masonry components of the building were adopted from the Italian Code (NTC2018) and compared with the value given by Basilio (2007). Table 6.1 summarises the model parameters adopted.

Masonry typology	fm	$\tau_0$	E	G	W
	[MPa]	[MPa]	[MPa]	[MPa]	[kN/m <sup>3</sup> ]
	min-max	min-max	min-max	min-max	min-max
Full brick	2.40	0.06	1200	400	
masonry with lime mortar	4.00	0.092	1800	600	18

Table 6.1. Mechanical properties of the masonry arch model

The assumed constitutive model was linear softening in tension and parabolic softening in compression. This behaviour is represented in Figure 6.4a, where  $G_f$  represents the tensile fracture energy of the material and  $f_t$  equals the tensile strength. The parabolic curve (Figure 6.4b) is a formulation based on fracture energy, according to Feenstra (1993) and it is described by three characteristic values  $G_c$  which defines the compressive fracture energy,  $f_c$  equals the compressive strength.

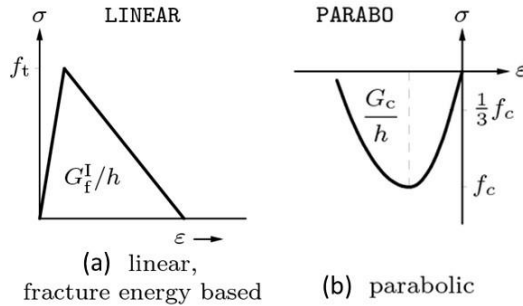


Figure 6.4. Arch 3D model : Tensile (a) and compressive behaviour (b)

On the basis of the numerical modelling approach, the level of accuracy and the complexity of the analysis must be thoroughly considered.

It is possible to choose a micro-modelling strategy if the goal is understanding the local behaviour, however, several approaches exist to perform micro-modelling as well. Furthermore, if the attention is given for the global behaviour, the macro-modelling is preferred (Lourenço, 2009).

In this case study a Macro-modelling approach has been used, in which bricks, mortar and brick-mortar interface is smeared out in a homogeneous continuum. The constitutive model based on total strain rotating crack is implemented for the FE model, this approach is improved along the bases of the Modified Compression Field Theory, originally proposed by Bentz et al. (2006)

Table 6.1 summarises the parameters adopted for the model, in particular, Young's modulus of 1800 MPa, Poisson coefficient equal to 0.2, mass density equal to 18 kN/m<sup>3</sup>, tensile strength equal to 0.4 MPa, tensile fracture energy is defined by the following formulation:

$$G_f = f_t d_{u,t} \quad (6.1)$$

Here, the ductility index ( $d_{u,t}$ ) equal 0.029 mm has been assumed; as suggested by Lourenço (2009), the  $G_f$  value equal to 0.015 N/mm is adopted. The compressive strength  $f_t$  equal to 4 MPa with the corresponding  $G_c$  equal to 9.6 N/mm (with  $d_{u,c}$  equal 2.4 mm) was adopted for analysis. The concrete abutments were assumed linear elastic with a Young's modulus equal to 30000 MPa, the Poisson coefficient equal to 0.2, mass density equal to 25 kN/m<sup>3</sup> were assumed for the analysis.

Solid elements CHX60 (Figure 6.5) were adopted for this numerical model. This is a twenty-node isoparametric solid brick element and is based on Gauss integration and quadratic interpolation. Typically, a rectangular brick element approximates the following strain and stress distribution over the element volume. The strain  $\varepsilon_{xx}$  and stress  $\sigma_{xx}$  vary linearly in x directions and quadratically in y and z direction. The strain  $\varepsilon_{yy}$  and stress  $\sigma_{yy}$  vary linearly in y direction and quadratically in x and z direction. The strain  $\varepsilon_{zz}$  and stress  $\sigma_{zz}$  vary linearly in z direction and quadratically in x and y direction. The stresses and strains are defined on the base evaluation of the form and stiffness of

the structural components, the degrees of freedom specified to each node, the applied actions, boundary conditions and the stress and strain history of the analysis.

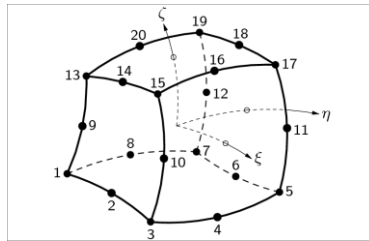


Figure 6.5. The CHX60 solid element

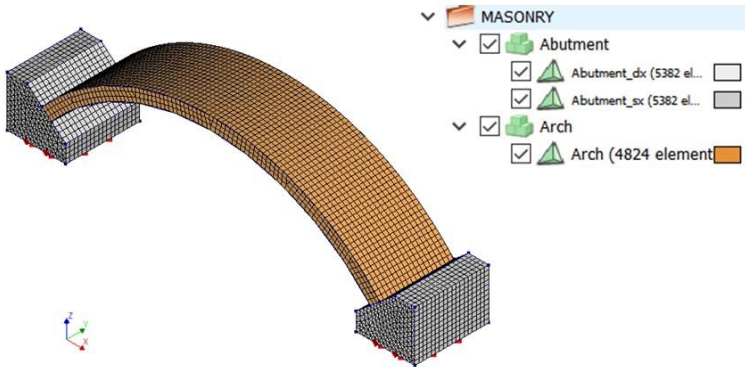


Figure 6.6. Arch 3D: view of the mesh type and the boundary conditions

The Finite Element Model (FEM) of the arch (Figure 6.6) , is based on the detailed geometric model. For the realization of the model, firstly the abutments were defined. These elements, for the reference scenario, are characterized at the base by perfect constraints. In continuity with the surface of the abutments, the arch solid part has

been made. In the optimized mesh of all the surface, an average size QUAD element (Figure 6.5) of 25 mm was considered.

In the beginning of the modal analysis, the 3D undamaged model was considered as the initial condition for the next non-linear static analysis.

### **6.2.3 Modal Dynamic Analysis**

A modal dynamic analysis was carried out to assess the models. Through this analysis, performing a free vibration eigenvalue analysis with DIANA solver. A modal dynamic analysis was carried out on the arch model. Through this analysis, free vibration eigenvalue analysis with DIANA solver was performed (Figure 6.8a,b). As shown before, this analysis was performed to better define the experimental dynamic tests. The range modes of vibration start from 35.34 up to 221.62 Hz and also there is no close frequencies either.



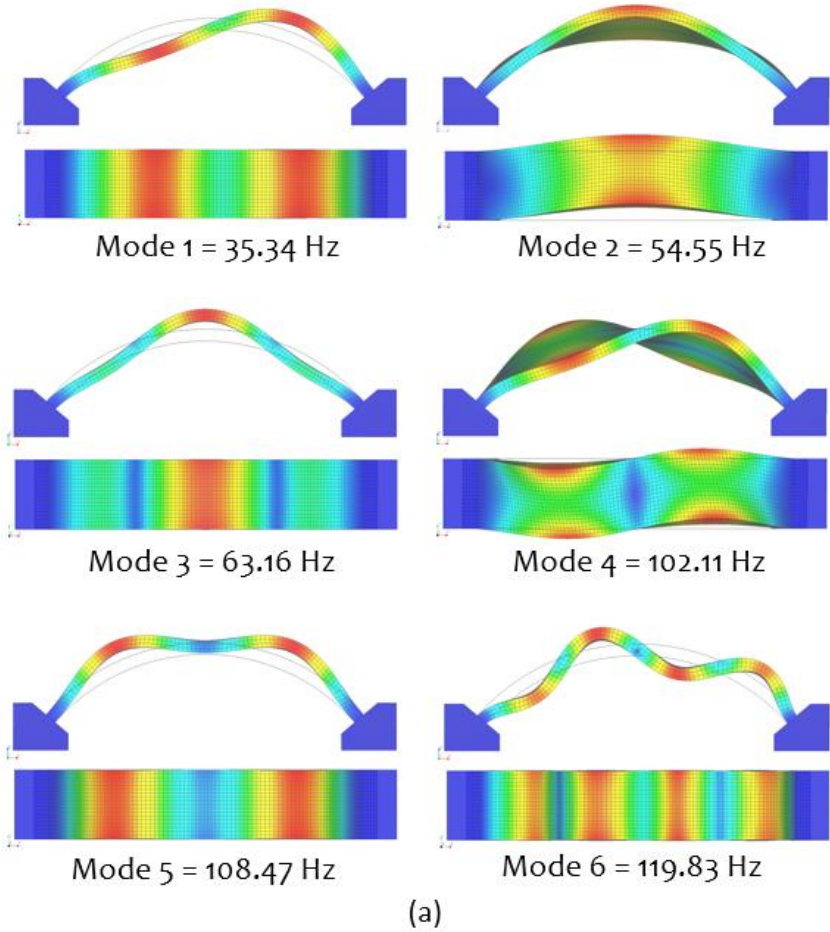


Figure 6.7. a) Numerical modal results - mode shape and frequency values

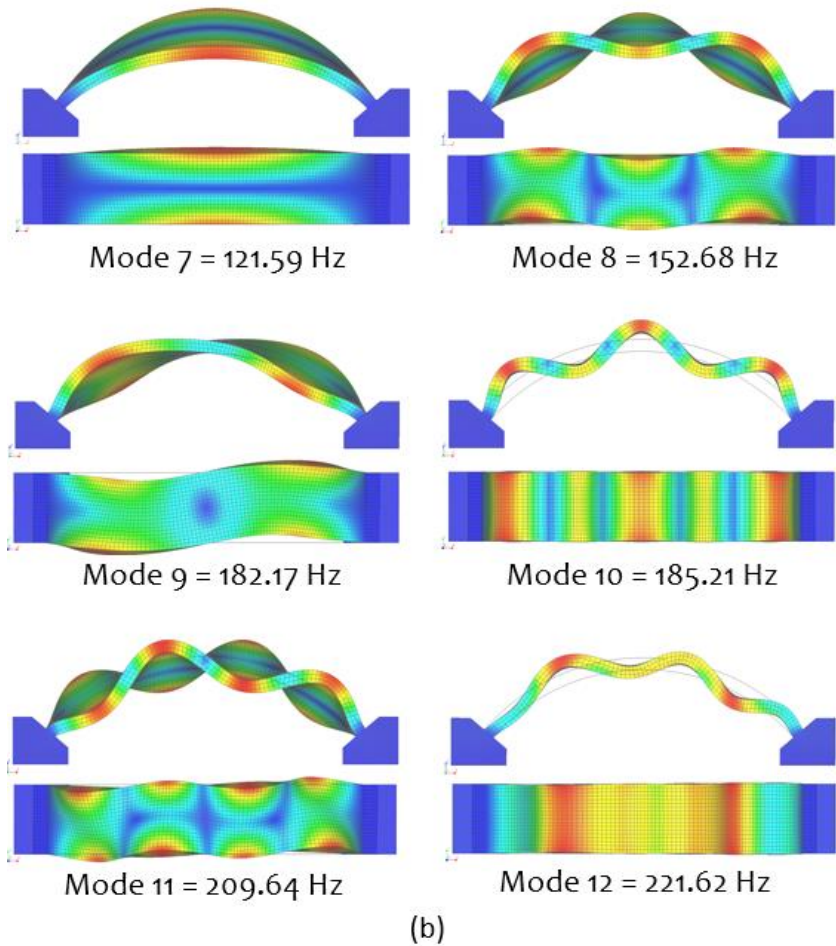


Figure 6.8. b) Numerical modal results - mode shape and frequency values

Therefore, for the experimental test, the sampling frequency of 400 Hz was defined. Consequently, it was expected to define experimentally, at least, ten distinct frequencies.

#### 6.2.4 Numerical prediction of damage locations

The FE model, previously used to perform the modal dynamic analysis, is subsequently subjected to an increasing displacement load to predict the possible location of damage. To simulate the non-linear behaviour of masonry, a standard smeared cracking model was used as described before. The displacement force was applied on the right abutment base (Figure 6.9). This is characterized to have only translation in the load displacement direction, so as to reproduce the same test conditions, while the right abutment is completely fixed.

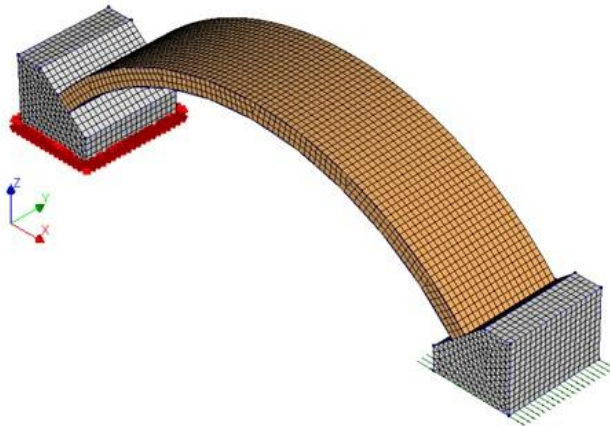


Figure 6.9. Edit boundary conditions

## Chapter 6 - Damage assessment: an old arch replica

---

The simulation tries to represent a displacement increasing load (0.1 mm by step) applied until the collapse. It should be stressed that the results are qualitative and they were useful only to predict the possible crack location and the corresponding displacement.

For the static response the analyses show three cracks (hinges) at ultimate load step. For the prediction model, the crack sequence shows the first two cracks appear simultaneously in the extrados in a symmetrical position close to the supports with a displacement of the support equal to 1.6 mm. The third and last crack appears in the intrados close to the crown position on the right side for a displacement equal to 8 mm.

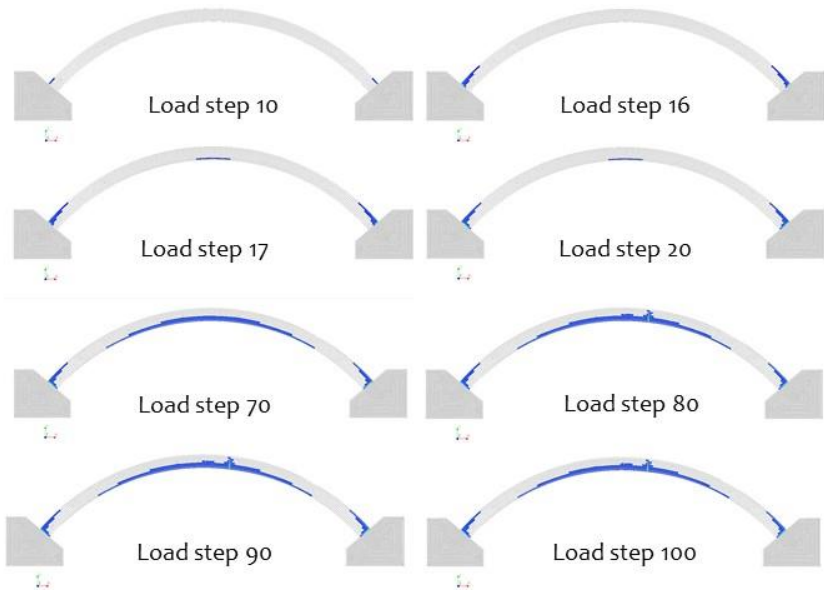


Figure 6.10. Numerical crack sequence prediction

The total displacement associated with the incremental load step has been plotted. Assuming that the interface between the support and the arch is not completely brokered, the results (Figure 6.11b), shows a higher similar displacement for the control points (Figure 6.11a) near the support that for the control point in key.

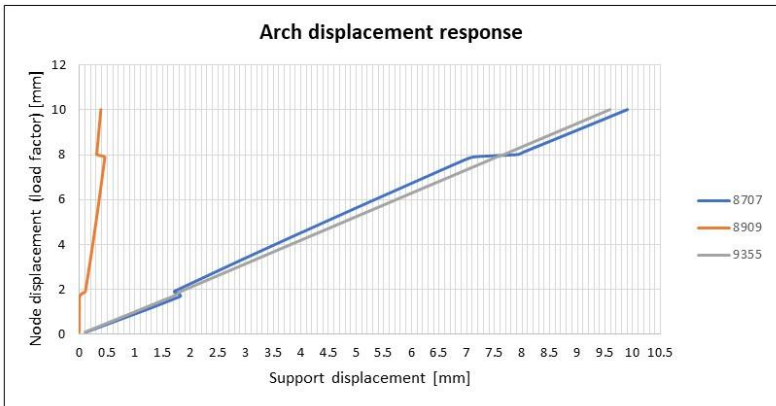
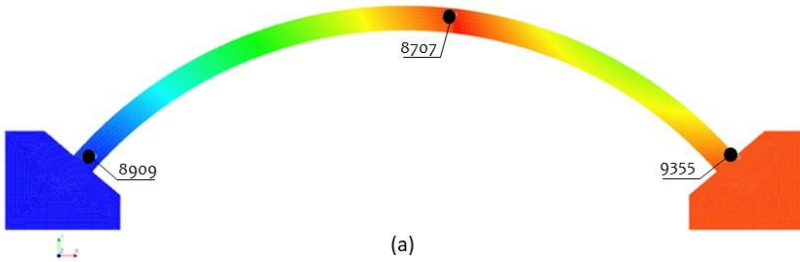


Figure 6.11. Prediction model analysis: (a)View of the control points; (b) displacement control of the arch

### 6.3 ARCH DAMAGE TEST IN DISPLACEMENT CONTROL

As per the information disseminated by the numerical model, a series of static tests were carried out with the aim of inducing progressive damage.

The tests were made with displacement-control by means of a hydraulic jack (Figure 6.12) . The load was applied with a slow linear velocity and without the recovery of the initial condition (support movement) for all seven Damage Scenarios (DSs).

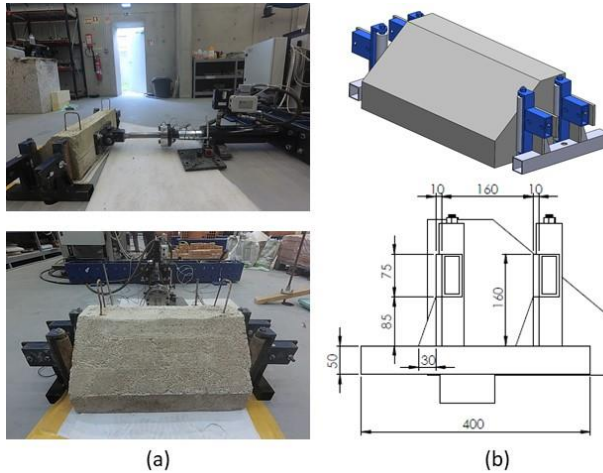


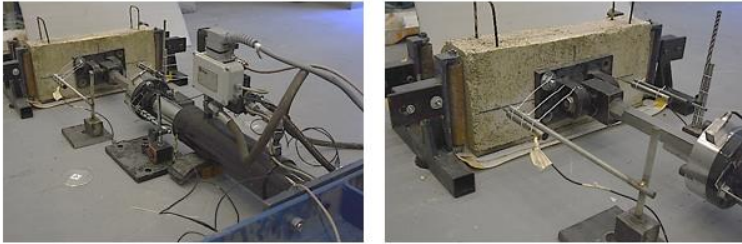
Figure 6.12. a) View of the actuator pre-test; b) rolls system design

In order to apply only a horizontal displacement a roll system was made and tested with the hydraulic actuator. As shown in Figure 6.12 the rolls were fixed on the floor close to the transverse surface of the free support were designed to limited eventually lateral and rotational movements.

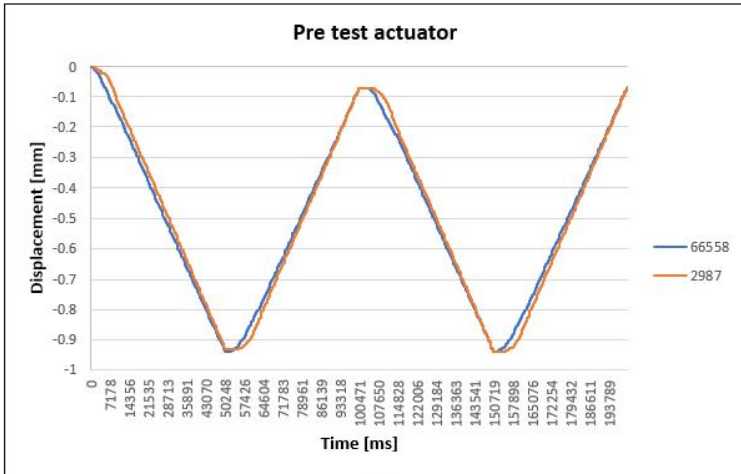
Through Two Linear Variable Displacement Transducers (LVDT), placed as in Figure 6.13a, the support's displacement was evaluated.

## Chapter 6 - Damage assessment: an old arch replica

The result shown in Figure 6.13b has confirmed the restraint system all the constraints necessary to resist the rotation movement.



(a)



(b)

Figure 6.13. Actuator test: a) View of LVDT controller; b) result of displacement test

### 6.3.1 System identification tests

In order to control the damage process, a series of static and dynamic test apparatus were used (Figure 6.14). The static instruments consisted five LVDTs as shown in Figure 6.15a.



These instruments were placed in such a way that one remained close to the fixed support and two near the support in movement, to evaluate respectively the horizontal arch's displacement and the absolute displacement for the all series.

The fourth LVDT was placed close to the hydraulic system, to compare the input displacement with the other horizontal values and the last LVDT was positioned on the key of the arch (Figure 6.14b) to check the vertical movements.



Figure 6.14. Arch test: a) view of the test apparatus; b) vertical LVDT

The resulting displacement in the arch for a single damage step is presented in Figure 6.15b. It is worthy to note that the vertical LVDT (5) and the LVDTs (2-3) on the right side presented the same displacement. While the result for the LVDT (4) close to the fixed support highlights comparatively less displacement similar to the numerical model result before.

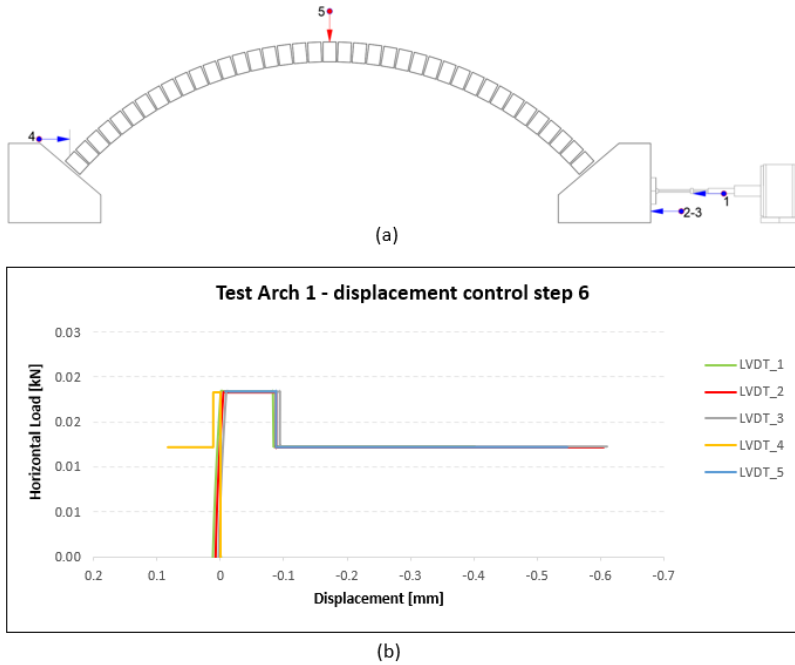


Figure 6.15. a) View of the LVDTs location during the static tests; b) results for the arch displacement control

In order to replicate the damage irreversibility, such as structural failures, cracks after earthquake, the displacement was incremented after each damage scenario.

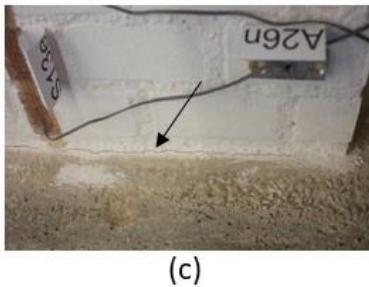
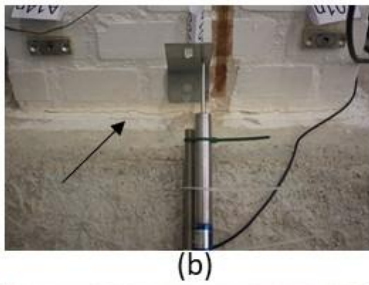
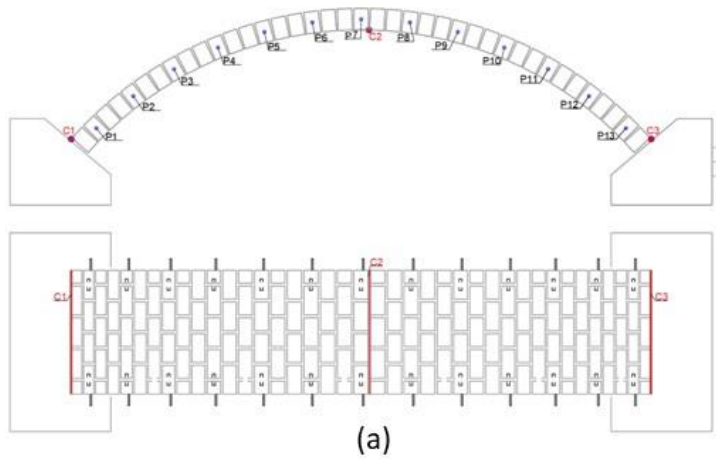


Figure 6.16. Arch damage: a) view of crack location; (b) crack C1; c) crack C2; d) crack C3

As in the numerical model prediction, three cracks progressively appeared during the static tests.

All cracks became visible from the third DS with a total displacement equal 1.6 mm, with the first two cracks (close to the right support and in key) that was visually detected during the displacement branch of DS<sub>II</sub>. The resulting crack pattern in the arch is shown in

Figure 6.16. The first crack (C1) was located in the extrados on the contact surface between the fixed support and the first brick courses, as expected, but without the opposite crack near the left abutment and with a displacement equal to 1 mm.

Crack C2 was detected at the crown, in the left side, between positions P7 and P8. The crack crossed all width at the last damage scenario DS<sub>VII</sub>, with the displacement equal to 3.7 mm.

The crack C3 appeared at the right support of the arch, in the extrados, corresponding to position P13.

### **6.3.2 Test setup**

The system identification tests were carried out according to the description below. The main equipment for the dynamic tests were strain gauges and accelerometers. The experimental dynamic tests consisted in the acquisition of the structural response of the arch along the testing to check its stiffness degradation with increasing damage.

As starting point, one qualitatively analysis was performed on the Reference Scenario (RS), used to compare it with the damage sequence.

The dynamic sensors are piezoelectric (*Model 393B12*) mono-directional accelerometers, with nominal sensitivity of 1000 mV/g, frequency interval ( $\pm 5\%$ ) from 0.15 to 1000 Hz (5%), 8  $\mu\text{g}$  of resolution and 210 g of weight, connected by coaxial cables to a data acquisition system (DAQ).

This type of accelerometers was selected because they have good accuracy for the dynamic response. From the numerical modal analysis, it was possible to define that all modes have significant modal displacements in the arch plan. While only the second and fifth modes show a significant mode shape.

That is why, it was decided to investigate only the response in the in-plan direction, by placing the sensors in the normal and tangential directions.

It was also decided to measure front and back edges of the arch (Figure 6.19b) to estimate the torsion modes and to detect any asymmetric behaviour.

In addition, two wireless vibrations sensor based on Micro-Electro-Mechanical Systems (MEMS) technology has been tested.

The BeanDevice® AX-3D XRange (Figure 6.17) is a tri-axial accelerometer sensor with built-in data logger, which is characterized by a waterproof (IP67/Nema 6) and a lightweight aluminium casing (100x60x31mm), an ultra-low power, a very low noise (45  $\mu\text{g}/\sqrt{\text{Hz}}$  for  $\pm 2\text{g}$  version), an integrated data logger that can store up to 8 million data logs.



Figure 6.17. BeanDevice® AX-3D XRange wireless vibrations sensor

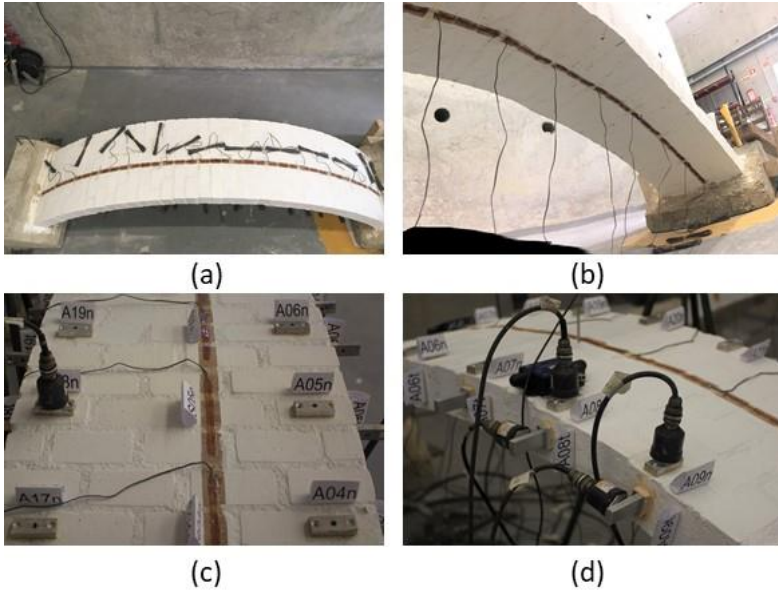


Figure 6.18. Sensors location: a) top view of the strain gauge systems; b) view from below of the strain gauge systems; c) strain gauges surface base across 3 bricks; d) disposition of the accelerometers

According to the configuration of the most significant numerical mode shapes, 13 measurement points (Figure 6.19), evenly spaced for the both edges of the arch were selected (front and back).

The accelerometers were fixed to aluminum plates that were directly glued in the arch edges to perform the normal and tangential measurements (Figure 6.18d).

Fourteen strain gauges in the extrados and intrados along the two sides of the arch middle line, as an attempt to study the possibility to measure strains for dynamic modal analysis has been used. The following figure shows the location of the measurement points.

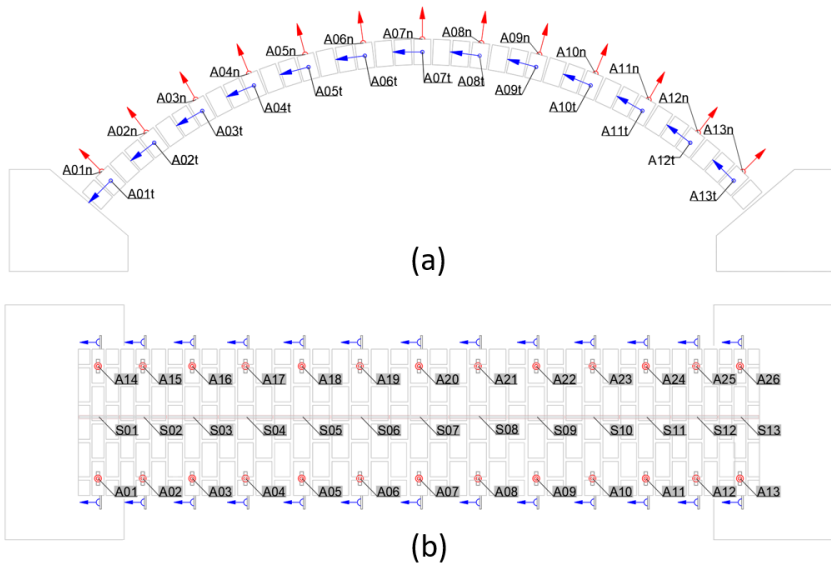


Figure 6.19. Location of the measuring points for the dynamic tests: (a) front view; (b) top view. Ai indicates accelerometers and Si indicates strain gauges.

## Chapter 6 - Damage assessment: an old arch replica

---

For the purpose to have a fine resolution in the modal estimation, altogether 56 accelerations (26 in normal direction and 26 in tangential direction - Figure 6.19) were measured. For this reason, 12 setups with four reference sensors in positions A09 and A18 and four moving sensors were placed in the front and back edges. For the measurement purpose, polyester strain gauge series were used (PL-120-11) . They are wire strain gauges utilizing a transparent plastic backing impregnated with polyester resin. The gauge length is 120mm with 120 resistances. Since the backing is transparent, the bonding position has been easily being checked in the installation works. The strain gauges were connected to the data acquisition system with lower resolution than the accelerometers but has the advantage to allow separate connections as well. Table 6.2 and Figure 6.20 summarize the sequential process. This resolution is enough to have the complete definition of the estimated modes and it is clear from the practical point of view that, too many points are unpractical and expensive for experimental tests in real structures.



	Ch.1	Ch.2	Ch.3	Ch.4	Ch.5	Ch.6	Ch.7	Ch.8
Setup	Ref.1	Ref.2	Ref.3	Ref.4	Mov.1	Mov.2	Mov.3	Mov.4
1	A09t	A09n	A18t	A18n	A01t	A01n	A14t	A14tn
2	A09t	A09n	A18t	A18n	A02t	A02n	A15t	A15n
3	A09t	A09n	A18t	A18n	A03t	A03n	A16t	A16n
4	A09t	A09n	A18t	A18n	A04t	A04n	A17t	A17n
5	A09t	A09n	A18t	A18n	A05t	A05n	A19t	A19n
6	A09t	A09n	A18t	A18n	A06t	A06n	A20t	A20n
7	A09t	A09n	A18t	A18n	A07t	A07n	A21t	A21n
8	A09t	A09n	A18t	A18n	A08t	A08n	A22t	A22n
9	A09t	A09n	A18t	A18n	A10t	A10n	A23t	A23n
10	A09t	A09n	A18t	A18n	A11t	A11n	A24t	A24n
11	A09t	A09n	A18t	A18n	A12t	A12n	A25t	A25n
12	A09t	A09n	A18t	A18n	A13t	A13n	A26t	A26n

Table 6.2. Test setups for accelerometers, n indicate normal direction and t tangential direction



(Setup01)



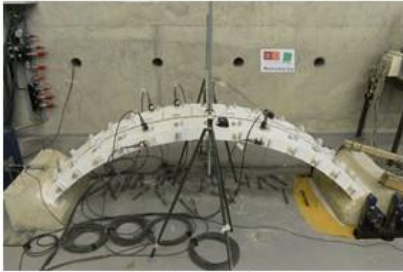
(Setup02)



(Setup03)



(Setup04)



(Setup05)



(Setup06)

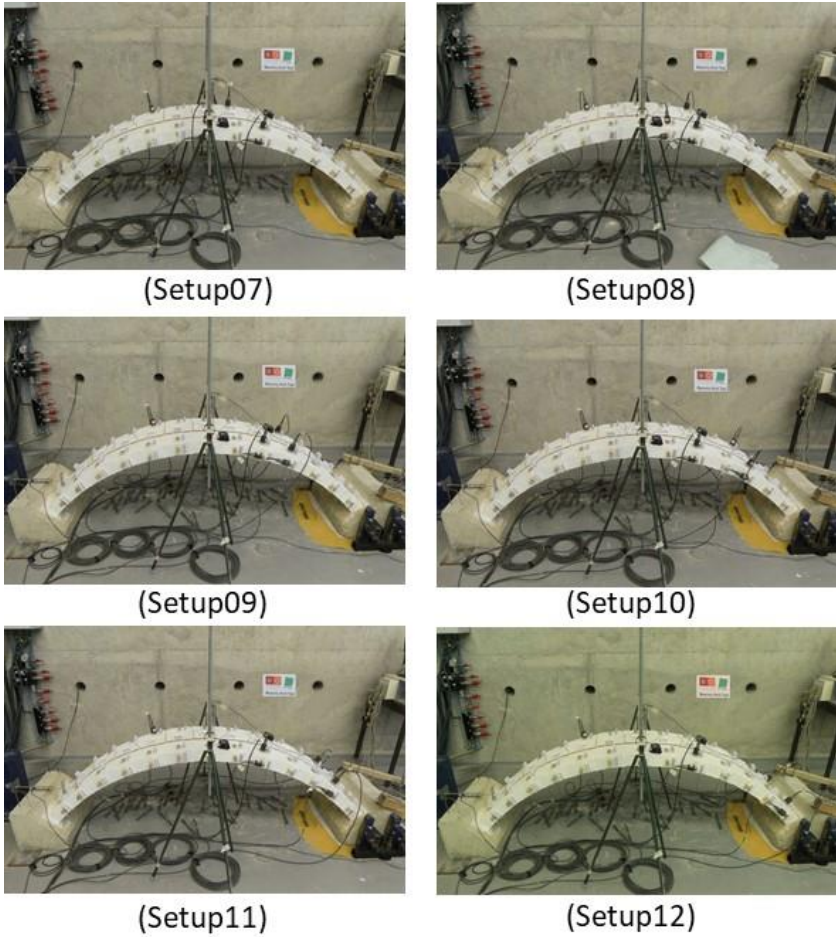


Figure 6.20. Dynamic test sequence, with the different setups

## Chapter 6 - Damage assessment: an old arch replica

Data acquisition, from the accelerometer was carried out by a measurement device with 16 bit resolution and on-board anti-aliasing filter. The data acquisition hardware is managed by software developed in LabView environment by StreGa Lab of University of Molise.

### 6.3.3 Types of Input data acquisition

Additional issue to address is the excitation type during the experimental tests. The intention was to validate if damage could be identified with ambient excitations or require stronger excitation.

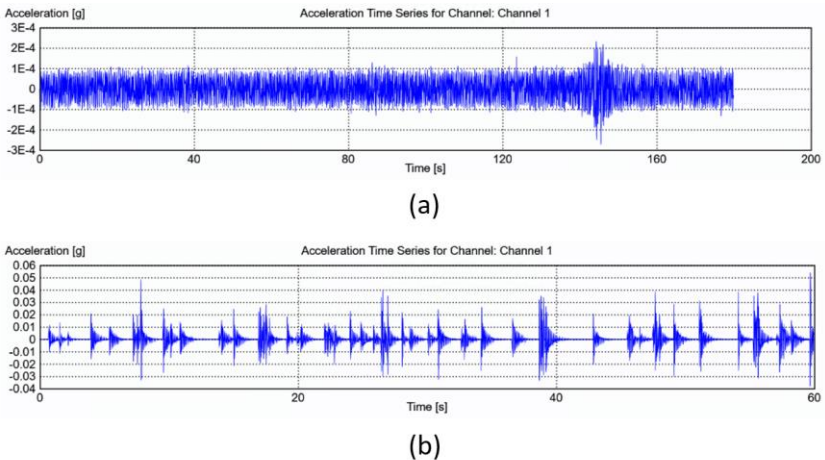


Figure 6.21. Data collection: a) ambient excitation; b) random impact excitation

As shown in the elaboration data below (Figure 6.23 and Figure 6.25), the ambient vibrations in the laboratory were not strong enough to excite the structure sufficiently to identify modal strains and also the ambient noise spectrum was presented in the frequency range of interest, due to the use of any sort of electrical equipment inside the laboratory that was not possible disconnected during the dynamic tests.

The signals from the accelerometric sensors were sampled at a frequency of 400 Hz per channel and a minimum measuring time of 60 s for the random impact and 180 s for the ambient excitations were fixed, with 24.000 data and 72.000 points per channel.

#### **6.3.4 Modal identification: Result for the damage evolution**

For both excitations the mode shapes and other dynamic parameters were defined. The acquired data were analysed with two different methods: the FDD and the SSI-Principal Component available in ARTeMIS software. Five mode shapes were clearly estimated with ambient and random excitations tests. Figure 6.23 and Figure 6.25 show the diagrams of the both input data acquired. It is evident that the random impact excitation test has better definition of the peaks and thus better modal estimation is possible.

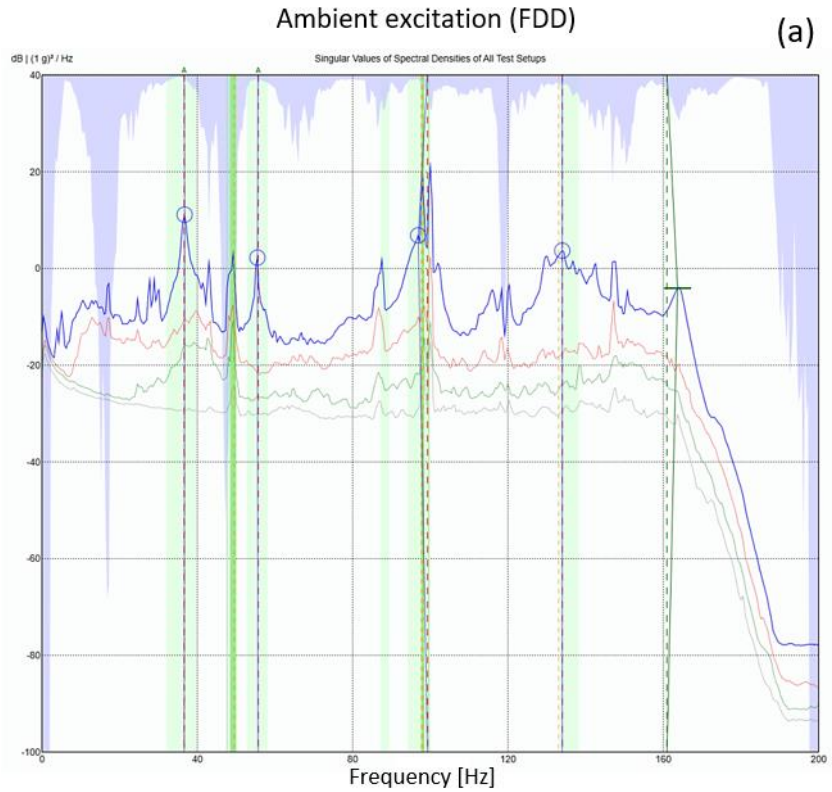


Figure 6.22. a) Reference scenario: diagram of estimated state space model with ambient excitation input ( FDD method)

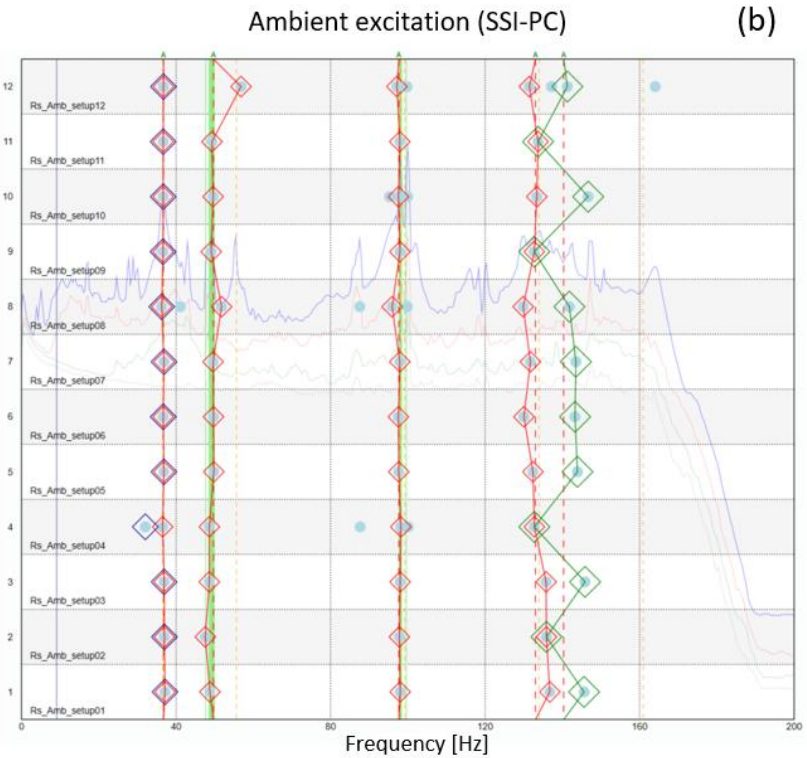


Figure 6.23. b) Reference scenario: diagram of estimated state space model with ambient excitation input (SSI-PC method)

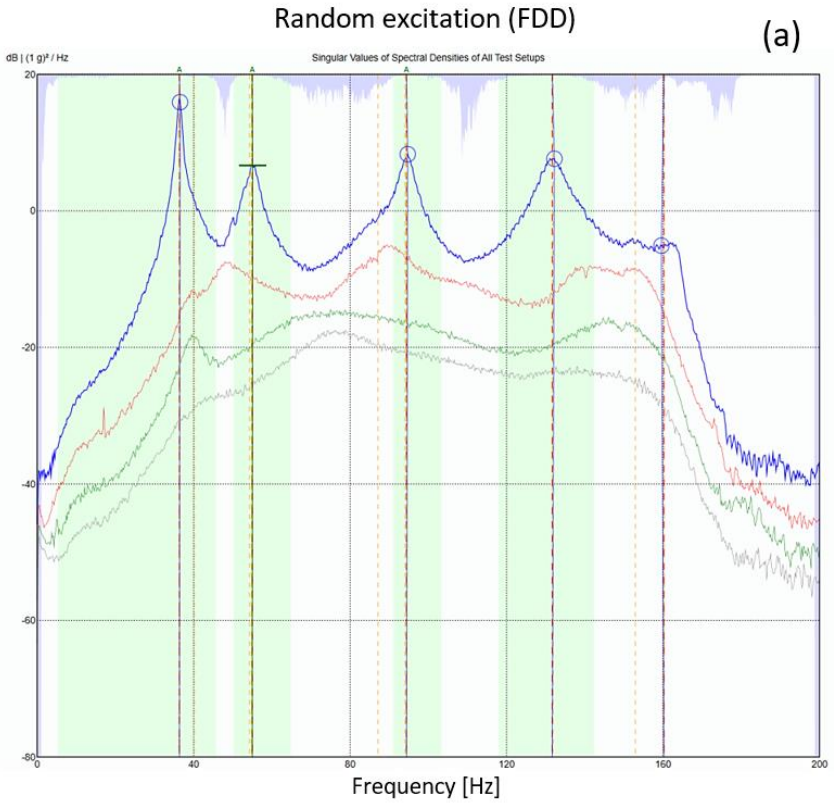


Figure 6.24. a) Reference scenario: diagram of estimated state space model with random excitation input (FDD method)



## Random excitation (SSI-PC) (b)

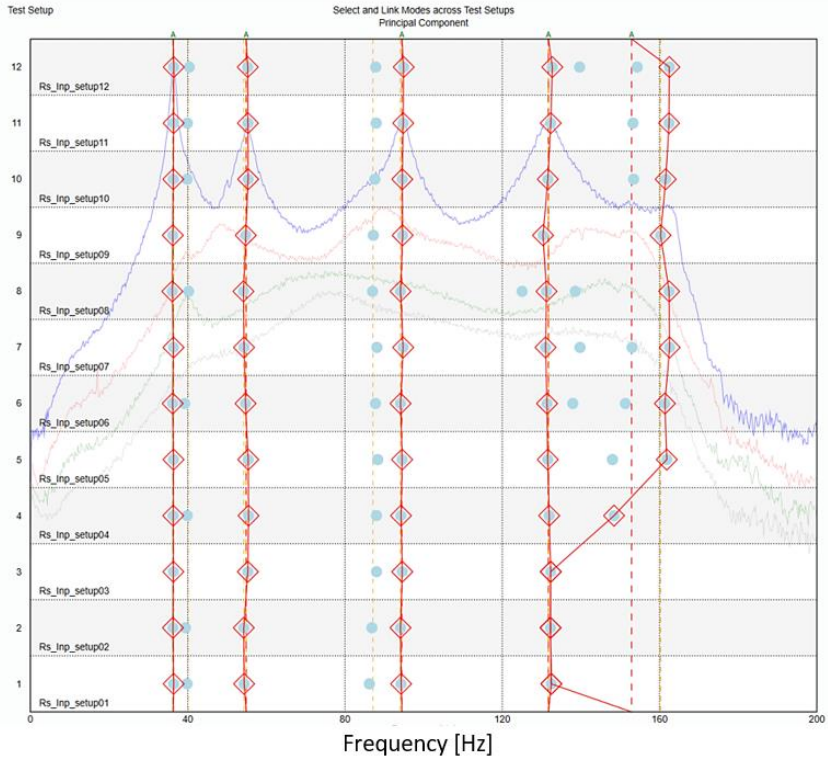


Figure 6.25. b) Reference scenario: diagram of estimated state space model with random excitation input (SSI-PC method)

Global results values are presented in Table 6.3 and Table 6.4 for the ambient excitation tests using the FDD and SSI-PC methods.

Chapter 6 - Damage assessment: an old arch replica

<b>FDD</b>		<b>Frequency <math>\omega</math> [Hz]</b>				
Damage	Mode 1	Mode 2	Mode 3	Mode 4	Mode 5	
Rs	36.60	55.67	99.26	133.98	160.95	
Ds01	33.49	49.41	87.70	127.92	147.70	
Ds02	33.02	49.22	83.20	129.85	141.70	
Ds03	30.42	49.02	80.59	124.23	137.31	
Ds04	29.84	48.78	78.19	122.76	132.19	
Ds05	29.07	48.24	77.70	122.26	133.40	
Ds06	28.94	46.66	76.04	120.46	132.02	
Ds07	28.97	46.38	76.11	120.05	133.19	

Table 6.3. Global scenario: FDD results from the ambient excitation test.

<b>SSI-PC</b>		<b>Frequency <math>\omega</math> [Hz]</b>				
Damage	Mode 1	Mode 2	Mode 3	Mode 4	Mode 5	
Rs	36.77	49.68	97.66	133.05	-	
Ds01	32.57	49.64	87.42	129.10	-	
Ds02	32.79	49.23	84.29	127.24	141.06	
Ds03	30.19	48.91	79.63	122.88	-	
Ds04	29.87	48.79	77.86	124.18	133.70	
Ds05	29.35	48.76	80.78	122.97	-	
Ds06	29.01	48.88	76.36	120.82	-	
Ds07	29.01	47.02	74.73	120.36	133.12	

Table 6.4. Global scenario: FDD results from the ambient excitation test.

SSI-PC Damage	Damping [%]				
	Mode 1	Mode 2	Mode 3	Mode 4	Mode 5
Rs	1.77	4.15	0.82	1.43	-
Ds01	3.04	1.18	1.38	1.48	-
Ds02	1.85	0.62	3.68	1.75	2.02
Ds03	3.19	4.89	7.96	1.23	-
Ds04	0.98	1.14	2.62	1.55	2.23
Ds05	0.52	1.31	3.60	1.85	-
Ds06	0.66	1.83	3.76	1.81	-
Ds07	1.08	3.01	4.01	1.73	1.79

Table 6.5. Global scenario: dumping results for the ambient excitation test

The MAC value results, for the ambient excitation as, shown in Table 6.6 are not accurate for frequencies and modal displacements, as few values of the MAC are greater than 0.9 except for mode 1.

MAC FDD -SSI				
Mode 1	Mode 2	Mode 3	Mode 4	Mode 5
1.00	0.59	0.85	0.70	-
0.99	0.95	0.87	0.88	-
1.00	0.99	0.88	0.68	0.64
1.00	0.99	0.93	0.62	-
1.00	0.99	0.97	0.86	-
1.00	0.99	0.84	0.51	-
1.00	0.94	0.95	0.59	-
1.00	0.71	0.47	0.95	0.46

Table 6.6. MAC values results

Chapter 6 - Damage assessment: an old arch replica

Table 6.7, Table 6.8 and Table 6.9 summarize the results concerning the frequency and damping values for the random impact excitation with the FDD and SSI-PC methods.

<b>FDD</b>	<b>Frequency <math>\omega</math> [Hz]</b>				
Damage Scenario	Mode 1	Mode 2	Mode 3	Mode 4	Mode 5
Rs	36.35	54.99	94.40	131.64	160.22
Ds01	33.25	51.29	85.40	127.79	148.57
Ds02	32.06	50.04	83.07	126.78	143.69
Ds03	30.46	48.53	80.71	124.95	137.71
Ds04	29.67	47.89	79.66	123.66	133.79
Ds05	29.21	47.58	79.33	123.43	133.53
Ds06	28.74	47.10	78.81	121.98	132.10
Ds07	28.61	46.54	77.94	121.99	130.83

Table 6.7. Global scenario: FDD results from the random impact test

<b>SSI-PC</b>	<b>Frequency <math>\omega</math> [Hz]</b>				
Damage Scenario	Mode 1	Mode 2	Mode 3	Mode 4	Mode 5
Rs	36.33	54.90	94.48	131.77	152.91
Ds01	33.16	51.26	84.05	128.47	149.41
Ds02	31.97	50.09	82.52	118.09	144.39
Ds03	30.39	48.44	80.32	125.07	138.48
Ds04	29.61	47.78	79.08	123.73	134.97
Ds05	29.17	47.42	78.89	123.48	134.00
Ds06	28.70	46.96	78.03	122.05	132.65
Ds07	28.59	46.46	77.36	122.02	132.62

Table 6.8. Global scenario: SSI-PC results from the random impact test

SSI-PC Damage Scenario	Damping [%]				
	Mode 1	Mode 2	Mode 3	Mode 4	Mode 5
Rs	1.382	3.399	2.051	2.392	2.806
Ds01	1.698	3.069	4.521	2.619	3.07
Ds02	1.791	2.61	4.128	1.877	2.916
Ds03	1.667	2.522	4.092	1.69	3.062
Ds04	1.576	2.586	4.589	1.59	2.673
Ds05	1.217	2.312	4.02	1.428	2.838
Ds06	1.39	2.466	6.096	1.825	1.854
Ds07	1.297	2.328	4.659	1.467	2.671

Table 6.9. Global scenario: dumping results for the random excitation test

MAC EFDD -SSI				
Mode 1	Mode 2	Mode 3	Mode 4	Mode 5
1.00	1.00	0.99	0.99	0.67
1.00	1.00	0.91	0.97	0.55
1.00	1.00	0.98	0.92	0.92
1.00	1.00	0.99	1.00	0.93
1.00	1.00	0.98	1.00	0.85
1.00	1.00	0.98	1.00	0.92
1.00	1.00	0.74	1.00	0.93
1.00	1.00	0.95	0.99	0.94

Table 6.10. MAC values results

The result from index MAC of random impact excitation, shows an higher accuracy in the modal displacements than before. The MAC values are greater than 0.9, except for mode 3 (in the DSVI) and in the

Mode 5. The main mode shapes configurations for the undamaged condition are shown in Figure 6.26.

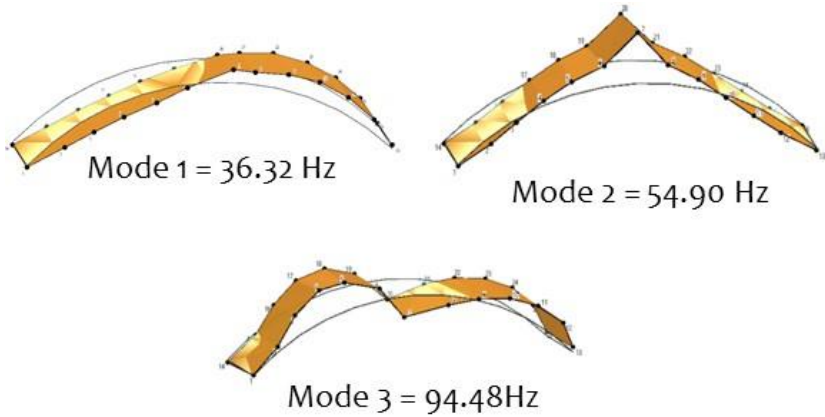


Figure 6.26. Mode shapes configuration for the reference scenario

### 6.3.5 Application of the spectral damage analysis

The damage analysis over the experimentally induced seven DSs was performed by studying the direct changes in the modal parameters of the arch as well as the changes in the derivatives of these modal parameters (Maria Giovanna Masciotta et al. 2016). This approach is discussed in Chapter 3 as well.

From the random impact test data, three square Power Spectral Density (PSD) matrices for each scenario were built in MATLAB (2010). Furthermore, two  $[26 \times 26]$  matrices from acceleration responses in both normal ( $z$ ) and tangential ( $x$ ) direction were also constructed.

In order to define the modal parameters and proceed with the damage analysis, each matrix is then decomposed in eigenvalues and eigenvectors. The eigenvalues decomposition (Figure 6.27), first performed with regard to the RS and then applied to the seven DSs, allowed to identify the eigenfrequencies to use as qualitative indicators in the damage analysis with global parameters. This type of analysis is essentially based on the observation of shifts in the resonant frequency values. If accurately estimated, direct changes in these modal parameters are proved to be a sensitive indicator of global structural damage.

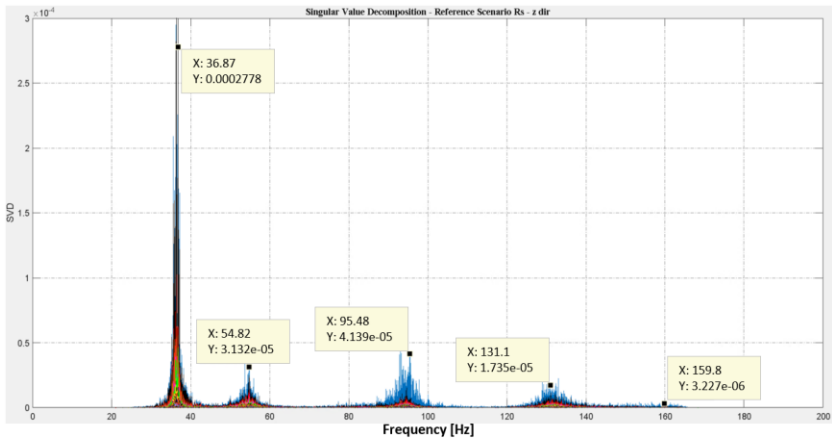


Figure 6.27. Spectral value decomposition for the random impact excitation

With the progress in displacement, the increase of the damage conjectures to the progressive degradation of the structural stiffness of the arch. Figure 6.28 shows the progressive frequency decrease with

increasing damage. The first significant frequency drop is observed from the beginning of the DS.

The results for the seven consecutive scenarios using the PSD technique are discussed below.

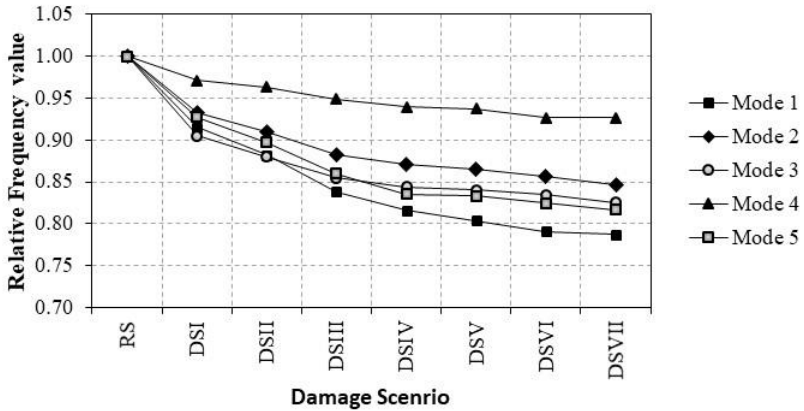


Figure 6.28. Relative frequency values for the identified modes obtained from the dynamic test



### 6.3.6 Results

For the spectral damage analysis, only the spectral output signal in normal direction have been used for the index computation because the contribution of the spectral output signals in tangential direction could be neglected due to low physical magnitude.

The results are shown in Figure 6.29 and comparison between  $RS$  and  $DS_I$  and  $R_s$  with  $DS_{VII}$  presented in Figure 6.30. In order to evaluate the sensitivity of the algorithm to the considered frequency bandwidth, two types of damage indices are computed and compared: A Broad-Band (BB) index and a Narrow-Band (NB) index. Detailed information can be found in Masciotta (2015).

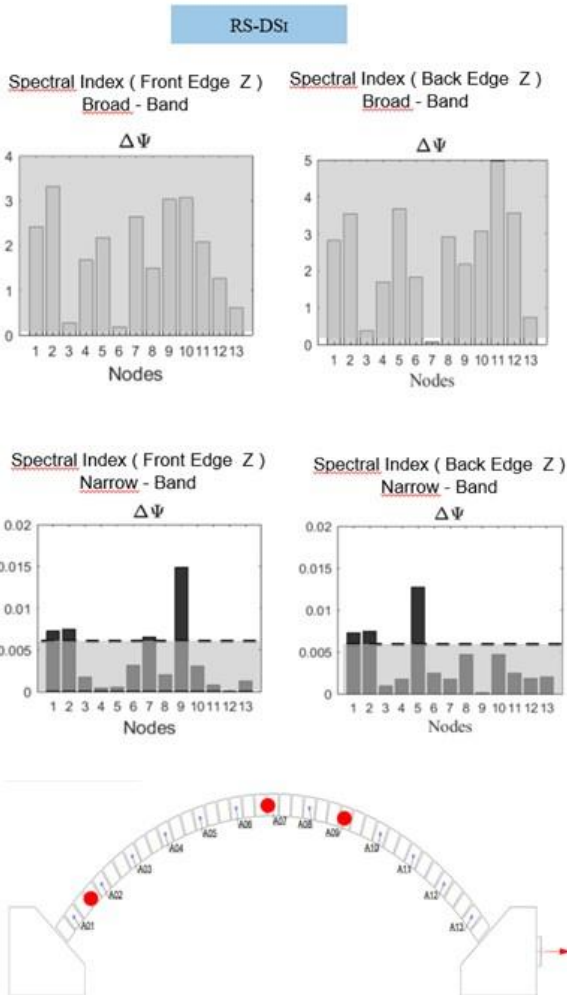


Figure 6.29. Damage analysis results (RS -DS<sub>r</sub>) for acceleration responses by BB index (light grey bars) and NB index (dark grey bars)

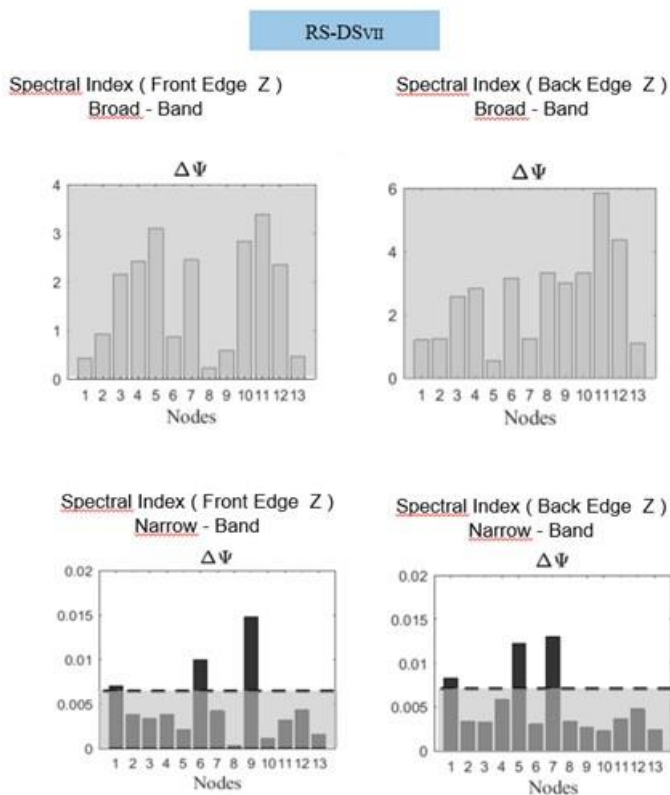


Figure 6.30. Damage analysis results (RS -DS<sub>VII</sub>) for acceleration responses by BB index (light grey bars) and NB index (dark grey bars)

Regarding the results of the comparison between RS and DSI and DSVII, it can be seen univocally the occurrence of cracks at positions A01 corresponding the right support, A07 corresponding the key of the arch and the last in the A09. The results in the absolute comparison show already the crack location before that it became visible (DSI). The

## Chapter 6 - Damage assessment: an old arch replica

---

last crack was not correctly detected, probably because the input data is affected by the noise of the lab. Finally, the NB damage index proved to be more accurate and reliable than the BB index in most of the cases, with regard to the crack sequence. Finally, in most of the cases, NB damage index results to be more accurate and safer than the BB index.

## Chapter 7

# CONCLUSIONS AND FUTURE DEVELOPMENTS

The present work reviewed some aspects of the dynamic response existing architectural complexes aiming at improving the approach to the seismic performance assessment of this peculiar class of structures. Their numerical analyses are often very complex due to widespread uncertainties in the characterization of material properties and structural behaviour. Besides, the reliability of seismic analyses is often jeopardized by the need of defining an appropriate structural and dynamic model. The unique structural configurations, the old construction techniques and the presence of stratified structural modifications occurred over the centuries make the definition of an appropriate and reliable numerical model very challenging. The available analysis approaches distinguish the local response of selected macro elements from the global response of the structure. However, these approaches are often univocally associated to a selected level of

## References

---

vulnerability assessment and based on assumptions derived from common masonry constructions.

In this work, in the field of local and global behaviour, some remarks on the vibration based methods for the structural assessment of the historical structures are proposed.

The research consisted of three phases: Background of the structural assessment of masonry structures in aggregates based on their dynamic response; review of basic dynamics and experimental testing and review of damage identification methods by means of vibration measurements; The review and careful consideration of a well-established vector correlation index, (MAC), made possible a novel field of application. A number of explanatory case studies were reported, pointing out how the proposed rational methodology can guide towards the selection of the most appropriate analysis procedure; the application of the identification tools for a real case to distinguish the global and local behaviour and the laboratory test for the damage assessment. The proposed techniques are attractive tool for historical masonry structures, as it is can be included in the non-destructive techniques.

The dynamic identification techniques and structural monitoring provide accurate global structural information and above all the evaluation of the actual behaviour of a structure. The illustrated procedures appear effective, especially due to their low level of complexity.

In a short-term perspective, for the index-based MAC, additional analyses on more complex structures are required for its exhaustive validation and to and to define a rational methodology can guide towards the selection of the most appropriate analysis procedure.

In the case of spectral-based algorithm be able to detect, locate and asses the structural damage the number of measuring points is extremely important for the quality and accuracy of the structural information. In this regard the reduction/optimization of the accelerometric sensors represent a long-term perspective and hence deserve further attention.

## REFERENCES

- Abdel Wahab, M. M., & De Roeck, G. (1999). Damage detection in bridges using modal curvatures: application to a real damage scenario. *Journal of Sound and Vibration*, 226(2), 217-235. <https://doi.org/10.1006/JSVI.1999.2295>.
- Allemang, R. J., & Brown, D. L. (1982). A correlation coefficient for modal vector analysis. In *Proceedings of The 1st International Modal Analysis Conference*. Orlando, FL, USA.
- Augusti, G., Ciampoli, M., & Giovenale, P. (2001). Seismic vulnerability of monumental buildings. *Structural Safety*, 23(3), 253-274. [https://doi.org/10.1016/S0167-4730\(01\)00018-2](https://doi.org/10.1016/S0167-4730(01)00018-2)
- Basilio, I. (2007). *Strengthening of Arched Masonry Structures with Composite Materials*. University of Minho.
- Bentz, E. C., Vecchio, F. J., & Collins, M. P. (2006). Simplified modified compression field theory for calculating shear strength of reinforced concrete elements. *ACI Structural Journal*, 103(4), 614-624. <https://doi.org/10.14359/16438>.



- Binda, L., & Saisi, A. (1996). State of the Art of Research on Historic Structures in Italy.
- Binda, L., & Saisi, A. (2005). Research on historic structures in seismic areas in Italy. *Progress in Structural Engineering and Materials*, 7(2), 71-85. <https://doi.org/10.1002/pse.194>.
- Binda, L., Saisi, A., & Tiraboschi, C. (2000). Investigation procedures for the diagnosis of historic masonries. *Construction and Building Materials*, 14(4), 199-233. [https://doi.org/10.1016/S0950-0618\(00\)00018-0](https://doi.org/10.1016/S0950-0618(00)00018-0).
- Boscato, G., Dal Cin, A., Ientile, S., & Russo, S. (2016). Optimized procedures and strategies for the dynamic monitoring of historical structures. *Journal of Civil Structural Health Monitoring*, 6(2), 265-289. <https://doi.org/10.1007/s13349-016-0164-9>.
- Brincker, R.; Zhang, L.; and Andersen, P. (2000). Modal identification from ambient responses using frequency domain decomposition, in Proceedings of the 18<sup>th</sup> International Modal Analysis Conference, San Antonio, Texas, USA, pp. 625-630.
- Brincker, R., Zhang, L., & Andersen, P. (2001). Modal identification of output-only systems using frequency domain decomposition, 10, 441-445.
- Calderoni, B., Cordasco, E. A., Sandoli, A., Onotri, V., & Tortoriello, G. (2015). Problematiche di modellazione strutturale di edifici in muratura esistenti soggetti ad azioni sismiche in relazione all'utilizzo di software commerciali. XVI *Convegno ANIDIS*, (October). <https://doi.org/10.1109/ICPP.2013.72>.

## References

---

- Carocci, C. F. (2012). Small centres damaged by 2009 L'Aquila earthquake: On site analyses of historical masonry aggregates. *Bulletin of Earthquake Engineering*, 10(1), 45-71. <https://doi.org/10.1007/s10518-011-9284-0>.
- Cattari, S., Lagomarsino, S., & Marino, S. (2015). Reliability of nonlinear static analysis in case of irregular urm buildings with flexible diaphragms. *SECED 2015 Conference: Earthquake Risk and Engineering towards a Resilient World*, 3(July), 1-10.
- CEN, European Committee For Standardization (2005). European standard EN1998-3. Eurocode 8: Design provisions for earthquake resistance of structures. Part 3: Assessment and retrofitting of buildings, Brussels, Belgium.
- C.M. 617/2009, Circolare Ministeriale n.°617 del 02/02/2009, Istruzioni per l'applicazione delle "Nuove Norme Tecniche per le Costruzioni" di cui al D.M. 2008.
- Chopra, A.K. (2001). Dynamics of structures: theory and applications to earthquake engineering. Englewood Cliffs, New Jersey: Prentice Hall.
- Courant, R. (1943). Variational Methods for the Solutions of Problems of Equilibrium and Vibrations. *Bulletin of the American mathematical Society*, 49.
- Craig, R.R., Bampton, M.C.C. (1968). Coupling of Substructures for Dynamic Analysis. *AIAA Journal*, 6(7):1313-1319.

- De Klerk, D., Rixen, D.J. De Jong, J. (2006). The Frequency Based Substructuring (FBS) Method Reformulated According to the Dual Domain Decomposition Method. In Proceedings of the Twenty Fourth International Modal Analysis Conference, St. Louis, MO, Bethel, CT. Society for Experimental Mechanics.
- De Klerk, D., Rixen, D.J., Voormeeren, S.N. (2008). General Framework for Dynamic Substructuring: History, Review, and Classification of Techniques. *AIAA Journal*, Vol. 43, No 5, pp. 1169-1181.
- DIANA (2018): DIANA Finite Element Analysis, User's Manual - Release 10.2, TNO, Netherlands.
- Elnashai, A.S. & Di Sarno, L. (2015). Fundamentals of Earthquake Engineering: from source to fragility, John Wiley and Sons, New York.
- Ewins, D.J. (2000). Modal testing: theory, practice and application. Second edition, Philadelphia, PA: Research Studies Press LTD, Baldock, Hertfordshire, England.
- Fanelli, F. (2014). "*Sulla valutazione sismica delle strutture in muratura a torre*". B.Sc. Thesis, University of Molise, Campobasso, Italy.
- Feenstra, P. (1993). Computational aspects of biaxial stress in plain and reinforced concrete. Delft University of Technology, The Netherlands. <https://doi.org/10.1021/es301297z>.

## References

---

- Formisano, A., Florio, G., Landolfo, R., & Mazzolani, F. M. (2015). Numerical calibration of an easy method for seismic behaviour assessment on large scale of masonry building aggregates. *Advances in Engineering Software*, 80(C), 116–138. <https://doi.org/10.1016/j.advengsoft.2014.09.013>.
- Friswell, M.I. & Mottershead, J.E. (1995). Finite Element Model Updating in Structural Dynamics. Kluwer Academic Publishers, Dordrecht, The Netherlands.
- Gladwell, G.M.L. (1964). Branch Mode Analysis of Vibrating Systems. *Journal of Sound and Vibration*, 1:41–59.
- Hrennikoff, A. (1941). Solution of problems of elasticity by the framework method. *ASME Journal of Applied Mechanics*, 8:619–715.
- Heylen W, Lammens S, Sas P (1998) Modal Analysis Theory and Testing. Katholieke Universiteit Leuven, Leuven.
- Hurty, W. C. (1960). Vibrations of Structural Systems by Component Mode Synthesis. *Journal of Engineering Mechanics, Division American Society of Civil Engineers*, 86(4):51–69.
- Lagomarsino, S., & Cattari, S. (2015). PERPETUATE guidelines for seismic performance-based assessment of cultural heritage masonry structures. *Bulletin of Earthquake Engineering*, 13(1), 13–47. <https://doi.org/10.1007/s10518-014-9674-1>.
- Lourenço, P. B. (2009). Recent Advances in Masonry Modelling: Micromodelling and Homogenisation. Guimarães, Portugal: Department of Civil Engineering, University of Minho. [https://doi.org/10.1142/9781848163089\\_0006](https://doi.org/10.1142/9781848163089_0006).

- MacNeal, R.H., Hybrid, A. (1971). Method of Component Mode Synthesis. *Computers & Structures*, 1(4):581–601.Guidl
- MATLAB (2017). *MATLAB User’s Manual*, Release 9.2.0, The Math Works, USA.
- Marra, A. (2015). Interdisciplinary approach to the conservation of cultural heritage in seismic areas. Ph.D. Thesis, Seismic Risk Doctoral Programme, XVII Cycle, University of Naples FedericoII.
- Marcari, G., & Fabbrocino, G. (2008). Survey and critical analysis of urban areas in Molise Region from a seismic standpoint : the case study of Oratino historic centre.
- Masciotta, M. G. (2015). *Damage Identification of Structures based on Spectral Output Signals Trabalho efectuado sob a orientação do.*
- Masciotta, M. G., Ramos, L. F., Lourenço, P. B., Vasta, M., & De Roeck, G. (2016). A spectrum-driven damage identification technique: Application and validation through the numerical simulation of the Z24 Bridge. *Mechanical Systems and Signal Processing*, 70–71, 578–600. <https://doi.org/10.1016/j.ymssp.2015.08.027>.
- Presidenza del Consiglio dei Ministri 2011. Valutazione e riduzione del rischio sismico del patrimonio culturale con riferimento alle norme tecniche per le costruzioni di cui al DM 14 Gennaio 2008. Direttiva P.C.M. 9 febbraio 2011.
- Peeters, B. (2000). System Identification and Damage Detection in Civil Engineering, PhD Thesis, Catholic University of Leuven, Belgium.

## References

---

- R. Plescu, G. Teodoriu, G. T. (2012). Infrared thermograohy applications for building investigation, *Tomu 1 LVI*. <https://doi.org/10.1007/s15006-012-1452-x>.
- Rainieri, C., Fabbrocino, G., & Cosenza, E. (2010). *Some remarks on experimental estimation of damping for seismic design of civile constructions*. *Shock and Vibration*, 17, 383-395.
- Rainieri, C., & Fabbrocino, G. (2014). *Operational Modal Analysis of Civil Engineering Structures: An Introduction and Guide for Applications*, Springer, New York, USA. <https://doi.org/10.1007/978-1-4939-07670>.
- Rainieri, C., & Fabbrocino, G. (2015). Development and validation of an automated operational modal analysis algorithm for vibration-based monitoring and tensile load estimation. *Mechanical Systems and Signal Processing*, 60-61, 512-534.
- Rainieri, C., Fabbrocino, G., & Cosenza, E. (2007). Automated Operational Modal Analysis as Structural Health Monitoring Tool: Theoretical and Applicative Aspects. *Key Engineering Materials*, 347, 479-484. <https://doi.org/10.4028/0-87849-4448.479>.
- Ramos, L. F. (2007). *Damage identification on masonry structures based on vibration signatures*. PhD Thesis. <https://doi.org/10.1038/nmat3777>.

- Ramos, L. F., & Lourenço, P. B. (2004). Modelling and vulnerability of historical city centers in seismic areas: A case study in Lisbon. *Engineering Structures*, 26(9), 1295-1310. <https://doi.org/10.1016/j.engstruct.2004.04.008>.
- Ramos, L. F., Marques, L., Lourenc, P. B., Roeck, G. De, Campos-costa, A., & Roque, J. (2010). Monitoring historical masonry structures with operational modal analysis: Two case studies, 24, 1291-1305. <https://doi.org/10.1016/j.ymsp.2010.01.011>.
- Rubin, S. (1975). Improved Component-Mode Representation for Structural Dynamic Analysis. *AIAA Journal*, 13:995-1006.
- Russo, S. (2013). On the monitoring of historical Anime Sante church damaged by earthquake in L'Aquila., *Structural Health Monitoring*, 20, pp 1226-1239
- SAP2000, (2017). SAP2000 Advanced User Manuals, Release 15, CSI Computers & Structures, Inc.
- Simões, A., Bento, R., Gago, A., & Lopes, M. (2012). Seismic Vulnerability of Old Masonry 'Gaioleiro' Buildings in Lisbon. 15 *Wcee*.
- Shih, C. Y.; Tsuei, Y. G.; Allemang, R. J.; and Brown, D. L. (1988). Complex mode indication function and its applications to spatial domain parameter estimation, *Mechanical Systems and Signal Processing*, vol. 2, no. 4, pp. 367-377.
- SOLIDWORKS, (2016). Finite Element Analysis, User's Manual - Release SP3.0, Dassault System, U.S.A.

## References

---

- SVS (2018): ARTeMIS Extractor Pro User Manual, Release .5.3.1.1, Structural Vibration Solutions, Aalborg, Denmark.
- van der Valk, P.L.C. (2010). Model Reduction & Interface Modelling in Dynamic Substructuring. M.Sc. Thesis, Mechanical, Maritime and Materials Engineering, Delft, Netherlands.
- VV. AA. (2002). La Carta di Cracovia 2000. Principi per la conservazione e il restauro del patrimonio costruito, Ed. Marsilio, 258 pp. (in Italian).
- Verderame, G. M., Ricci, P., Esposito, M., & Sansiviero, F. C. (2011). Le Caratteristiche Meccaniche degli Acciai Impiegati nelle Strutture in c.a. realizzate dal 1950 al 1980. *XXVI Convegno Nazionale AICAP*.
- Yam, L.H.; Yan, Y.J.; and Wei, Z. (2004). Vibration-based non-destructive structural damage detection, *Key Engineering Materials*, vol. 270–273, pp. 1446–1453.